DEVELOPMENT OF POLYOLEFIN-BASED MULTIPLE AND REVERSIBLE SHAPE MEMORY POLYMERS

DEVELOPMENT OF POLYOLEFIN-BASED MULTIPLE AND REVERSIBLE SHAPE MEMORY POLYMERS

By YUAN GAO, B.ENG., M. ENG.

A Thesis Submitted to the School of Graduate Studies

in Partial Fulfilment of the Requirements for

the Degree Doctor of Philosophy

DOCTOR OF PHILOSOPHY (2019) McMaster University

(Chemical Engineering) Hamilton, Ontario

TITLE: Development of polyolefin-based multiple and reversible shape memory polymers

AUTHOR: Yuan Gao

B.Eng. (Zhejiang University, China)

M.Eng. (Zhejiang University, China)

SUPERVISOR: Dr. Shiping Zhu

CO-SUPERVISOR: Dr. Michael Thompson

NUMBER OF PAGES: xvii, 188

Lay abstract

Shape memory polymer (SMP) is stimuli-responsive capable of “memorizing” a temporary shape and yet recovering to its permanent shape upon a certain external trigger. SMPs are widely studied and applied in the areas of aerospace, biomedicine, textile, etc. On the other hand, a reversible shape memory polymer (RSMP) is a new type of SMP that can shift back and forth between two different temporary shapes without the need of reprogramming between transitions, and has been applied in soft actuators, microrobotics, and artificial muscles. In this thesis, unique polyolefin-based RSMP were developed with good reprocessability and shown in new application scenarios. Firstly, a thermoplastic semicrystalline polymer was demonstrated to exhibit the reversible shape memory effect (RSME) by using a lab-designed ethylene/1-octene diblock copolymer and commercial polyolefin elastomer blends. Subsequently, the reprocessability of a crosslinked poly(ethylene-co-vinyl acetate) (PEVA) RSMP was improved by introducing a dynamic covalent polymer network. Finally, transitional changes between shapes was amplified by developing a RSMP foam by utilizing polyolefin elastomer blends. This thesis represents significant progress in the study of polyolefin-based RSMPs.

Abstract

A shape memory polymer (SMP) is stimuli-responsive with the fantastic capacity to “memorize” a temporary shape under certain conditions and to recover to its permanent shape upon exposure to certain external stimulus (e.g. heat, light, electromagnetic field). In the past few decades, various SMPs have been investigated and applied in the area of aerospace, biomedicine, and textiles, etc. Recently, a special type of SMP called a ‘two-way reversible shape memory polymer’ or ‘reversible shape memory polymer’ (RSMP) capable of transitioning between two temporary shapes without the need for reprogramming after each change has attracted the attention of many researchers. In this class of polymer, the semicrystalline RSMP was studied considerably due to the various chain structures produced by relatively simple synthesis routes. The crystallization-induced elongation (CIE) and melting-induced contraction (MIC) of the oriented crystal domains has been theorized as the main mechanism of semicrystalline RSMP. However, most RSMPs are predominantly thermosets, which implies significant drawbacks regarding reprocessing and recycling.

This thesis focuses on the development of RSMP based on polyolefin materials, especially novel high-performance polyolefin elastomers, due to the advantages of high crystallizability, varying chain structures, tunable and broad melting transitions, and low cost. The thesis starts off by demonstrating the reversible shape memory effect (RSME) of the thermoplastic ethylene/1-octene diblock copolymer, which contains the ethylene-rich hard segments and the 1-

octene-rich soft segments. The delicately designed chain structure exhibited a broad melting transition and strong physical crosslinks, which contributed to the resulting RSME and the CIE/MIC effect at load-free conditions. Furthermore, the commercially available polyolefin elastomer blends demonstrated the RSME. The utilization of commercial products and simple processing method to achieve a thermoplastic RSMP offers easy production in large scale and low costs. The second part of the thesis developed a polyolefin-based RSMP with reconfigurable network by introducing a transesterification catalyst into a crosslinked poly(ethylene-co-vinyl acetate). The network reconfiguration achieved a dynamic covalent polymer network by breaking the ester bonds and reconnecting. The third part of the thesis explored a new RSMP foam material developed by utilizing polyolefins. The polyolefin elastomers of differing compositions were blended and foamed to fabricate the porous structure. The RSME in a load-free condition was then demonstrated successfully. This thesis represents significant progress in the development of polyolefin-based RSMPs, outlining new structural design, processability improvements, and potential applications.

Acknowledgements

When I started writing this acknowledgement after completing all the chapters in this thesis, I felt it was really a fantastic experience to study here at McMaster University. There are so many people I would like to give my sincere gratefulness to during this journey.

First, I would like to thank my greatest supervisor Dr. Shiping Zhu for giving me the opportunity to study as his student and work on this interesting project in his research group. Dr. Zhu shaped my thinking in an engineer way during every meeting and discussion time, which is a great treasure for me in the research. His passion, tirelessness, open mind, humor, wisdom and the philosophy of life will always point the direction to what a man I should be. Thank you, Dr. Zhu!

I would like to thank my co-supervisor Dr. Michael Thompson for his exceptional guidance and the critical thinking on my research. Every time after discussing with him I feel I gain a lot from a different perspective. I am very appreciated for his supervision.

I would like to thank my supervisor committee member Dr. Li Xi for the valuable suggestions. His excellent knowledge and working attitude inspire me a lot in these years.

I would also like to thank Dr. Weifeng Liu, who gave me the best guidance in the group when I first came here. I am very appreciated for him sharing his experience and knowledge to me in my research. He is the best colleague I have

ever met, and I will never forget the days we spent to discuss the experiments, the paper drafts, and daily life.

I am thankful to current and former members of PolyMac Zhu research group. We shared the office, the lab, and the joy every day. Because of you, I didn't feel alone in the beginning, because of you I learned a lot from a different culture. No matter where we are in the future, our friendship will never fade away.

I am thankful to the great faculty members in the Chemical Engineering Department, and the friends I met here. You made my life as a Ph.D. student colorful and unforgettable.

I am also grateful to Dr. Paul Charpentier and his students, Mr. Yixing Tang and Miss Rayehe Samimi Haghgozar from the University of Western Ontario, for their kindly help that opened the DMA to me and let my research continue smoothly.

Last but never least, I will give my deepest gratitude to my family. My lovely wife, Qianqian Chen, always gives me the strongest support since I planned to be abroad for my doctoral study. I appreciate so much that we can reunite in Canada and have a wonderful life in the latest two years. And no matter how far I live from home, my heart will be there with my parents, who always take pride in me and encourage me to fight for a new life.

Table of contents

List of figures

List of Schemes

List of tables

Declaration of academic achievement

This thesis is organized based on a “sandwich” style, which consists of 2 published journal articles, one submitted manuscript and one prepared manuscript. The contributions of the authors in each work are summarized as below:

- Yuan Gao is the primary author of all the articles and manuscripts in this thesis. (Chapter 3-6).
- Dr. Weifeng Liu is a coauthor for the three original works (Chapter 3-5). He synthesized the polymer used in Chapter 3 and provided necessary revision to the manuscript drafts of the three works.
- Dr. Shiping Zhu is the supervisor in all the works. He provided the ideas, guidance and revision of the manuscript drafts.
- Dr. Michael Thompson is the supervisor in one prepared manuscript (Chapter 6). He provided valuable discussion and revision of the manuscript draft.

List of publications

- Gao, Y.; Liu, W.; Zhu, S., Thermoplastic Polyolefin Elastomer Blends for Multiple and Reversible Shape Memory Polymers, *Industrial & Engineering Chemistry Research*, **2019**, *58(42)*, 19495-19502.
- Gao, Y.; Liu, W.; Zhu, S., Reversible Shape Memory Polymer from Semicrystalline Poly(ethylene-co-vinyl acetate) with Dynamic Covalent Polymer Networks, *Macromolecules*, **2018**, *51(28)*, 8956-8963.
- Gao, Y.; Liu, W.; Zhu, S., Polyolefin Thermoplastics for Multiple Shape and Reversible Shape Memory, *ACS Applied Materials & Interfaces*, **2017**, *9(5)*, 4882-4889.

1 INTRODUCTION

This chapter gives an overview of the research objectives and the thesis organization.

§ 1.1 Introduction

As a representative stimuli-responsive polymer, shape memory polymers can memorize one or several temporary shapes and recover to their permanent shape under external triggering conditions, such as heat, light, electromagnetic field, etc. Nowadays, shape memory polymers have attracted many researchers due to their fantastic advantages of low cost, wide sources, light weight, tunable structures and properties. They show great potential in both academia and industry, especially in the fields of textiles, aerospace facilities and biomedical devices.

The more or less conventional one-way shape memory effect, which means the shape-changing direction is one-way during a programming-recovering cycle, is a great drawback for the shape memory polymers applying in applications such as microrobots, artificial muscles. Recently, a series of soft actuators based on shape memory polymers have been reported. These novel actuators can shift between their different temporary shapes driven by external stimuli and without the need of new programming step. This novel shape memory polymer with bidirectionally shape-changing ability was thus named as two-way shape memory polymer or reversible shape memory polymer. The mechanism of crystallization-induced elongation (CIE) and melting-induced contraction (MIC) are critical to the transition in shapes.

Till now, reported semicrystalline reversible shape memory polymers have been mainly polyester, polyether and polyolefin materials. However, single-component polyester or polyether-based reversible shape memory polymers require an external force to induce the oriented crystallization necessary to achieve the reversible shape memory effect, making them only “quasi-reversible”. They usually need other polymer components to achieve a fully reversible shape memory effect under load-free conditions, which increases the complexity of their synthesis and hence increases their production costs. In comparison, polyolefin materials have been largely overlooked as reversible shape memory polymers but offer the advantages of high crystallizability, various chain structures, tunable and broad melting transitions near room temperature. Their excellent

weatherability, chemical resistance, and low cost would also be advantages for potential applications.

Most of the current reversible shape memory polymers are thermosets and their permanent shapes cannot be reconfigured, which is an obvious drawback for their re-processing and recycling. Thus, exploration of thermoplastic reversible shape memory polymer systems is of great significance for applications.

Thus, this thesis focuses on the development of reversible shape memory polymers based on thermoplastic polyolefin materials, especially the novel high-performance polyolefin elastomers. As the world's most consumable polymer material, polyolefin-based materials have many commercially available products, various polymerization methods, and precisely controllable chain structure, so that appropriate materials with much needed broad melting transitions can be developed to produce novel reversible shape memory polymers. The resulted materials will expand on the application areas of polyolefin-based materials.

§ 1.2 Research objectives

The thesis is organized to introduce several new polyolefin-based reversible shape memory polymers. It first demonstrates the reversible shape memory effects of pure polyolefins and provides a simple method for their production on large scale. The subsequent studies introduced a polyolefin-based reversible shape memory polymer with reconfigurable network structure, along with its

application as the foam material. The research objectives of each chapter are summarized in detail below.

- To develop a novel thermoplastic reversible shape memory polymer based on lab-designed polyolefin elastomer materials with precise chain structure control. (Chapter 3)
- To fabricate commercially available thermoplastic polyolefin elastomer blend systems to realize reversible shape memory effect (Chapter 4)
- To develop a reversible shape memory polymer with a dynamic covalent network by poly(ethylene-co-vinyl acetate) system to realize both good shape reversibility and re-processability. (Chapter 5)
- To apply reversible shape memory polymer in polyolefin elastomer foam materials (Chapter 6)

§ 1.3 Thesis organization

This thesis is organized in the “sandwich” style and includes seven chapters. Chapter 3 and Chapter 5 represent two published research articles in peer-reviewed journals, while Chapter 4 and Chapter 6 represent two prepared manuscripts for peer-review journals. The published articles were copied into the thesis with copyright permits from the publishers placed at the beginning of each chapter. The numbers of all the tables and figures of the copied articles have been adjusted for consistency throughout the thesis, while the bibliographic formats have been modified.

This thesis starts from Chapter 2 with a literature review of shape memory polymers and focuses on the current development of reversible shape memory polymers and the application of polyolefin materials in shape memory polymers. This review indicates that this class of material is full of opportunities and challenges to fabricate reversible shape memory polymers from new materials and with new functions.

The following chapters report studies on various polyolefin-based elastomers applied in multiple and reversible shape memory polymer.

Since chemical crosslinks are often considered necessary in a reversible shape memory polymer, which limits the re-processability or recyclability, it is a challenge to develop the thermoplastic reversible shape memory system. **Chapter 3** focuses on a thermoplastic polyolefin elastomer as a potential reversible shape memory polymer. Several lab-designed ethylene/1-octene diblock copolymers with well-controlled hard block and soft block contents are investigated. The new thermoplastic polyolefin elastomers are demonstrated with broad melting transitions as well as broad crystal size distributions. This delicate structure design endows the diblock copolymers with not only multi-shape memory effects but also a novel reversible shape memory effect. The mechanism of the reversible shape memory effect is also confirmed to be based on crystallization-induced elongation (CIE) and melting-induced contraction (MIC). .This diblock copolymer with precise chain structure design and control is

the first pure hydrocarbon thermoplastic polyolefin material that can be demonstrated the reversible shape memory effect. It also expands the application of polyolefin elastomers in the smart polymer field.

However, lab-designed polyolefin elastomers with precise chain structure control will be limited in their manufacture on a large scale and can result in high production costs. It is a challenge to fabricate reversible shape memory polymers economically. Furthermore, in **Chapter 4**, a simple blending method is introduced to fabricate thermoplastic reversible shape memory polymers based on commercially available polyolefin elastomers. Several thermoplastic polyolefin elastomers are blended in the different recipes and the resulting elastomer blends demonstrate broad melting transitions. The crystal size distributions of the blends are also broadened during blending. The resulted elastomer blends demonstrate one-way dual- and multi-shape memory effects as well as a reversible shape memory effect. The mechanism of the reversible shape memory effect is confirmed at the end. This chapter demonstrates a simple blending method, which can be used for fabricating thermoplastic reversible shape memory polymers. This method also expands the material resource for reversible shape memory polymers. The commercially available raw materials will also help to produce reversible shape memory polymer in large scale.

Chapter 5 reports on an idea to improve the re-processability of crosslinked poly(ethylene-co-vinyl acetate) (PEVA) reversible shape memory polymers. Once

a transesterification catalyst is introduced into a crosslinked PEVA system, the system becomes a dynamic covalent polymer network, which can achieve network reconfiguration through ester bonds breaking and reconnecting. The resulted system has also demonstrated the orthogonality between the reversible shape memory effect and network reconfiguration. Thus, the reprocessing of the permanent shape of the current PEVA system can be achieved. This work is the first attempt to introduce the dynamic covalent network into polyolefin-based reversible shape memory polymer. It provides an opportunity for the design and synthesis of shape memory polymers having good reprocessing, mechanical and reversible shape memory properties through simple modification of commercially available polymers.

Chapter 6 focus on one application of polyolefin-based reversible shape memory polymer in foams. Several polyolefin foams are fabricated with different polyolefin elastomer blends using a chemical blowing agent and a crosslinking agent. The resulted foams demonstrate the reversible shape memory effect successfully in tension and bending modes. The mechanism of the reversible shape memory effect is also discussed in the context of a foam. Since all current reversible shape memory polymer foams are based on polycaprolactone materials, this work is the first reversible shape memory polymer foam fabricated by polyolefin elastomer blends. It shows the various possibility of application of commercially available polyolefin-based reversible shape memory polymers.

Chapter 7 is the conclusion of the thesis and summarizes all the contributions and recommendations for further research.

2 LITERATURE REVIEW

This chapter presents a literature review on shape memory polymers, with a brief introduction followed by recent developments of reversible shape memory polymers. It summarizes all types of current reversible shape memory polymer materials.

§ 2.1 Abstract

In the past few decades, remarkable progresses have been made in shape memory polymers due to the development of mechanism knowledge, structure design, and synthesis methods. Shape memory polymers have potential applications in biomedicine, aerospace, and textures. In this chapter, a brief overview of shape memory polymers is discussed in terms of phenomena, mechanisms, and behaviors. An overview on the novel reversible or two-way

shape memory polymers will also be provided, followed by the recent developments in this field. Lastly, the unique class of polyolefin-based shape memory polymers is discussed.

§ 2.2 Introduction

In recent times, smart materials (otherwise known as stimuli-responsive materials) have been developed in an increasingly rapid manner for their significant roles in human life. As a representative type of smart materials, shape memory polymer is considered as a material that can “memorize” a temporary shape during a programming step under appropriate conditions, and recover to its permanent shape when exposed to an external stimulus, such as heat, light, electric and magnetic field, redox, pH, solvents, and etc. The full category of shape memory materials includes shape memory alloys, shape memory ceramics, and shape memory polymers (SMP). Among them, SMP has attracted the most attention in both academia and industry due to its advantages of low cost, light weight, good processability, various types, and easy modification. Due to their interesting and unique behaviors, SMPs have been considered for many potential applications in such areas as textiles, biomedical devices, aerospace facilities, etc.[1-7]

Although widely and deeply studied since the 1990s, SMPs were actually reported and applied industrially more than half a century ago. The earliest reported SMP could be traced to a US patent in the 1940s,[8] in which an “elastic

memory" was described in some materials. Then in the 1960s, a heat shrinkable polyethylene was commercialized, which was considered a SMP.[9] In 1984, the word "shape memory polymer" was applied to the development of a polynorbornene-based SMP, which was fabricated by CdF Chimie Company (France).[10] From then on, the development of SMP has been growing fast, first in industrial research and later in academic research. Various mechanisms and types of SMPs have been investigated, with quite a few reviews published in the field.[11-19]

SMPs can be classified in different ways. Using the external trigger as the means to classify, there are thermally-induced SMP,[20] light-induced SMP,[21] electricity-induced SMP,[22] magnet-induced SMP,[23] etc. When the classification is focused on the reversible switch for fixing a temporary shape, there are crystalline SMP,[24] and amorphous SMP.[25] When the classification focuses on the number of temporary shapes that a SMP can hold, there are dual-SMP,[26] triple-SMP,[27] and multi-SMP.[28] And when the shape-changing direction is the means of classification, there are one-way SMP,[29] and two-way or reversible SMP.[30] The simplest SMP is typically thermally-induced one-way dual-SMP, which is an ideal model polymer for studies on the phenomenon and mechanism of shape memory effects (SME).

The demonstration of a typical shape memory cycle for a thermally-induced one-way dual-SMP is shown in Figure 2.1, including a programming step and a recovery step. The SMP usually needs a pre-processing step, such as pressing,

extrusion, etc., to set the “permanent shape” or the original shape. In the programming step, the SMP is heated to a programming temperature (T_p) above a certain “switch temperature” (T_{sw}), but below the pre-processing temperature. An external force is then added to the SMP to set the temporary shape. This external force is applied as the SMP is being cooled from T_p to a low temperature (T_{low}) below T_{sw}. Once the external force is removed, the temporary shape is fixed, that is, the temporary shape is “memorized”. In the following recovery step, the SMP is reheated to T_p, and the fixed temporary shape recovers to its permanent shape. Thus, a typical shape memory cycle is completed.

In quantitative SME studies, dynamic mechanical analysis (DMA) is usually used for “memory” measurements in the tension mode. In a thermally-induced dual-SME test, the strain of the permanent shape for a SMP sample at T_p is recorded as ε_{f0}. In the programming step, the external force stretches the sample to a maximum strain ε_m, while temperature decreases from T_p to T_{low}. When the external force is removed, the sample usually recovers a little until a temporary shape is fixed and its fixed strain is ε_f. In the recovery step, the temperature increases again to T_p and the SMP sample begins to shrink to its permanent shape and finally reaches the recovery strain ε_r. However, the sample strain usually cannot completely recover to ε_{f0}, due to stress relaxation during the test. From the DMA measurements, there are two important parameters, which must

be calculated in the quantitative evaluation of SME: the shape fixing ratio (R_f) and the shape recovery ratio (R_r):[20]

$$R_f = \frac{\varepsilon_f - \varepsilon_{f0}}{\varepsilon_m - \varepsilon_{f0}}$$

$$R_r = \frac{\varepsilon_f - \varepsilon_r}{\varepsilon_f - \varepsilon_{f0}}$$

The shape fixing ratio represents the ability of SMP to fix the temporary shape, while the shape recovery ratio represents the ability of SMP to recover its permanent shape. For an ideal SMP, both the shape fixing ratio and the shape recovery ratio should be 100%.

The measurement methods and the important parameters for multi-SME and reversible SME are similar to those described above, which will be discussed in the following chapters.

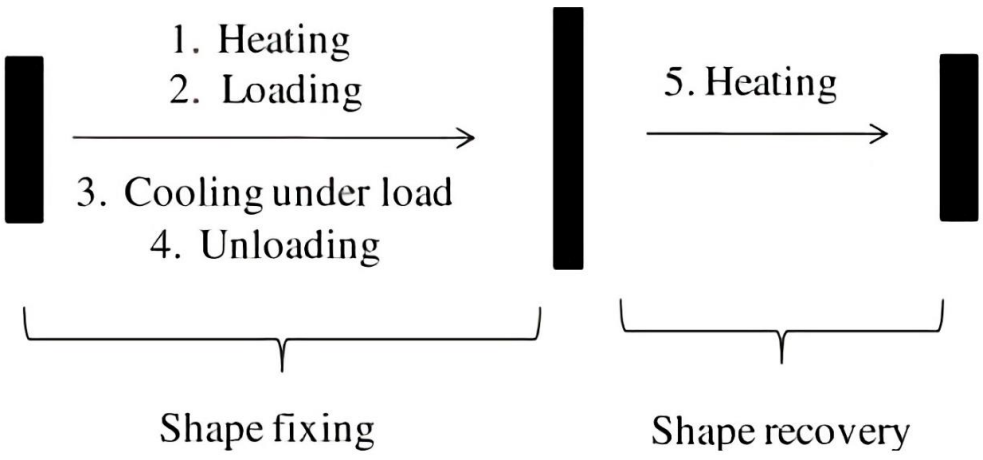

Figure 2.1. Schematic illustration of a one-way thermally-induced dual-SME.[1]

§ 2.3 One-way shape memory polymers

A conventional SMP has one-way SME, which can be programmed and fixed into one temporary shape at a time under certain conditions and which can be subsequently transformed back to its permanent shape under an external trigger, such as heat, light, etc.

A typical mechanism of SMP is as follows. Generally speaking, a SMP possesses at least two structures, one is a stable network and the other is a reversible switch transition, that can respond to an external trigger.[18] As shown in Figure 2.2, the stable network fixes a permanent shape of the SMP material. The deformation of this phase induces an entropic elasticity for shape recovery. This stable network can be achieved by chemical or physical crosslinks. The reversible switch transition can be phase segregation or a reversible crosslinking. It can fix the temporary shape by two types of interactions. The first is a separated phase formed by crystallization or glass transition, for example. The second is crosslinks containing reversible covalent bonds or non-covalent bonds, for example. Among them, the most important reversible switch transitions are melting transition and glass transition. The melting transition can be utilized in crosslinked elastomers and semicrystalline polymers, as well as some thermoplastic polymers. Polyolefin,[31, 32] polyethers,[33, 34] and polyesters[35, 36] are the most investigated SMPs that take advantage of melting transitions. These

SMPs are often stiffer and have faster recovery than other SMPs.[4] The glass transitions can similarly be utilized in chemically crosslinked or thermoplastic polymers, such as epoxy,[20, 25] polyurethane,[37, 38] and polymethacrylate networks.[39, 40] These SMPs often have slower recovery than other SMPs because of their relatively broad glass transitions.[6] Actually, those SMPs utilizing melting transitions can also feature glass transitions for the reversible switch transitions. However, since their glass transition temperatures are usually much lower than room temperature, these SMEs using their glass transition temperatures as T_{sw} are not discussed.

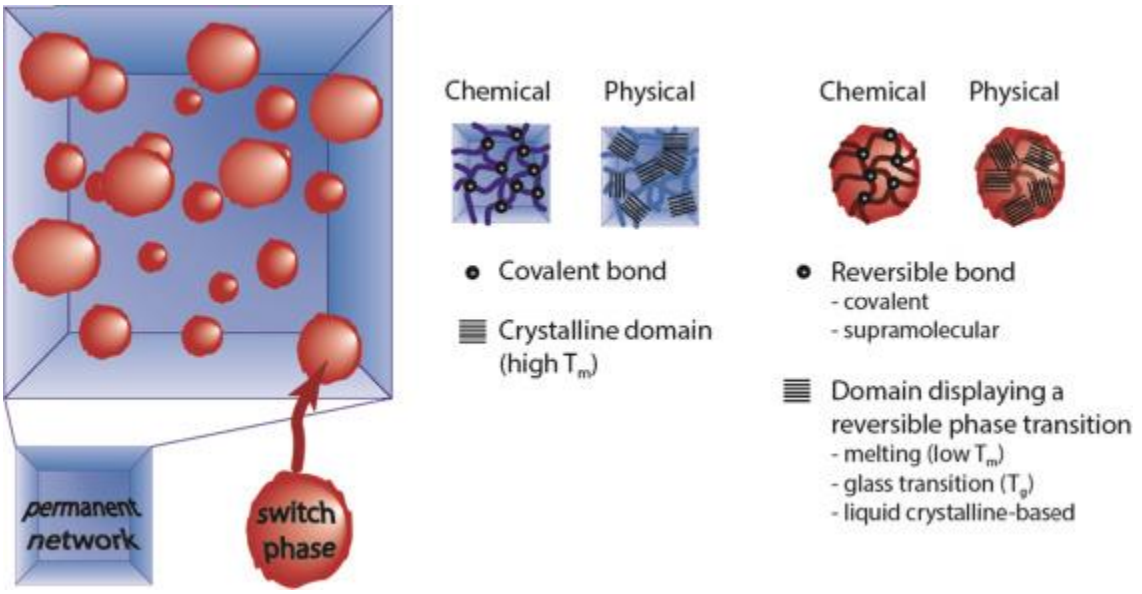

Figure 2.2. General structure of SMPs consisting of a stable network, which fixes the permanent shape and a reversible switch, which can fix temporary shape and can be triggered by external stimuli.[18]

The temporary shape can also be fixed by reversible crosslinks. Several examples utilizing reversible covalent bonds and supramolecular interactions have been reported, such as bonds formed by Diels-Alder reaction,[41, 42] and hydrogen bonds.[43, 44]

In considering the mechanism of some thermally-induced SMPs, if the fixation interaction can be regarded as a “lock” that fixes the temporary shape, the “key” will be the trigger, which is heat in this case. This “key-lock” model can be helpful for us to understand the mechanism of SME.

It is easy to understand that, in a SMP, the number of locks is always equal to the number of temporary shapes, while the number of keys may not be the same temperature. This understanding can result in a multi-SMP material, which can fix and recover at least two temporary shapes, as shown in Figure 2.3, in contrast to the examples described above. The polymer transforms from one shape to another, induced by one trigger (usually heat). There are two important strategies for the design of multi-SMPs: (i) introducing multiphase structures to the polymer material; or (ii) utilizing polymers with a very broad thermal transition. The latter strategy is more popular in research due to the simple requirement whereas many polymers can fit, such as gradient styrene/methyl acrylate copolymer,[45] PMMA/PEG semi-interpenetrating polymer network,[46] and some commercially available polymers, e.g. Nafion.[28, 47] Those materials have a broad glass transition or melting transition, and as a result, the triple-SME and even quadruple-SME of the polymers have been demonstrated.

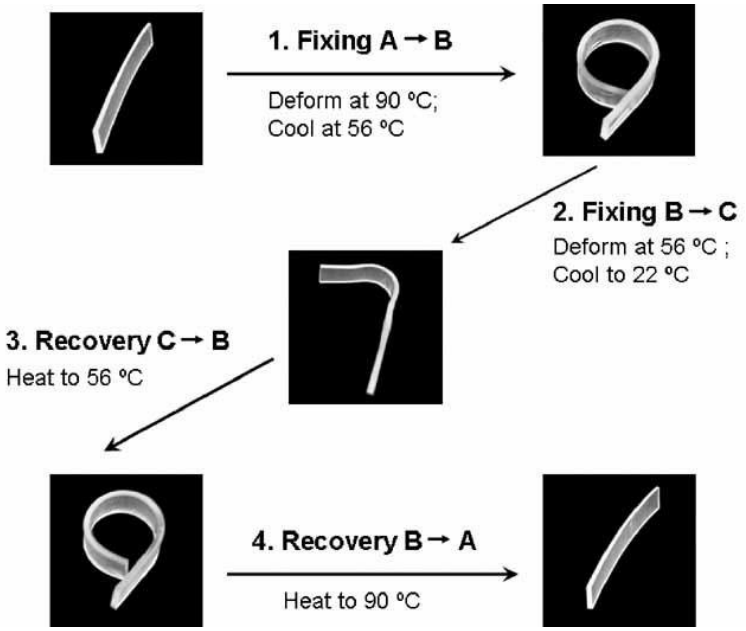

Figure 2.3. Visual illustration of a triple-SME.[48]

SMP has been widely applied in the areas of wrapping, aerospace, biomedicine, and textile. The early application of SMP was heat-shrinkable tubes made of polyethylene for insulation protection of cable connections.[31] Based on the same idea, heat shrinkable films made of SMP are now widely used in the wrapping industry. The advantages of SMP, such as light weight and low cost, are useful for fabricating self-deployable structures, such as solar arrays, solar sails, and sunshields in the aerospace industry.[14] SMP can also be applied in biomedical areas by selecting appropriate materials and processing methods to obtain biocompatible SMPs. Lendlein et al.[49] generated a self-tightening suture with biodegradable polyester SMP. The suture was first deformed to an elongated form, and then used to close up the wound. The loose suture shrinks at body temperature to tighten the knot, avoiding secondary damage during

surgery. Similarly, Erndt-Marino et al.[50] prepared a biocompatible PCL foam material to repair irregularly damaged bones.

§ 2.4 Reversible shape memory polymers

Some categories of conventional SMPs have been reviewed. All of them are one-way SMPs, that is, the direction of shape changing is one-way during a programming-recovering process and the polymers cannot change between two shapes without external deformation.[51, 52] This is a great drawback of conventional SMPs for many applications. In fact, there are some investigations aiming to solve this problem. The key is to introduce an internal “driving force” to the SMP system for the back transformation in order to achieve a reversible shape memory effect (RSME), which is challenging.

An approach for design of reversible shape memory polymers (RSMPs) is based on liquid crystal elastomers (LCE),[53, 54] which exhibit reversible contraction/extension behavior between its anisotropic and isotropic phases.[55] A LCE expands when the temperature is below its transition temperature due to an orientation effect. The discovery of this phenomenon opened doors to achieving RSMPs. However, the difficulty in synthesis of the materials limits research in their production and applications.

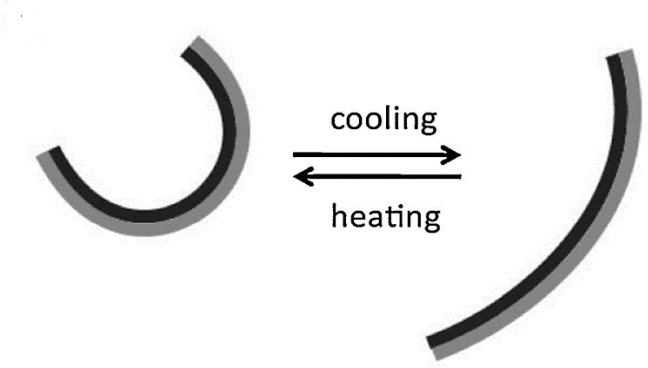

Figure 2.4. Schematic illustration of the RSME achieved by polymer laminates.[17]

Another approach for making RSMPs is to fabricate polymer laminate materials. Pre-programmed dual-SMP is combined with an elastic polymer into a laminate structure, as shown in Figure 2.4. The recovery force of SMP can be an internal driving mechanism to achieve reversible shape change. Chen et al.[56, 57] pre-programmed a shape memory polyurethane (SMPU) film by stretching into a film and then adhered to a non-stretched elastic polyurethane (PU) film to form a laminate structure. Upon heating, the pre-programmed SMPU layer shrunk and drove the whole sample to bend towards the SMPU side. A temporary shape was fixed when the recovery force of SMPU layer was equal to the bending force of PU layer. Upon cooling, the bending PU layer acted as a spring and reversed the sample to another temporary shape, while SMPU layer was stretched again. After two cycles of heating and cooling between 25 °C and 60 °C, this shape-changing cycle became stable and the RSME was achieved. Tamagawa et al.[58] combined a carbon fiber reinforced epoxy layer and a pure epoxy layer to make a laminate.

Due to the significantly different thermal expansion coefficients between the two layers, upon heating, the layer with the high expansion coefficient experienced a higher volumetric rate change, leading to the laminte bending toward the side of the other layer. Upon cooling, it would also reverse back in its shape. Though the mechanism was different from that in Chen's work, it also achieved a RSME.

Based on the same idea, Westbrook et al.[59] designed a core-shell structure to achieve RSME. They used pre-stretched crosslinked polycyclooctene (PCO) as its core and affixed an elastic matrix as a shell to fabricate RSMP. Its reversible ratio reached 10%.

It is a simple method to achieve RSME by fabricating polymers into laminate or core-shell structures. However, this method has many limitations. For example, the reversible shape changes can be achieved only between bending shapes.

A comparable behavior to LCE was found within semicrystalline polymer systems. In 2008, Chung et al.[60] first reported PCO with chemical cross-linking that featured a crystallization-induced elongation (CIE) upon cooling and a melt-induced contraction (MIC) upon heating under an external stress, which resulted in RSME. When an external force was applied to the sample at a temperature higher than PCO's melting temperature, the strain increased to a value ε_1 as the PCO chains became oriented in the stretching direction. Upon cooling, the crystals in the PCO sample formed from the oriented chains and led to an elongation in the stretching direction up to a strain ε_2, due to CIE. With the

remaining external force, the oriented crystals melted upon heating and the sample contracted to a strain ε_3, due to MIC. The sample's extent of strain could shift between ε_2 and ε_3 during the cycles of heating and cooling under an external force and hence, demonstrated RSME. Later, Zotzmann et al.[61] reported the CIE and MIC effect in poly(ω-pentadecalactone) (PPD) and poly(ε-caprolactone) (PCL) networks. However, since an external force was required to realize RSME, that is, the only programming method was stretching, the application of this material was also limited. Development of semicrystalline RSMPs with an internal driving force was desired.

Various approaches have been attempted to construct semicrystalline RSMP systems applicable under stress-free conditions. Recently, there were a few reports on the progress in this field. The reported work can be divided into two categories: i) by one-step crosslinking, and ii) by two-step crosslinking.

For one-step crosslinked polymers, there are crystal domains and amorphous domains co-existing in a single semicrystalline polymer network having a broad range of transition temperatures. The oriented polymer chains can be fixed first by crystal domains of relatively high melting temperature, that act as a skeletal framework. Li et al.[62] demonstrated that crosslinked poly(ethylene-co-vinyl acetate) (PEVA) could exhibit RSME. Behl et al.[63] extended the research of crosslinked PEVA and further studied the thermal memory effect of PEVA. Zhou et al.[30] systematically studied a poly(octylene adipate) (POA) network that also exhibited a broad melting transition and RSME.

The authors synthesized POA networks with multiple components, as well as with different crosslink densities and switch temperatures. They revealed that the key factor affecting RSME was crosslink density. In their report, RSME of POA increased initially with crosslink density, but decreased then if the crosslink density was higher than 70%. It was believed that almost any crosslinked semicrystalline elastic polymer would exhibit RSME using some programming method and an appropriate temperature range. Besides the above single component RSMPs, various polymer networks containing multiple components have also been studied. Behl et al.[64] synthesized a polyesterurethane (PEU) network with PPD and PCL segments. The two polyesters provided a high T_m around 64 °C and a low T_m around 34 °C, respectively, that is, the polymer contained two types of crystalline phases with two distinguishable melting temperatures. The crosslinked network kept the permanent shape by having the oriented PPD crystal domains with high T_m acting as a skeleton. When the temperature decreased, the PCL crystals crystallized along with the skeleton as the CIE effect. This design is ideal in realizing RSME without an external stress. The material had a high reversible strain and a switch temperature that could be adjusted to body temperature for biomedical applications. Saatchi et al.[65] synthesized polycaprolactone/n-butyl acrylate copolymer with a broad melting transition and demonstrated RSME at human body temperature. When the crystal domain content increased, the reversible strain increased from 12.5% to 17.1%. Yang et al.[66] reported that poly(ethylene glycol)/n-butyl acrylate (PEG/BA)

copolymer network could exhibit body temperature responsive RSME and moisture responsive RSME. The RSME could be tuned by adjusting the molecular weight of PEG and BA contents.

In the one-step crosslinked semicrystalline RSMPs, different melting transition temperatures are required for both single component and multiple component polymers. The chemical crosslinks fix the permanent shape. The large crystal domains of high melting temperature fix the oriented polymer chains, whereas the small crystal domains act as actuators through the elongation and contraction of the polymer. A single component RSMP is affected by its crosslink density and switch temperature, while a multiple component RSMP is affected by the combined influence of crosslink density and component contents.

In the two-step crosslinked RSMPs, the first crosslinking step aims to fix the permanent shape of the polymer, while the second crosslinking step aims to fix the oriented polymer network after deformation by an external stress, in contrast to the one-step crosslinked RSMP where the oriented polymer network is fixed by large crystal domains of high melting temperature. Wu et al.[67] synthesized an interpenetrating polymer network (IPN) by PCL and poly(tetramethylene ether) glycol (PTMEG). In their report, PCL was first crosslinked by UV light. The resulting gel was stretched to 100% strain. PTMEG was then crosslinked at 80 °C to fix the oriented PCL network. In the IPN, the PCL crystal domains acted as the actuator, while the elastic PTMEG network acted as the spring to provide an internal reversing force. The reversible strain could reach 5.5%. Meng et al.[68]

studied a PCL/polyacrylate system. They first crosslinked PCL network by thiol-ene reaction and then stretched the polymer to several specified strains. The dangling acrylates were then subsequently crosslinked by UV light. A RSME was demonstrated with the reversible strain higher than 15%. Fan et al.[69] used a single crosslinker to realize a two-step crosslinking process with the SBS/PU system. The PCL-based PU was first crosslinked by trimethylolpropane tris(3-mercaptopropionate) (TMPMP) at 60 °C. The polymer was then stretched to 500% strain and cooled to room temperature. In the second step, crosslinking occurred in the SBS phase, and between the SBS and PU phases, when the polymer was exposed to UV light. The reversible strain was 8.7% in the following seven cycles of heating and cooling between -20 °C and 60 °C. It should be noted that all of the above reported RSMPs were covalently crosslinked during the second crosslinking step, that is, the shapes of these RSMPs are not reconfigurable or recyclable. Jin et al.[70] utilized reversible covalent bonds to tackle the problem. They added nitro-cinnamic acid to PCL network, which could undergo photo-reversible dimerization, when exposed to 312 nm and 254 nm UV light. The introduced reversible covalent bonds improved recyclability and reprocessability of RSMP after crosslinking, and also provided new synthesis routes for fabricating novel RSMPs. However, there are still some remaining challenges. First, the synthetic route was not simple, which limited their large-scale fabrication. Second, they could not be easily reprocessed because of the thermoset nature.

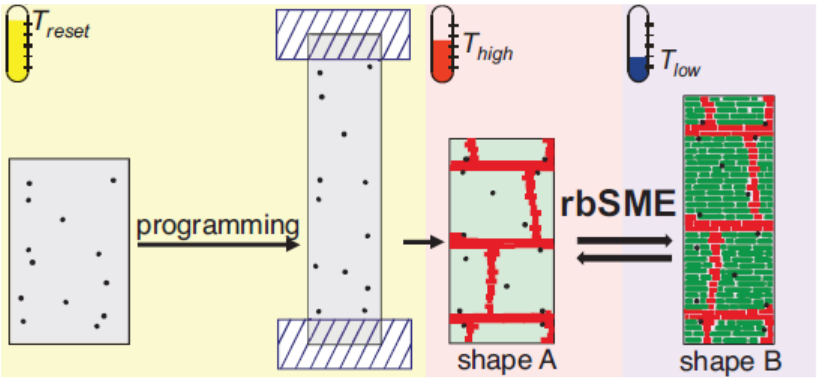

Figure 2.5. Illustration of RSME achieved by polyesterurethane (PEU) network with PPD and PCL segments.[64]

Thermoplastic RSMPs have rarely been reported so far. Recently, Lu et al.[71] found that a commercial ionomer, semi-crystalline poly(ethylene-co-methacrylic acid), could exhibit tunable reversible actuation. Shortly after, Biswas et al.[72] reported a thermoplastic polyurethane that exhibited reversible shape memory performance. In the well-designed PU, soft segments acted as actuator domains, which expanded with cooling and collapsed with heating. The hard segments acted as a skeleton and facilitated crystallization of the soft segments. Thermoplastic polymers have clear advantages in regards to ease of processing, in which the permanent shape of RSMPs can be easily reformed.

Despite the different material designs of RSMPs, CIE and MIC effects are the only working mechanism up to now. It should be noted that since multi-level reversible transitions are required for both one-way multi-SME and RSME, RSMP can also exhibit one-way multi-SME. Bai et al.[73] grafted PCL onto polydopamine and showed that the resulting polymer network could exhibit both one-way triple-

SME and RSME under appropriate conditions, which has an advantage of high modulus and high recovery strain.

RSMP requires only a single programming step to realize reversible actuation. It can be anticipated that RSMPs will have more applications, especially in biomedicine, soft actuator,[74] bionic areas, and so on.

§ 2.5 Polyolefin materials applied in shape memory polymer

As the leader in the global polymer production and consumption, polyolefins have considerable potential as SMP materials due to their high crystallizability and versatile chain structures. The “memory effect” of polyethylene had been realized,[75] leading to heat-shrinkable products in the packaging, cable, and electrotechnical industries.[31, 76] Numerous efforts have been made to study the heat-shrinkability of polyolefin materials, such as LDPE,[31] HDPE,[77] polyolefin blend with chlorosulphonated polyethylene,[78] and LDPE blend with PU elastomer.[79] Since then, the SME of polyolefins based on their semicrystalline nature has been explored. A variety of polyolefin-based SMPs with melting temperatures between 20 to 100 °C were synthesized, such as, crosslinked short-chain branched polyethylene,[32] trans-polyisoprene,[80] polycyclooctene,[81] and poly(1,4-butadiene).[82] Compared to other semicrystalline SMPs such as polyethers and polyesters, polyolefin-based SMPs formed a complete microphase separation structure, due to their nonpolar nature and absent H-bonds in the polyolefin networks.[80] Polyolefin-based SMPs are also the ideal

model compounds for studying SME theoretically.[83] Nowadays, the development of novel high-performance thermoplastic polyolefin elastomers has opened a new door to the fabrication of various SMPs.[84-86] Hoeher et al.[87] used an ethylene-co-1-octene blend with LDPE and HDPE to fabricate a multi-SMP. Zhang et al.[88, 89] used commercial olefin block copolymer (OBC) as the supporting polymer to fabricate phase change materials, which could also exhibit SME.

Polyolefin-based RSMPs have also been reported over the recent years. Kolesov and Dolynchuk et al.[90, 91] theoretically studied RSME of crosslinking linear and short-chain branched polyethylene. Hedden et al.[92] reported an enhanced RSME of crosslinked polyethylene by adding carbon black nanoparticles.

Polyolefins have excellent chemical resistance, outstanding weatherability, low density, low costs, and easily obtained monomers. It is very important to study SME of polyolefin-based materials, and it is desirable to develop novel polyolefin-based SMPs.

§ 2.6 Summary

In this chapter, the concept of shape memory polymer (SMP) is introduced from the perspectives of definition, history, classification, and some applications. Among them, the novel reversible shape memory polymer (RSMP) is focused due to its superior behavior that can realize shape changing between two temporary shapes when exposed to an external trigger (i.e. heat), without a new

programming step. There are mainly three types of RSMPs, namely, LCE, polymer laminates, and semicrystalline polymers, which have attracted many attentions of researchers, because of high potential applications in biomedicine, soft actuator, and bionic areas. Despite the variety of semicrystalline RSMPs, the CIE and MIC effect is confirmed as the only mechanism of RSME for the current semicrystalline RSMP. As the world's leader in polymer production and consumption, commodity polyolefin materials serve as good candidates for SMP applications for low costs and for versatility. Polyolefin-based SMPs have been emerged in the recent years, however, the area is still largely untouched. The development of polyolefin SMPs and RSMPs is a promising area worth of great research efforts.

§ 2.7 References

(1) Xie, T., Recent advances in polymer shape memory. *Polymer* **2011**, 52, (22), 4985-5000.

(2) Lendlein, A.; Kelch, S., Shape-Memory Polymers. *Angew. Chem., Int. Ed.* **2002**, 41, (12), 2034-2057.

(3) Behl, M.; Zotzmann, J.; Lendlein, A., Shape-Memory Polymers and Shape-Changing Polymers. In *Shape-Memory Polymers*, Lendlein, A., Ed Springer Berlin Heidelberg: Berlin, Heidelberg, **2010**, 1-40.

(4) Liu, C.; Qin, H.; Mather, P. T., Review of progress in shape-memory polymers. *J. Mater. Chem.* **2007**, 17, (16), 1543-1558.

(5) Mather, P. T.; Luo, X.; Rousseau, I. A., Shape Memory Polymer Research. In *Annual Review of Materials Research*, **2009**, 39, 445-471.

(6) Hu, J.; Zhu, Y.; Huang, H.; Lu, J., Recent advances in shape‐memory polymers: Structure, mechanism, functionality, modeling and applications. *Prog. Polym. Sci.* **2012**, 37, (12), 1720-1763.

(7) Meng, H.; Mohamadian, H.; Stubblefield, M.; Jerro, D.; Ibekwe, S.; Pang, S.; Li, G., Various shape memory effects of stimuli-responsive shape memory polymers. *Smart Mater. Struct.* **2013**, 22, (9), 93001.

(8) Vernon, L. B.; Vernon, H. M. Process Of Manufacturing Articles Of Thermoplastic Synthetic Resins. US2234993A, **1941**.

(9) Rainer, W. C.; Redding, E. M.; Hitov, J. J.; Sloan, A. W.; Stewart, W. D. Polyethylene product and process. US3144398A, **1964**.

(10) World's First Shape Memory Polymer. *CEER* **1984**, 16, (5), 34.

(11) Behl, M.; Razzaq, M. Y.; Lendlein, A., Multifunctional Shape-Memory Polymers. *Adv. Mater.* **2010**, 22, (31), 3388-3410.

(12) Wu, X.; Huang, W.; Zhao, Y.; Ding, Z.; Tang, C.; Zhang, J., Mechanisms of the Shape Memory Effect in Polymeric Materials. *Polymers* **2013**, 5, (4), 1169-1202.

(13) Meng, H.; Li, G., A review of stimuli-responsive shape memory polymer composites. *Polymer* **2013**, 54, (9), 2199-2221.

(14) Liu, Y.; Du, H.; Liu, L.; Leng, J., Shape memory polymers and their composites in aerospace applications: a review. *Smart Mater. Struct.* **2014**, 23, (2), 23001.

(15) Berg, G. J.; Mcbride, M. K.; Wang, C.; Bowman, C. N., New directions in the chemistry of shape memory polymers. *Polymer* **2014**, 55, (23), 5849-5872.

(16) Cavicchi, K. A., Shape Memory Polymers from Blends of Elastomers and Small Molecule Additives. *Macromol. Symp.* **2015**, 358, (1), 194-201.

(17) Zhao, Q.; Qi, H. J.; Xie, T., Recent progress in shape memory polymer: New behavior, enabling materials, and mechanistic understanding. *Prog. Polym. Sci.* **2015**, 49-50, 79-120.

(18) Hager, M. D.; Bode, S.; Weber, C.; Schubert, U. S., Shape memory polymers: Past, present and future developments. *Prog. Polym. Sci.* **2015**, 49-50, 3-33.

(19) Hasan, S. M.; Nash, L. D.; Maitland, D. J., Porous shape memory polymers: Design and applications. *J. Polym. Sci., Part B: Polym. Phys.* **2016**, 54, (14), 1300-1318.

(20) Xie, T.; Rousseau, I. A., Facile tailoring of thermal transition temperatures of epoxy shape memory polymers. *Polymer* **2009**, 50, (8), 1852-1856.

(21) Lendlein, A.; Jiang, H. Y.; Junger, O.; Langer, R., Light-induced shape-memory polymers. *Nature* **2005**, 434, (7035), 879-882.

(22) Fei, G.; Li, G.; Wu, L.; Xia, H., A spatially and temporally controlled shape memory process for electrically conductive polymer – carbon nanotube composites. *Soft Matter* **2012**, 8, (19), 5123-5126.

(23) Mohr, R.; Kratz, K.; Weigel, T.; Lucka-Gabor, M.; Moneke, M.; Lendlein, A., Initiation of shape-memory effect by inductive heating of magnetic nanoparticles in thermoplastic polymers. *Proc. Natl. Acad. Sci. U. S. A.* **2006**, 103, (10), 3540.

(24) Lendlein, A.; Schmidt, A. M.; Schroeter, M.; Langer, R., Shape-memory polymer networks from oligo(ϵ-caprolactone)dimethacrylates. *J. Polym. Sci., Part A: Polym. Chem.* **2005**, 43, (7), 1369-1381.

(25) Rousseau, I. A.; Xie, T., Shape memory epoxy: Composition, structure, properties and shape memory performances. *J. Mater. Chem.* **2010**, 20, (17), 3431-3441.

(26) Shi, X.; Wang, X.; Fu, C.; Ran, X., Dual-shape memory effect in radiation crosslinked thermoplastic blends: fabrication, optimization and mechanisms. *RSC Adv.* **2015**, 5, (76), 61601-61611.

(27) Kashif, M.; Chang, Y., Triple-shape memory effects of modified semicrystalline ethylene – propylene – diene rubber/poly(ε -caprolactone) blends. *Eur. Polym. J.* **2015**, 70, 306-316.

(28) Xie, T., Tunable polymer multi-shape memory effect. *Nature* **2010**, 464, (7286), 267-270.

(29) Collins, D. A.; Yakacki, C. M.; Lightbody, D.; Patel, R. R.; Frick, C. P., Shape-memory behavior of high-strength amorphous thermoplastic poly(para-phenylene). *J. Appl. Polym. Sci.* **2015**, n/a-n/a.

(30) Zhou, J.; Turner, S. A.; Brosnan, S. M.; Li, Q.; Carrillo, J. Y.; Nykypanchuk, D.; Gang, O.; Ashby, V. S.; Dobrynin, A. V.; Sheiko, S. S., Shapeshifting: Reversible Shape Memory in Semicrystalline Elastomers. *Macromolecules* **2014**, 47, (5), 1768-1776.

(31) Morshedian, J.; Khonakdar, H. A.; Mehrabzadeh, M.; Eslami, H., Preparation and properties of heat-shrinkable cross-linked low-density polyethylene. *Adv. Polym. Technol.* **2003**, 22, (2), 112-119.

(32) Kolesov, I. S.; Kratz, K.; Lendlein, A.; Radusch, H., Kinetics and dynamics of thermally-induced shape-memory behavior of crosslinked short-chain branched polyethylenes. *Polymer* **2009**, 50, (23), 5490-5498.

(33) Luo, X.; Zhang, X.; Wang, M.; Ma, D.; Xu, M.; Li, F., Thermally stimulated shape-memory behavior of ethylene oxide-ethylene terephthalate segmented copolymer. *J. Appl. Polym. Sci.* **1997**, 64, (12), 2433-2440.

(34) Niu, Y.; Zhang, P.; Zhang, J.; Xiao, L.; Yang, K.; Wang, Y., Poly(p-dioxanone) – poly(ethylene glycol) network: synthesis, characterization, and its shape memory effect. *Polym. Chem.* **2012**, 3, (9), 2508-2516.

(35) Ping, P.; Wang, W.; Chen, X.; Jing, X., Poly(ε -caprolactone) Polyurethane and Its Shape-Memory Property. *Biomacromolecules* **2005**, 6, (2), 587-592.

(36) Peponi, L.; Navarro-Baena, I.; Sonseca, A.; Gimenez, E.; Marcos-Fernandez, A.; Kenny, J. M., Synthesis and characterization of PCL – PLLA polyurethane with shape memory behavior. *Eur. Polym. J.* **2013**, 49, (4), 893-903.

(37) Alteheld, A.; Feng, Y.; Kelch, S.; Lendlein, A., Biodegradable, Amorphous Copolyester-Urethane Networks Having Shape-Memory Properties. *Angew. Chem., Int. Ed.* **2005**, 44, (8), 1188-1192.

(38) Jeong, H. M.; Lee, S. Y.; Kim, B. K., Shape memory polyurethane containing amorphous reversible phase. *J. Mater. Sci.* **2000**, 35, (7), 1579-1583.

(39) Safranski, D. L.; Gall, K., Effect of chemical structure and crosslinking density on the thermo-mechanical properties and toughness of (meth)acrylate shape memory polymer networks. *Polymer* **2008**, 49, (20), 4446-4455.

(40) Yakacki, C. M.; Shandas, R.; Safranski, D.; Ortega, A. M.; Sassaman, K.; Gall, K., Strong, Tailored, Biocompatible Shape-Memory Polymer Networks. *Adv. Funct. Mater.* **2008**, 18, (16), 2428-2435.

(41) Yamashiro, M.; Inoue, K.; Iji, M., Recyclable Shape-memory and Mechanical Strength of Poly(lactic acid) Compounds Cross-linked by Thermo-reversible Diels-Alder Reaction. *Polym. J.* **2008**, 40, 657.

(42) Defize, T.; Riva, R.; Jérôme, C.; Alexandre, M., Multifunctional Poly(ϵ-caprolactone)-Forming Networks by Diels‐Alder Cycloaddition: Effect of the Adduct on the Shape-Memory Properties. *Macromol. Chem. Phys.* **2012**, 213, (2), 187-197.

(43) Chen, S.; Hu, J.; Yuen, C.; Chan, L., Supramolecular polyurethane networks containing pyridine moieties for shape memory materials. *Mater. Lett.* **2009**, 63, (17), 1462-1464.

(44) Chen, S.; Hu, J.; Zhuo, H.; Yuen, C.; Chan, L., Study on the thermal-induced shape memory effect of pyridine containing supramolecular polyurethane. *Polymer* **2010**, 51, (1), 240-248.

(45) Luo, Y.; Guo, Y.; Gao, X.; Li, B.; Xie, T., A General Approach Towards Thermoplastic Multishape-Memory Polymers via Sequence Structure Design. *Adv. Mater.* **2013**, 25, (5), 743-748.

(46) Li, J.; Liu, T.; Xia, S.; Pan, Y.; Zheng, Z.; Ding, X.; Peng, Y., A versatile approach to achieve quintuple-shape memory effect by semi-interpenetrating polymer networks containing broadened glass transition and crystalline segments. *J. Mater. Chem.* **2011**, 21, (33), 12213-12217.

(47) Li, J.; Xie, T., Significant Impact of Thermo-Mechanical Conditions on Polymer Triple-Shape Memory Effect. *Macromolecules* **2011**, 44, (1), 175-180.

(48) Xie, T.; Xiao, X.; Cheng, Y., Revealing Triple-Shape Memory Effect by Polymer Bilayers. *Macromol. Rapid Commun.* **2009**, 30, (21), 1823-1827.

(49) Lendlein, A.; Langer, R., Biodegradable, Elastic Shape-Memory Polymers for Potential Biomedical Applications. *Science* **2002**, 296, (5573), 1673.

(50) Erndt-Marino, J. D.; Munoz-Pinto, D. J.; Samavedi, S.; Jimenez-Vergara, A. C.; Diaz-Rodriguez, P.; Woodard, L.; Zhang, D.; Grunlan, M. A.; Hahn, M. S., Evaluation of the Osteoinductive Capacity of Polydopamine-Coated Poly(*ε*-caprolactone) Diacrylate Shape Memory Foams. *ACS Biomater. Sci. Eng.* **2015**, 1, (12), 1220-1230.

(51) Zhou, J.; Sheiko, S. S., Reversible shape-shifting in polymeric materials. *J. Polym. Sci., Part B: Polym. Phys.* **2016**, 54, (14), 1365-1380.

(52) Meng, H.; Li, G., Reversible switching transitions of stimuli-responsive shape changing polymers. *J. Mater. Chem. A* **2013**, 1, (27), 7838-7865.

(53) Xie, P.; Zhang, R., Liquid crystal elastomers, networks and gels: advanced smart materials. *J. Mater. Chem.* **2005**, 15, (26), 2529-2550.

(54) Finkelmann, H.; Kock, H.; Rehage, G., Investigations on liquid crystalline polysiloxanes 3. Liquid crystalline elastomers — a new type of liquid crystalline material. *Makromol. Chem., Rapid Commun.* **1981**, 2, (4), 317-322.

(55) Qin, H.; Mather, P. T., Combined One-Way and Two-Way Shape Memory in a Glass-Forming Nematic Network. *Macromolecules* **2009**, 42, (1), 273-280.

(56) Chen, S.; Hu, J.; Zhuo, H.; Zhu, Y., Two-way shape memory effect in polymer laminates. *Mater. Lett.* **2008**, 62, (25), 4088-4090.

(57) Chen, S.; Hu, J.; Zhuo, H., Properties and mechanism of two-way shape memory polyurethane composites. *Compos. Sci. Technol.* **2010**, 70, (10), 1437-1443.

(58) Tamagawa, H., Thermo-responsive two-way shape changeable polymeric laminate. *Mater. Lett.* **2010**, 64, (6), 749-751.

(59) Westbrook, K. K.; Mather, P. T.; Parakh, V.; Dunn, M. L.; Ge, Q.; Lee, B. M.; Qi, H. J., Two-way reversible shape memory effects in a free-standing polymer composite. *Smart Mater. Struct.* **2011**, 20, (6), 65010.

(60) Chung, T.; Romo-Uribe, A.; Mather, P. T., Two-Way Reversible Shape Memory in a Semicrystalline Network. *Macromolecules* **2008**, 41, (1), 184-192.

(61) Zotzmann, J.; Behl, M.; Hofmann, D.; Lendlein, A., Reversible Triple-Shape Effect of Polymer Networks Containing Polypentadecalactone- and Poly(*ε*-caprolactone)-Segments. *Adv. Mater.* **2010**, 22, (31), 3424-3429.

(62) Li, J.; Rodgers, W. R.; Xie, T., Semi-crystalline two-way shape memory elastomer. *Polymer* **2011**, 52, (23), 5320-5325.

(63) Behl, M.; Kratz, K.; Noechel, U.; Sauter, T.; Lendlein, A., Temperature-memory polymer actuators. *Proc. Natl. Acad. Sci. U. S. A.* **2013**, 110, (31), 12555-12559.

(64) Behl, M.; Kratz, K.; Zotzmann, J.; Nöchel, U.; Lendlein, A., Reversible Bidirectional Shape-Memory Polymers. *Adv. Mater.* **2013**, 25, (32), 4466-4469.

(65) Saatchi, M.; Behl, M.; Nöchel, U.; Lendlein, A., Copolymer Networks From Oligo(ε -caprolactone) and n-Butyl Acrylate Enable a Reversible Bidirectional Shape-Memory Effect at Human Body Temperature. *Macromol. Rapid Commun.* **2015**, 36, (10), 880-884.

(66) Yang, G.; Liu, X.; Tok, A. I. Y.; Lipik, V., Body temperature-responsive two-way and moisture-responsive one-way shape memory behaviors of poly(ethylene glycol)-based networks. *Polym. Chem.* **2017**, 8, (25), 3833-3840.

(67) Wu, Y.; Hu, J.; Han, J.; Zhu, Y.; Huang, H.; Li, J.; Tang, B., Two-way shape memory polymer with "switch–spring" composition by interpenetrating polymer network. *J. Mater. Chem. A* **2014**, 2, (44), 18816-18822.

(68) Meng, Y.; Jiang, J.; Anthamatten, M., Shape Actuation via Internal Stress-Induced Crystallization of Dual-Cure Networks. *ACS Macro Lett.* **2015**, 4, (1), 115-118.

(69) Fan, L. F.; Rong, M. Z.; Zhang, M. Q.; Chen, X. D., A Facile Approach Toward Scalable Fabrication of Reversible Shape-Memory Polymers with Bonded Elastomer Microphases as Internal Stress Provider. *Macromol. Rapid Commun.* **2017**, 38, (16), 1700124.

(70) Jin, B.; Song, H.; Jiang, R.; Song, J.; Zhao, Q.; Xie, T., Programming a crystalline shape memory polymer network with thermo- and photo-reversible bonds toward a single-component soft robot. *Sci. Adv.* **2018**, 4, (1), o3865.

(71) Lu, L.; Li, G., One-Way Multishape-Memory Effect and Tunable Two-Way Shape Memory Effect of Ionomer Poly(ethylene-co-methacrylic acid). *ACS Appl. Mater. Interfaces* **2016**, 8, (23), 14812-14823.

(72) Biswas, A.; Aswal, V. K.; Sastry, P. U.; Rana, D.; Maiti, P., Reversible Bidirectional Shape Memory Effect in Polyurethanes through Molecular Flipping. *Macromolecules* **2016**, 49, (13), 4889-4897.

(73) Bai, Y.; Zhang, X.; Wang, Q.; Wang, T., A tough shape memory polymer with triple-shape memory and two-way shape memory properties. *J. Mater. Chem. A* **2014**, 2, (13), 4771.

(74) Camacho-Lopez, M.; Finkelmann, H.; Palffy-Muhoray, P.; Shelley, M., Fast liquid-crystal elastomer swims into the dark. *Nat. Mater.* **2004**, 3, (5), 307-310.

(75) Charlesby, A., CHAPTER 13 - POLYETHYLENE. In *Atomic Radiation and Polymers*, CHARLESBY, A., Ed Pergamon: **1960**, 1, 198-257.

(76) Mishra, J. K.; Das, C. K., Heat Shrinkable Polymer Blends Based on Grafted Low Density Polyethylene and Polyurethane Elastomer — Part II. *J. Elastomers Plast.* **2001**, 33, (2), 137-153.

(77) Khonakdar, H. A.; Morshedian, J.; Mehrabzadeh, M.; Wagenknecht, U.; Jafari, S. H., Thermal and shrinkage behaviour of stretched peroxide-crosslinked high-density polyethylene. *Eur. Polym. J.* **2003**, 39, (8), 1729-1734.

(78) Patra, P. K.; Das, C. K., Blends of Polyolefins and Chlorosulphonated Polyethylene (CSM) with Special Reference to their Shrinkability and Flame Retardancy. *Int. J. Polym. Mater. Polym. Biomater.* **1997**, 35, (1-4), 103-118.

(79) Mishra, J. K.; Raychowdhury, S.; Das, C. K., Heat-shrinkable polymer blends based on grafted low-density polyethylene and polyurethane elastomer. Part I. *Polym. Int.* **2000**, 49, (12), 1615-1623.

(80) Sun, X.; Ni, X., Block copolymer of trans-polyisoprene and urethane segment: Crystallization behavior and morphology. *J. Appl. Polym. Sci.* **2004**, 94, (6), 2286-2294.

(81) Liu, C.; Chun, S. B.; Mather, P. T.; Zheng, L.; Haley, E. H.; Coughlin, E. B., Chemically Cross-Linked Polycyclooctene: Synthesis, Characterization, and Shape Memory Behavior. *Macromolecules* **2002**, 35, (27), 9868-9874.

(82) Sakurai, K.; Shirakawa, Y.; Kashiwagi, T.; Takahashi, T., Crystal transformation of styrene-butadiene block copolymer. *Polymer* **1994**, 35, (19), 4238-4239.

(83) Khonakdar, H. A.; Jafari, S. H.; Rasouli, S.; Morshedian, J.; Abedini, H., Investigation and Modeling of Temperature Dependence Recovery Behavior of Shape-Memory Crosslinked Polyethylene. *Macromol. Theory Simul.* **2007**, 16, (1), 43-52.

(84) Arriola, D. J., Catalytic Production of Olefin Block Copolymers via Chain Shuttling Polymerization. *Science* **2006**, 312, (5774), 714-719.

(85) Liu, W.; Wang, W.; Fan, H.; Yu, L.; Li, B.; Zhu, S., Structure analysis of ethylene/1-octene copolymers synthesized from living coordination polymerization. *Eur. Polym. J.* **2014**, 54, 160-171.

(86) Liu, W.; Zhang, X.; Bu, Z.; Wang, W.; Fan, H.; Li, B.; Zhu, S., Elastomeric properties of ethylene/1-octene random and block copolymers synthesized from living coordination polymerization. *Polymer* **2015**, 72, 118-124.

(87) Hoeher, R.; Raidt, T.; Krumm, C.; Meuris, M.; Katzenberg, F.; Tiller, J. C., Tunable Multiple-Shape Memory Polyethylene Blends. *Macromol. Chem. Phys.* **2013**, 214, (23), 2725-2732.

(88) Zhang, Q.; Feng, J., Difunctional olefin block copolymer/paraffin form-stable phase change materials with simultaneous shape memory property. *Sol. Energy Mater. Sol. Cells* **2013**, 117, 259-266.

(89) Zhang, Q.; Cui, K.; Feng, J.; Fan, J.; Li, L.; Wu, L.; Huang, Q., Investigation on the recovery performance of olefin block copolymer/hexadecane form stable phase change materials with shape memory properties. *Sol. Energy Mater. Sol. Cells* **2015**, 132, 632-639.

(90) Dolynchuk, O.; Kolesov, I.; Androsch, R.; Radusch, H., Kinetics and dynamics of two-way shape-memory behavior of crosslinked linear high-density and short-chain branched polyethylenes with regard to crystal orientation. *Polymer* **2015**, 79, 146-158.

(91) Kolesov, I.; Dolynchuk, O.; Jehnichen, D.; Reuter, U.; Stamm, M.; Radusch, H., Changes of Crystal Structure and Morphology during Two-Way Shape-Memory Cycles in Cross-Linked Linear and Short-Chain Branched Polyethylenes. *Macromolecules* **2015**, 48, (13), 4438-4450.

(92) Ma, L.; Zhao, J.; Wang, X.; Chen, M.; Liang, Y.; Wang, Z.; Yu, Z.; Hedden, R. C., Effects of carbon black nanoparticles on two-way reversible shape memory in crosslinked polyethylene. *Polymer* **2015**, 56, 490-497.

3 POLYOLEFIN THERMOPLASTICS FOR MULTIPLE SHAPE AND REVERSIBLE SHAPE MEMORY

In this chapter, the multiple and reversible shape memory effect of a polyolefin elastomer material, ethylene/1-octene diblock copolymer, is demonstrated and represented. This chapter is based on the peer-reviewed published journal paper as follows: “Gao, Y.; Liu, W.; Zhu, S., Polyolefin Thermoplastics for Multiple Shape and Reversible Shape Memory, *ACS Applied Materials & Interfaces*, **2017**, *9(5)*, 4882-4889. (DOI: 10.1021/acsami.6b14728) Reprinted with permission from *ACS Applied Materials & Interfaces*, **2017**, *9(5)*, 4882-4889. Copyright 2015 American Chemical Society.

Author contributions

Yuan Gao conducted the experiments and wrote the first draft of the manuscript under the guidance of Dr. Shiping Zhu and Dr. Weifeng Liu. Dr. Weifeng Liu provided the synthesize polymer and the first revision of the manuscript. The final revision was provided by Dr. Zhu.

§ 3.1 Abstract

This work reports the first pure hydrocarbon thermoplastic polyolefin material with reversible shape memory effect under stress-free or very small external loading condition. A thermoplastic ethylene/1-octene diblock copolymer with designed chain microstructure was synthesized. The polyolefin material performed not only the conventional one-way multishape memory effects, but also a two-way reversible shape memory effect (RSME). The elongation and contraction induced by oriented crystallization with heating was confirmed as the mechanism of RSME without chemical crosslinking. This work demonstrated that the thermoplastic reversible shape memory could be achieved through careful design of chain microstructure, based on sole hydrocarbon materials such as ethylene-1-octene copolymer.

§ 3.2 Introduction

Shape memory polymer (SMP) is a representative type of smart materials with a broad range of potential applications such as surface coatings, textiles, biomedical devices, aerospace facilities, etc.[1-5] SMPs can store temporary shapes and recover to their original permanent shapes under stimulation of external triggers. Many types of triggers have been applied to SMP systems such as temperature,[6] light,[7] electric and magnetic field,[8,9] and redox.[10] Over the decades, a large variety of SMPs have been synthesized and reported.[3] However, design and preparation of multiple and reversible SMPs are still challenging and require much further research effort.

Conventional one-way SMPs with dual-shape memory effect can only be recovered from one temporary shape to their original permanent shape in one way.[2] The polymers cannot be shifted back and forth between temporary and permanent shapes without additional programming. In the past decade, the multishape memory effect has also attracted much attention, as it can memorize more than one temporary shapes, such as triple-shape or quadruple-shape memory effects.[11-14] To achieve the multishape memory effect, a carefully designed programming with multiple deformations must be implemented. However, regardless of the great effort, the reported multiple SMPs are still in one-way shifting only, as they cannot go back to temporary shapes, nor can they

shift between temporary shapes without a new programming process after one shape memory cycle.[2]

Recently, great progress has been achieved in developing reversible shape memory polymers (RSMP).[15] There have been several types of materials designed for RSMP applications, such as laminates,[16] liquid crystalline elastomers (LCE),[17] and semicrystalline polymers.[18] In the material design, LCE was synthesized as an elastic polymer with liquid crystalline units on the main or side chains. The shift between anisotropic and isotropic phases of the liquid crystals could lead to reversible contraction and elongation upon heating and cooling, exhibiting reversible shape memory effect (RSME).[17] However, the synthesis of LCE is challenging.

In the recent years, RSMPs based on simple semicrystalline polymers have attracted great attention. Mather et al.[18] has demonstrated a cross-linked poly(cyclooctene) (PCO) film exhibiting reversible shape memory performance under a tensile load. The reversibility in this polymer system stems from the mechanism of oriented crystallization and further crystallization induced elongation upon cooling.

This mechanism has been actively explored in designing RSMP from semicrystalline polymers.[19-30] Lendlein et al. ingeniously constructed several cross-linked multiphase copolyester-urethane networks[19] and PEVA networks[28] with distinguished or continuous broad melting temperatures so that the oriented

crystallization can be induced by the “skeleton” crystals with high melting temperature, resulting in a free-standing RSME upon cooling and heating without constantly applied tensile loading. Sheiko et al. studied the effect of partial melting of crystals on reversible shape memory performance of cross-linked poly(octylene adipate),[29,30] and applied switchable micropatterned surface topographies,[31] and dynamic optical gratings.[32] Anthamatten et al. reported a two-step cross-linking procedure to introduce an internal stress into polymer film to induce crystallization for free-standing RSMP.[33]

Most published works focused on thermoset RSMPs and considered the chemical cross-linking a must for RSMPs.[19,29] Thermoplastic two-way RSMPs have been rarely reported so far. Very recently, Li et al.[34] found that a commercial ionomer, semicrystalline poly(ethylene-co-methacrylic acid), exhibited tunable reversible actuation. Shortly after, Maiti et al.[35] reported a thermoplastic polyurethane that exhibited reversible shape memory performance. In the well-designed PU, soft segments acted as actuator domains, which expanded in cooling and collapsed in heating. The hard segments acted as skeleton and assisted crystallization of the soft segments. Thermoplastic polymers have clear advantages for easy processing in which the permanent shape of RSMPs can be easily reformed.

Polyolefins, the world’s largest polymer in production and consumption, have also been investigated for shape memory polymer applications.[11,36-38] Polyolefin materials have very good chemical resistance, excellent weatherability, low

density, low cost, cheap and easily obtained monomers.[39] Development of high-value added applications for polyolefins definitely represents one of the most attractive pursuits for polymer scientists. In fact, the oriented crystallization effect of polyolefins has been well studied as “necking”, which is exploited in the design of cross-linked RSMPs.[40] For example, Kolesov et al. reported reversible shape memory behavior of cross-linked HDPE/poly(*ε*-caprolactone) blends under stress.[41] RSMEs of crosslinked HDPE and poly(ethylene/1-octene) copolymer blends were also studied by experimental and theoretical methods.[40,42] Hedden et al. reported that adding carbon black nanoparticles as physical cross-linkers could affect the reversible shape memory behavior of cross-linked polyethylene such as actuation ratio and switching temperature.[43]

To the best of our knowledge, polyolefin-based SMPs studied so far are thermosets and their permanent shapes could not be reformed.[11,40] Polyolefin materials account for half of the world’s total polymer products. It is important to develop SMPs from this class of polymers. It is also easy to remold thermoplastic polyolefins into new permanent shapes. The recent progress in the synthesis of high-performance polyolefin thermoplastic elastomers has provided a great opportunity for designing RSMPs. Our previous work on the synthesis of diblock ethylene/1-octene copolymers showed that the chain microstructure of polyolefins can be precisely designed, resulting in a tunable distribution of crystal sizes and a continuous wide range of melting temperature.[44] On the basis of our understanding of the two-way reversible shape memory effect, we hypothesized

that polyolefin elastomers having a well-designed hard and soft segment distribution could be good candidates for developing RSMPs. Harder segments are expected to form larger crystals, acting as higher temperature skeletons for holding softer segments crystallizable at lower temperature. In this work, we report the first pure carbon-hydrogen thermoplastic polyolefin elastomer as a two-way reversible shape memory material.

§ 3.3 Experimental Section

3.3.1 Materials and Preparation

Synthesis of ethylene/1-octene diblock copolymers was reported in the previous work.[44] Provided here is a brief description for readers' convenience. Polymerization-grade ethylene and 1-octene were used as monomer and comonomer. Bis[N-(3-methylsalicylidene)-2,3,4,5,6-pentafluoroanilinato] titanium(IV) dichloride was used as catalyst and dried methylaluminoxane (MAO) used as cocatalyst. Anhydrous toluene was used as solvent. Ethylene/1-octene copolymerization was carried out in a semibatch autoclave reactor. The reactor temperature was controlled at 25 °C during the polymerization. Purified ethylene monomer was first filled into the reactor. Toluene solvent, 1-octene, cocatalyst (MAO in toluene solution) and catalyst solution were sequentially injected into the reactor under nitrogen protection. Ethylene was fed immediately after the catalyst injection. To obtain diblock copolymer, ethylene pressure in the reactor was initially maintained at atmosphere pressure for 5 min, followed by a sudden

increase to 20 bar in a stepwise fashion for 0.5 min. The comonomer feeding ratio was kept at about 0.90 in the first step and decreased to less than 0.30 in the second step. The experiment was stopped by shutting off ethylene gas and pouring the resulting mixture into acidified alcohol. The polymer sample was washed with excess alcohol and dried in vacuum at 50 °C for 8 h.

The resulting polyolefin samples were molded in hot press at 160 °C and 13.8 MPa to form flat films of 40 × 40 × 0.5 mm dimension. The characterization data for the diblock copolymers are presented in the Supporting Information.

3.3.2 Polymer characterization

Melting temperature T_m and crystallization temperature T_c were measured by DSC 2910 (TA Instruments). Samples between 5.0 and 7.0 mg were first heated to 160 °C and kept isothermally for 5 min to remove thermal history. Temperature was then cooled to −20 °C at a rate of 10 °C/min, maintained at −20 °C for 3 min, and finally raised to 160 °C at 10 °C/min. T_c was measured from the cooling curve and T_m was obtained from the second heating curve.

The temperature-dependent modulus test was carried out using DMA 2980 (TA Instruments) in a tensile mode. The sample film of 20 × 2 × 0.5 mm was first cooled to −70 °C, then heated to 60 °C at a rate of 3 °C/min. The storage modulus and loss modulus were measured with the frequency of 1 Hz and the amplitude of 0.3% strain.

The shape memory effects were measured by DMA 2980 (TA Instruments) in a tensile mode. The elastomers were first cut into 20 × 2 × 0.5 mm films. For one-way two-shape memory testing, the sample was first heated to 82 °C under 0.006 N loading for 4 min, setting the original strain ε_{f0}. It was stretched by a stress around 0.4 MPa, and then cooled from 82 to 5 °C at a rate of 10 °C/min. It was kept isothermal at 5 °C for 3 min under the stress to obtain the maximum elongated strain ε_m. The stress was then removed and the sample was maintained at 5 °C for 2 min to obtain the fixed strain ε_f. Finally the sample was heated back to 82 °C and obtained the recovery strain ε_r. The fixing ratio R_f and recovery ratio R_r were calculated as:

$$R_{\mathrm{f}} = \frac{\varepsilon_{\mathrm{f}} - \varepsilon_{\mathrm{f0}}}{\varepsilon_{\mathrm{m}} - \varepsilon_{\mathrm{f0}}} \text{ and } R_r = \frac{\varepsilon_{\mathrm{f}} - \varepsilon_{\mathrm{r}}}{\varepsilon_{\mathrm{f}} - \varepsilon_{\mathrm{f0}}}$$

In one-way triple-shape memory testing, the sample was first heated to 82 °C under 0.006 N loading for 4 min, setting the original strain ε_{f0}. It was stretched by a stress around 0.4 MPa and then cooled down to 53 °C at a rate of 10 °C/min. It was kept isothermal at 53 °C under the stress for 3 min to obtain the first maximum elongated strain ε_{m1}. The stress was then removed and the sample was maintained at 53 °C for 2 min to get the fixed strain ε_{f1}. The sample was further cooled down from 53 to 5 °C at a rate of 10 °C/min and kept isothermal at 5 °C under the stress for 3 min to obtain the second maximum elongated strain ε_{m2}. The stress was then removed and the sample was maintained at 5 °C for 2 min to get the fixed strain ε_{f2}. The sample was heated back to 53 °C at a rate of

5 °C/min and kept isothermal at 55 °C for 10 min to obtain the first recovery length ε_{r1}. Finally the sample was heated up to 82 °C to obtain the final recovery strain ε_{r0}. The fixing ratio R_f and recovery ratio R_r were calculated as:

$$R_{\mathrm{fi}} = \frac{\varepsilon_{\mathrm{fi}} - \varepsilon_{\mathrm{f(i-1)}}}{\varepsilon_{\mathrm{mi}} - \varepsilon_{\mathrm{f(i-1)}}} \text{ and } R_{ri} = \frac{\varepsilon_{\mathrm{fi}} - \varepsilon_{\mathrm{r(i-1)}}}{\varepsilon_{\mathrm{fi}} - \varepsilon_{\mathrm{f(i-1)}}}$$

For one-way quadruple- (multi-) shape memory testing, the experimental procedure and the fixing/recovery ratio calculation were similar to the above.

To measure the reversible shape memory effect, a typical procedure is as follows: The sample was heated to 82 °C for 4 min for the original strain ε_{f0}. It was stretched by a stress around 0.4 MPa. The temperature was then decreased from 82 to 5 °C at a rate of 10 °C/min and the sample was annealed under the stress at 5 °C for 3 min. In the stress-free testing, the stress was removed and the sample was maintained at 5 °C for 2 min. It was then heated to 60 °C and annealed for 3 min to obtain the reversible length ε_{rb}. After another cooling process to 5 °C, a stable length of ε_s was obtained. The cooling-heating cycles between 5 and 60 °C were repeated for 5 times. In the load testing, the stress was maintained constant during all cooling-heating cycles. The reversible ratio R_{rb} was calculated as:

$$R_{\mathrm{rb}} = \frac{\varepsilon_{\mathrm{s}} - \varepsilon_{\mathrm{rb}}}{\varepsilon_{\mathrm{s}} - \varepsilon_{\mathrm{f0}}}$$

X-ray diffraction (XRD) analysis was performed on a Bruker D8 DISCOVER with DAVINCI.DESIGN diffractometer using Co as the anode material. The sample was scanned from 12° to 35° with a scanning increment of 0.02°at 35 kV generator voltage and 45 mA current.

§ 3.4 Results and Discussion

For prove of the concept, we prepared the gradient ethylene/1-octene diblock copolymer samples. The results of structural characterization were provided in the Supporting Information. This type of ethylene/1-octene diblock copolymers possessed excellent thermoplastic elastomeric performance.[44] Sample1 having 42% hard segment content was selected in this work for the detailed study. Figure 3.1 shows the DSC cooling and second heating curves of Sample1. The heating curve clearly showed a broad melting temperature range. It probably started to melt as soon as the glass transition process completed at about −40 °C and it totally melted at about 95 °C. The maximum melting peak was about 78 °C. When the melt was cooled down, a sharp exothermic peak was first found at about 60.6 °C in the cooling curve, which is the major crystallization temperature. The short-ordered ethylene segments continued to crystallize as the temperature was further cooled down and a second small exothermic peak was found between 0 to 10 °C. The harder segments having longer crystalline ethylene sequence length crystallized at higher temperatures and formed relatively larger crystal domains, while the softer segments having shorter crystalline ethylene sequence length formed crystal domains of smaller sizes. The broad crystal size

distribution contributed to the wide melting temperature range. In the synthesis, 1-octene incorporation and hard/soft segment lengths are easily tunable by adjusting the monomer feeding policy. From this perspective, the chain microstructure of the diblock copolymer could be precisely designed, and it becomes practical to synthesize thermoplastic polyolefin elastomers with a desired range of melting temperatures. The temperature-dependent modulus from −70 °C to 60 °C measured by DMA gave the T_g of Sample1 about −51 °C (Figure S3.3).

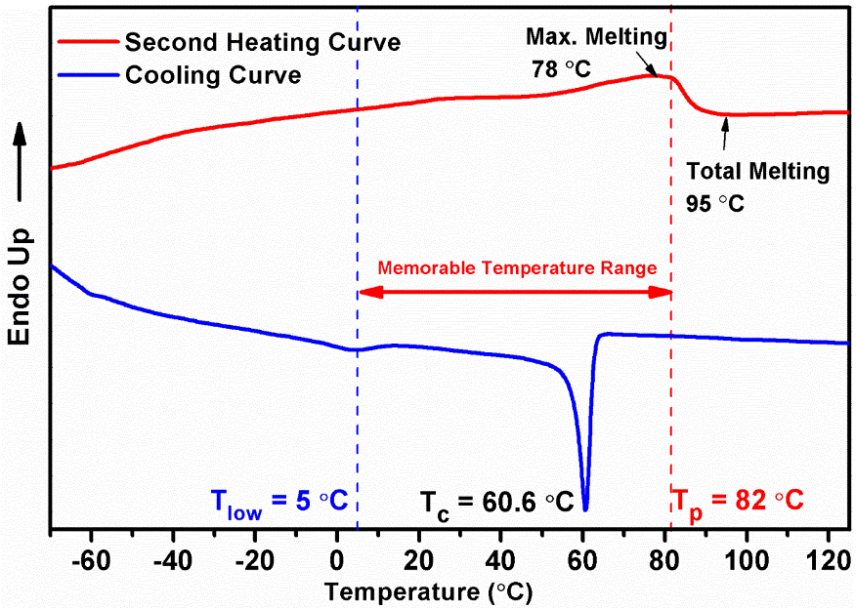

Figure 3.1. DSC cooling and heating curves of the ethylene/1-octene diblock copolymer Sample1.

3.4.1 One-Way Shape Memory Effect

One-way shape memory effect of the diblock copolymer was measured by DMA and the result is shown in Figure 3.2. The diblock copolymer in this study possessed a broad crystal size distribution and exhibited a broad range of melting temperature, which allowed the realization of multishape memory effects. On the basis of DSC data, 82, 55, and 35 °C were selected as the programming temperatures T_p, and 5 °C as the fixing temperature T_{low} (see Figure 3.1). As the total melting temperature was about 95 °C, 82 °C was a partial melting temperature. At this temperature, some large crystals were still not melted, allowing the sample to keep its permanent solid shape. The fixing ratio R_f was 79.6% and the recovery ratio R_r reached 95.9% (Figure 3.2a), indicating a good one-way dual-shape memory effect, especially for the recoverability.

The shape fixing ratio was affected by elasticity of the diblock copolymer at low temperature. In a thermoplastic polyolefin elastomer, both crystal domains and chain entanglements contribute to physical cross-linking networks, rendering a large dragging force inside the elongated elastomer matrix. We employed two more samples having different hard/soft segment contents for further illustration. In one-way dual-shape memory effect test (see Figure S3.4), it has been demonstrated that Sample2 having lower hard segment content (23%) exhibited a lower fixing ratio but a higher recovery ratio (R_f = 69.1%, R_r = 99.9%), whereas Sample3 having higher hard segment content (48%) exhibited a higher fixing

ratio and a lower recovery ratio (R_f = 82.5%, R_r = 76.6%). The result showed that the high hard segment content provide high fixability at low temperature due to the high crystallizability, while the high soft segment content provide high elasticity for high recoverability. As a result, varying chain microstructure through designing the length and ratio of hard and soft segments could tune the shape memory performance of diblock copolymers.

To demonstrate the triple shape memory effect, we selected 82 °C as the first programming temperature T_{p1} with the external load of 0.38 MPa, and 53 °C as the second programming temperature T_{p2} with the external load of 0.77 MPa, and 5 °C as the fixing temperature T_{low}. The resulted fixing ratios for the two temporary shapes R_{f1} and R_{f2} were 41.3% and 67.0%, while the recovery ratios R_{r2} and R_{r1} were 86.0% and 93.2%, respectively, as shown in Figure 3.2b, c.

For better demonstration of the multishape memory effect, the copolymer film was programmed into three shapes, as shown in Figure 3.2d. The film edge was painted red for better observation. The film was in a flat permanent shape at 82 °C, then deformed to a temporary spiral shape (the first temporary shape), when cooled down to 53 °C. It was further deformed to a “ω” shape (the second temporary shape) when cooled down to 5 °C. The “ω” shape was stable at temperature below 5 °C. When heated up to 53 °C, the film recovered to the spiral shape automatically and in a short time. This spiral shape was very stable at temperature below 53 °C. It was finally recovered to its original flat shape when

it was further heated up to 82 °C. Triple-shape memory effect of the diblock copolymer was clearly demonstrated. From “ω” to spiral, it exhibited excellent shape memory performance, in which it could recover from a simple shape to a complex shape. This is not an easy task with thermoset SMPs.[45] Similarly, quadruple-shape memory effect with three temporary shapes was also demonstrated, with programming condition, shape fixity and recovery ratio shown in Figure 3.2c. Similar to dual-shape memory effect testing, the fixity for each temporary shape was significantly affected by elasticity of the amorphous phase, as well as amount and size of the crystal domains.

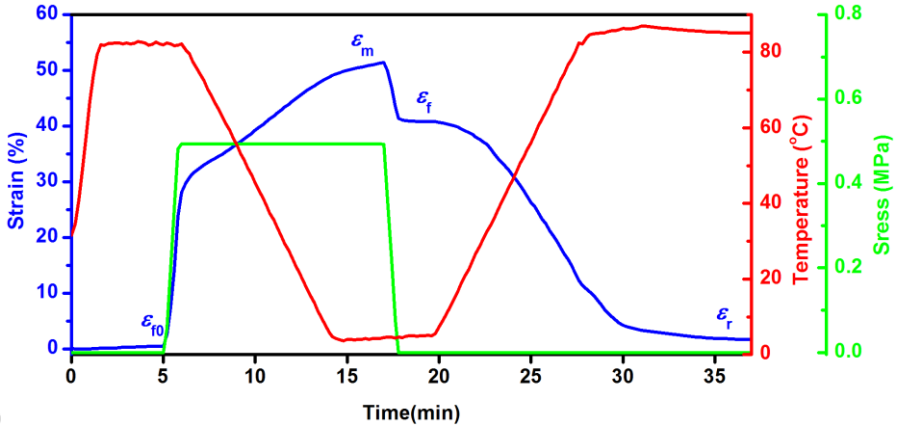

(a)

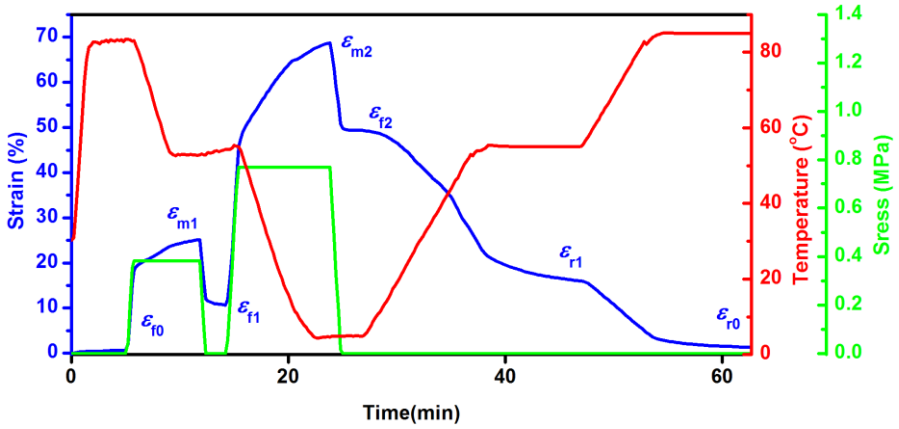
Strain (%)
Temperature (°C)
Sress (MPa)
Time(min)
ε_{m2}
ε_{f2}
ε_{m1}
ε_{r1}
ε_{f0}
ε_{f1}
ε_{r0}

(b)

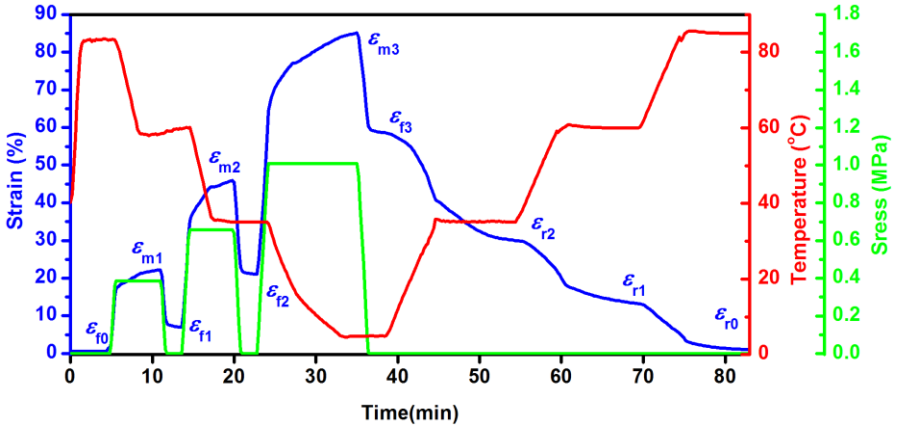
Strain (%)
Temperature (°C)
Sress (MPa)
Time(min)
ε_{m3}
ε_{f3}
ε_{m2}
ε_{r2}
ε_{m1}
ε_{f2}
ε_{r1}
ε_{f0}
ε_{f1}
ε_{r0}

(c)

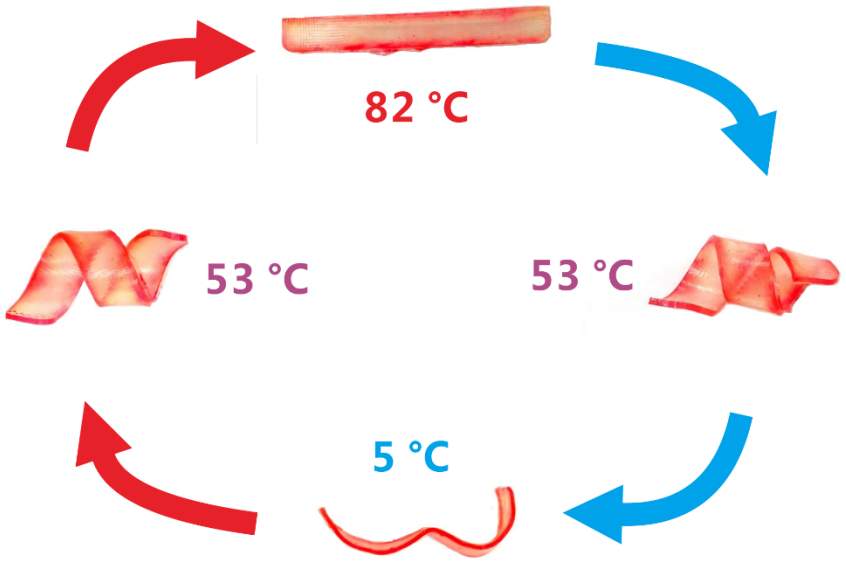

(d)

Figure 3.2. One-way shape memory effect of ethylene/1-octene diblock copolymer Sample1 by DMA. (a) One-way dual-shape memory effect: Tp = 82 °C, Tlow = 5 °C, Rf = 79.6%, Rr = 95.9%. (b) One-way trishape memory effect: Tp1 = 82 °C, Tp2 = 53 °C, Tlow = 5 °C, Rf1 = 41.3%, Rf2 = 67.0%, Rr2 = 86.0%, Rr1 = 93.2%. (c) One-way quadruple-shape memory effect: Tp1 = 82 °C, Tp2 = 60 °C, Tp3 = 35 °C, Tlow = 5 °C, Rf1 = 28.0%, Rf2 = 36.5%, Rf3 = 59.1%, Rr3 = 76.0%, Rr2 = 54.8%, Rr1 = 100%. (d) Photo demonstration of triple-shape memory effect at 82, 53, and 5 °C.

3.4.2 Reversible Shape Memory Effect

It is well-known that achieving reversible shape memory effects represents a challenging task. A majority of RSMPs require chemically cross-linked networks, which limit processing and remolding of permanent shape. It is therefore of great

interest to develop thermoplastic RSMPs. In this work, a reversible switching angle upon cooling and heating was found in the thermoplastic polyolefin film, as shown in Figure 3.3 and video S3.1. The film was first heated to 82 °C, folded to a small angle and then quenched to 5 °C. When the external force was removed, an angle of 34.6° was fixed. The film was clamped to a clip in air, as shown in Figure 3.3a. A stream of hot air was blown to the film from left side, through which the temperature of the film reached 55 °C. As temperature increased, the angle of the film changed to 58.1°. A stream of cold air was then blown to the film from bottom, decreasing the film temperature to about 5 °C. The angle was recovered to 36.8°. This angle switching upon heating and cooling was repeated for 5 cycles with good reproducibility, as shown in Figure 3.3b. We believe this is the first RSME free of external loading, ever observed with thermoplastic polyolefin elastomer materials.

(a)

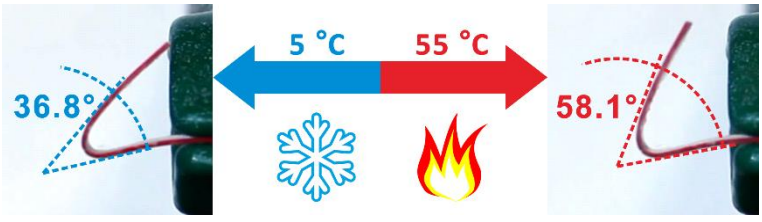

(b)

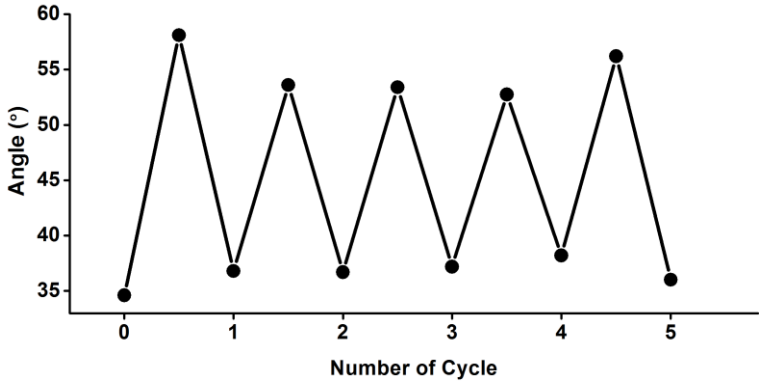

Figure 3.3. Reversible shape memory effect of the diblock olefin copolymer Sample1 film without external loading. (a) Photographs of the angle change, (b) plot of the angle change vs cycles.

To date, the only feasible mechanism for RSME is the oriented-crystallization-induced elongation upon cooling and melting-induced contraction. RSME can occur under external loading or stress-free condition, according to the material design. To exclude a possibility of “cold shrinkage and thermal expansion” effect, which might also induce the angle change, and to further investigate the reversibility, a series of quantitative shape memory tests by DMA were performed.

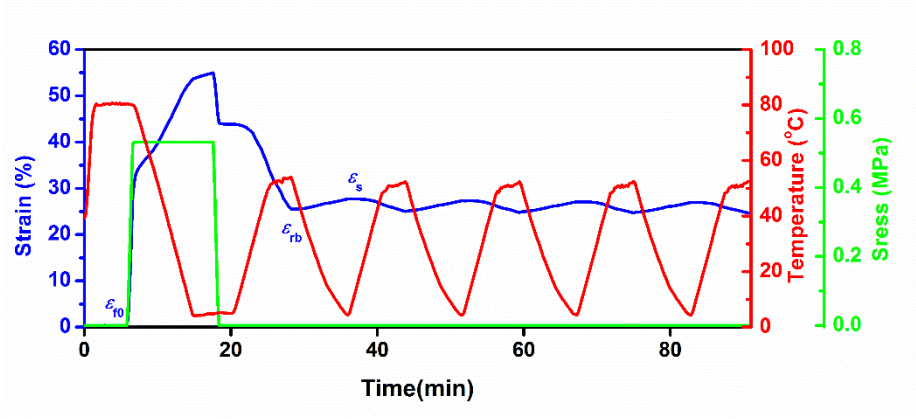

(a)

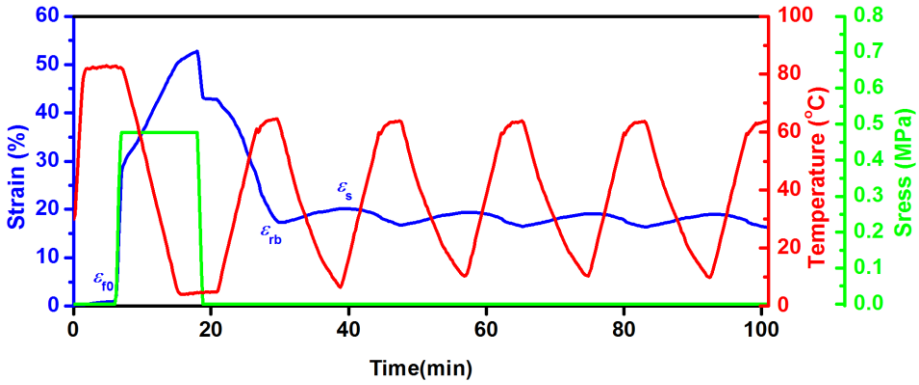

(b)

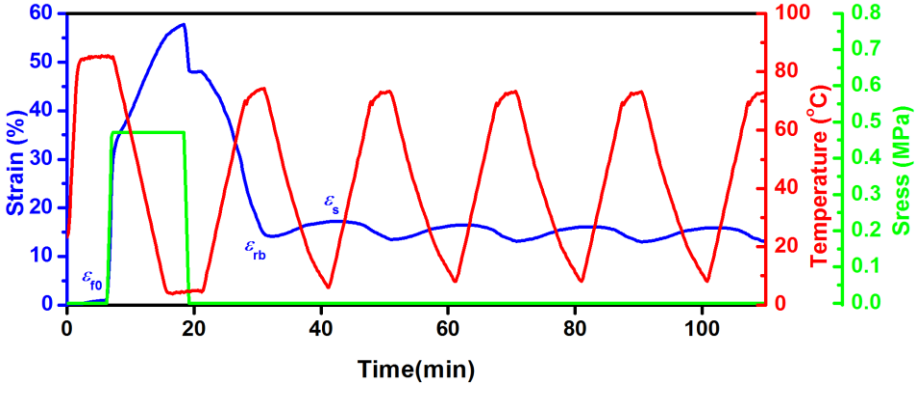

(c)

Figure 3.4. Reversible shape memory effect of ethylene/1-octene diblock copolymer Sample1 by DMA under stress-free condition. T_p = 82 °C, T_{low} = 5 °C, and (a) T_{high} = 50 °C, (b) 60 °C, (c) 70 °C.

RSME was first tested under stress-free condition at three different temperatures, as shown in Figure 3.4. Similar to the one-way shape memory tests, the sample was first programmed with external stress of about 0.4 MPa at T_p = 82 °C, then it was cooled to the fixing temperature T_{low} = 5 °C under loading. After isothermal at 5 °C for 3 min, the external load was released to zero. The temperature was increased to a higher level, T_{high}, at which the elongated sample partially recovered. After that, the temperature was cooled and heated between T_{low} and T_{high} for four times under stress-free condition. It is evident in Figure 3.4 that all the tests clearly showed reversible "cold extension and thermal contraction", while Figure S3.5 showed that the strain caused by thermal extension under heating was only 0.25%, therefore the possibility of "cold shrinkage and thermal expansion" could be excluded. When T_{high} was set to 50, 60, and 70 °C, the reversible strain became 2.2, 2.8, 3.0% and the reversible ratio was 8.6, 14.0, and 17.7%, respectively. This reversible ratio under stress-free condition was higher than other thermoplastic RSMPs reported in literature.[34,35] Up to date, the reported reversible strains for thermoplastic RSMPs were 3.4 and 6% at 100% prestrain within similar temperature range, and the reversible ratios were 5.2 and 8%, respectively.[34,35] The diblock copolymer Sample1 yielded higher reversible ratios than the reported values (Figure S3.6). In this work, the reversible strain was obviously increased with a larger prestrain (e.g., 120%) applied to the sample film (See Figure S3.6), and the reversible ratio was even competitive with some thermoset RSMPs.[28] The result also indicated

that the larger temperature variation between T_{high} and T_{low}, the higher reversible ratio could be achieved. This is because the bigger crystal domains formed at higher temperature possess a larger fixing ability than smaller crystal domains, so that a stronger crystal "skeleton" could be formed, resulting in better crystallization orientation and thus increased reversibility.

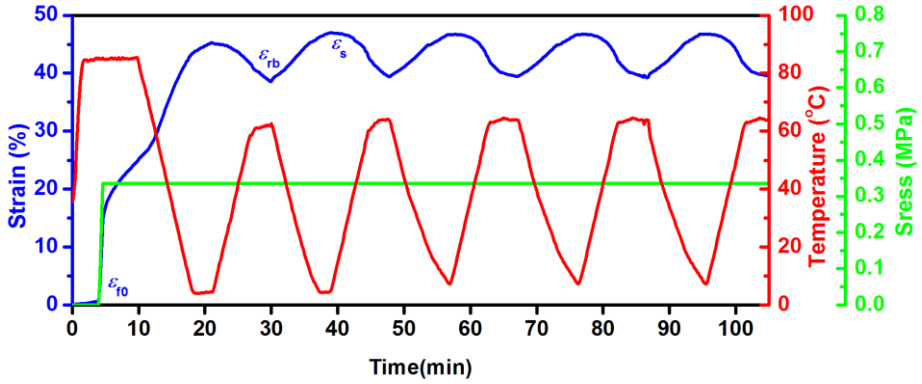

(a)

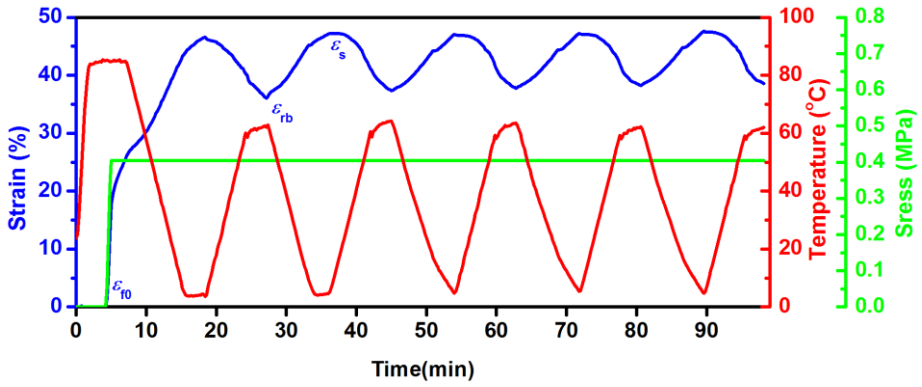

(b)

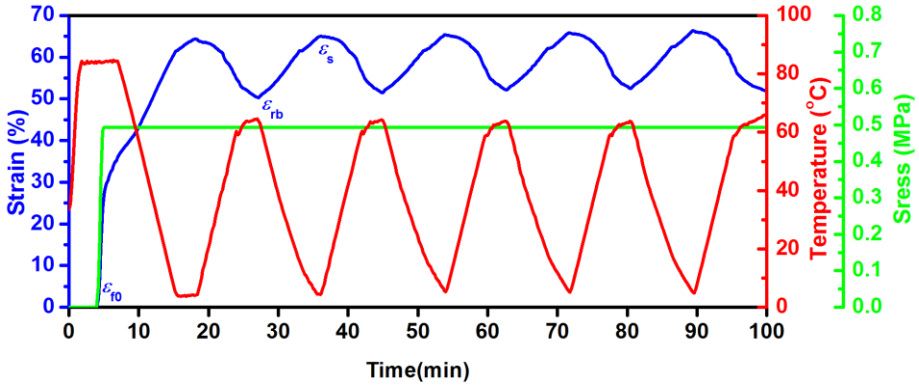

(c)

Figure 3.5. Reversible shape memory effect of ethylene/1-octene diblock copolymer Sample1 by DMA. T_p = 82 °C, T_{low} = 5 °C, T_{high} = 60 °C under external loading of (a) 0.33, (b) 0.40, and (c) 0.49 MPa

To further improve the reversible ratio, RSME was also studied under loading, as external loading could more effectively stretch polymer chains facilitating crystallization orientation. There have been many research reports on RSME under external loading.[18,22,23,40] DMA test procedure was similar as stress-free testing, except that external loading was remained after programing. The result was shown in Figure 3.5. It is clear that when a small stress was loaded, reversible elongation increased significantly from the stress-free condition. At 0.33, 0.40, and 0.49 MPa, the reversible strain reached 7.6, 10.5, and 14.1%, and the reversible ratio was 16.1, 22.6, and 21.8%, respectively, indicating that larger stress would induce higher reversibility in the studied stress range. There was no obvious creeping observed in this thermoplastic polyolefin film after five cycles.

3.4.3 Mechanism for RSME without chemical crosslinking

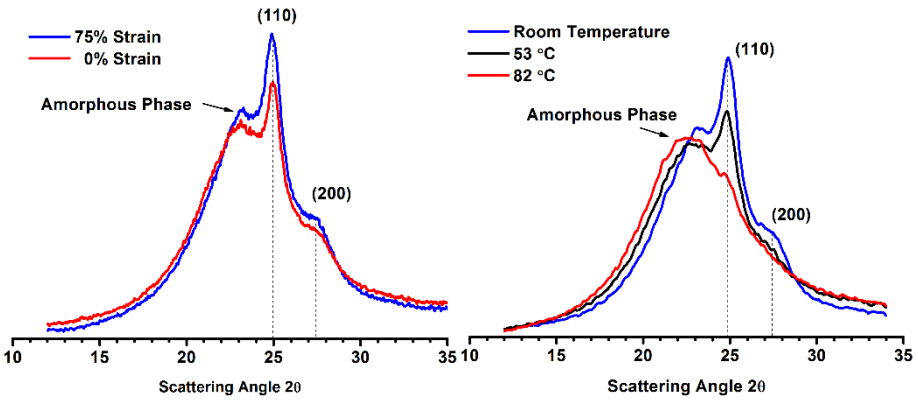

(a) (b)

Figure 3.6. XRD curves of the diblock copolymer Sample1, (a) sample with 0% and 75% strain at room temperature; (b) 75% prestrained sample at room temperature, 53, and 82 °C.

It can be speculated that RSME of the diblock copolymer was induced by its broad crystal size distribution and oriented crystallization. Figure 3.6 shows XRD analysis of the sample for further explanation. The sample without prestrain was first tested at room temperature. It was then deformed at 82 °C and quenched to 5 °C to fix the prestrain at 75%. The prestretched sample was then measured at room temperature, 53 and 82 °C to test crystallinity at the different temperatures. Figure 3.6a compares the results from 0% and 75% strain at room temperature. The sharp peak near 25° was attributed to the reflection of (110) crystallographic plane, (200) crystallographic plane was also found between 27° and 28°, the broad peak near 23° was attributed to amorphous phase. The prestretched

sample with 75% strain showed obviously higher reflection intensity of (110) plane than the nonstretched sample at room temperature, indicating that the deformation at 82 °C and subsequent quenching could induce chain orientation and give higher crystallinity. Figure 3.6b shows the crystallinity variation in the prestretched sample at different temperatures. As temperature increased to 53 °C, the crystallinity decreased but it still retained a certain amount of crystals as the reflection of (110) plane was still obvious. The prestretched sample partially recovered at 53 °C. When temperature further increased to 82 °C, the sample fully recovered to its initial shape and there was almost no crystal reflection at 82 °C, as a majority of crystals were melted (shown in DSC melting curve in Figure 3.1). Due to variance of temperature and oriented chain crystallization induced by external deformation, crystallinity of the diblock copolymer film was tunable.

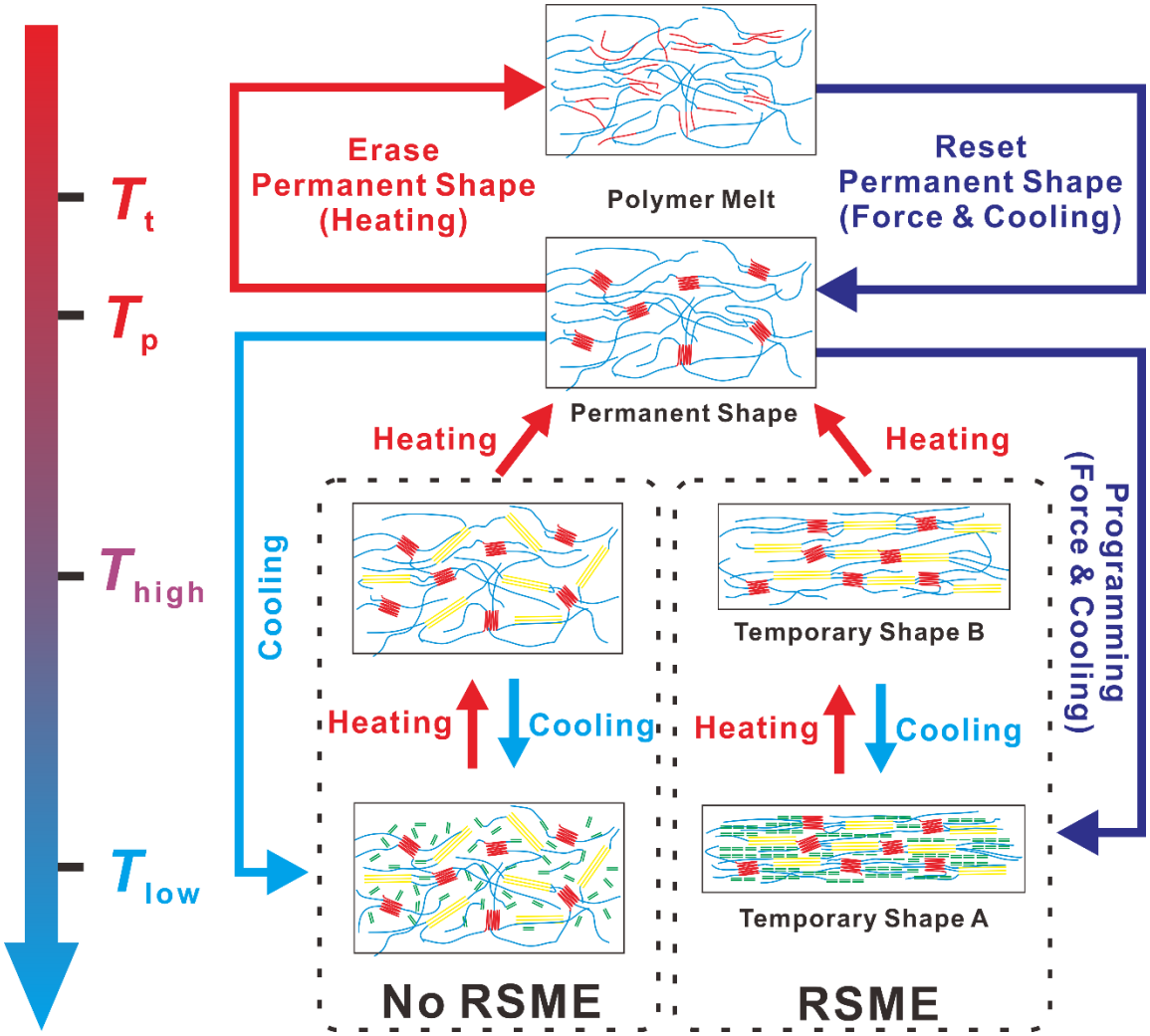

Figure 3.7. Schematic graph of reversible shape memory effect of thermoplastic polyolefin elastomer

A plausible mechanism for RSME with the thermoplastic polyolefin elastomer is proposed in Figure 3.7. The thermoplastic polyolefin elastomer could be molded or remolded into different permanent shapes above T_t, at which polymer was totally melted. When cooled to T_p, the permanent shape could be fixed by partially crystallized large crystals, as well as chain entanglements in amorphous

phase. If there was no external force that deformed or programmed the elastomer sample at T_p, crystal domains of broad size distribution could form and act as physically cross-linked points when temperature continuously cooled down to T_{low}, giving the material a good elasticity. As the crystal domains would form isotopically, there was no evident shape change upon cooling and heating. Therefore, the material showed only elasticity but no RSME. In contrast, if there was an external force deforming or programing the sample at T_p, polymer chains would be oriented by stretching in the microscopic level. As sample was cooled down to T_{low} under loading, oriented-crystallization-induced elongation occurred. After external load was released, a temporary shape was fixed at T_{low}. As the sample in this study was an ethylene/1-octene diblock copolymer having hard and soft segments, the hard segments with longer crystalline ethylene sequence would crystallize first and form relatively larger crystal domains. These larger crystal domains could act as a skeleton and constrain crystallization behavior of the soft segments. The soft segments with shorter crystalline ethylene sequence length formed small crystals (fringed micelles or bundled crystals) along the stretch direction. When sample was heated back to T_{high}, the small crystals melted and induced contraction. Although there were still some large crystal domains existed in the sample, a temporary shape could be fixed at T_{high}. When cooled down to T_{low}, small crystals could form again along skeleton of the larger crystal domains. The oriented-crystallization-induced elongation was thus maintained. These two temporary shapes could reversibly shift between each

other upon cooling and heating under constant external loading or even stress-free condition. The reversible shape memory effect was thus achieved.

§ 3.5 Conclusion

In summary, a thermoplastic ethylene/1-octene diblock copolymer with designed chain microstructure has been demonstrated to perform not only traditional one-way multishape memory effect, but also two-way reversible shape memory effect under loading or stress-free condition. A plausible mechanism for RSME without chemical cross-linking was proposed. The hard segments with large crystal domains and high melting temperature act as a skeleton in keeping permanent shapes. The soft segments with small crystal size and low melting temperature act as an actuator and fix temporary shapes. Crystallization of soft segments must be constrained by skeleton of hard segments, otherwise there was no oriented crystallization. The oriented-crystallization-induced elongation makes the material extend under cooling and contract on heating, leading to a reversible shape memory performance. This work reports the first thermoplastic polyolefin material with reversible shape memory effect at stress-free or very small external loading condition. The idea of tunable reversible shape memory polymer by chain structure design would promote the development in this area. It especially opens a door to design pure hydrocarbon thermoplastic reversible shape memory material.

§ 3.6 References

(1) Xie, T., Recent Advances in Polymer Shape Memory. *Polymer* **2011**, *52* (22), 4985-5000.

(2) Hu, J., Zhu, Y., Huang, H., Lu, J., Recent Advances in Shape–Memory Polymers: Structure, Mechanism, Functionality, Modeling and Applications. *Prog. Polym. Sci.* **2012**, *37* (12), 1720-1763.

(3) Berg, G. J., McBride, M. K., Wang, C., Bowman, C. N., New Directions in the Chemistry of Shape Memory Polymers. *Polymer* **2014**, *55* (23), 5849-5872.

(4) Hager, M. D., Bode, S., Weber, C., Schubert, U. S., Shape Memory Polymers: Past, Present and Future Developments. *Prog. Polym. Sci.* **2015**, *49-50*, 3-33.

(5) Zhao, Q., Qi, H. J., Xie, T., Recent Progress in Shape Memory Polymer: New Behavior, Enabling Materials, and Mechanistic Understanding. *Prog. Polym. Sci.* **2015**, *49-50*, 79-120.

(6) Lendlein, A., Schmidt, A. M., Schroeter, M., Langer, R., Shape-Memory Polymer Networks From oligo(ϵ-caprolactone)dimethacrylates. *J. Polym. Sci., Part A: Polym. Chem.* **2005**, *43* (7), 1369-1381.

(7) Lendlein, A., Jiang, H. Y., Junger, O., Langer, R., Light-Induced Shape-Memory Polymers. *Nature* **2005**, *434* (7035), 879-882.

(8) Cho, J. W., Kim, J. W., Jung, Y. C., Goo, N. S., Electroactive Shape-Memory Polyurethane Composites Incorporating Carbon Nanotubes. *Macromol. Rapid Comm.* **2005**, *26* (5), 412-416.

(9) Schmidt, A. M., Electromagnetic Activation of Shape Memory Polymer Networks Containing Magnetic Nanoparticles. *Macromol. Rapid Comm.* **2006**, *27* (14), 1168-1172.

(10) Harris, R. D., Auletta, J. T., Motlagh, S. A. M., Lawless, M. J., Perri, N. M., Saxena, S., Weiland, L. M., Waldeck, D. H., Clark, W. W., Meyer, T. Y., Chemical and Electrochemical Manipulation of Mechanical Properties in Stimuli-Responsive Copper-Cross-Linked Hydrogels. *ACS Macro Lett.* **2013**, *2* (12), 1095-1099.

(11) Luo, Y., Guo, Y., Gao, X., Li, B., Xie, T., A General Approach Towards Thermoplastic Multishape-Memory Polymers via Sequence Structure Design. *Adv. Mater.* **2013**, *25* (5), 743-748.

(12) Li, W., Liu, Y., Leng, J., Selectively Actuated Multi-Shape Memory Effect of a Polymer Multicomposite. *J. Mater. Chem. A* **2015**, *3* (48), 24532-24539.

(13) Zhang, Q., Hua, W., Feng, J., A Facile Strategy to Fabricate Multishape Memory Polymers with Controllable Mechanical Properties. *Macromol. Rapid Comm.* **2016**, *37* (15), 1262-1267.

(14) Li, M., Song, F., Chen, L., Wang, X., Wang, Y., Flexible Material Based On Poly(lactic Acid) and Liquid Crystal with Multishape Memory Effects. *ACS Sustainable Chem. Eng.* **2016**, *4* (7), 3820-3829.

(15) Zhou, J., Sheiko, S. S., Reversible Shape-Shifting in Polymeric Materials. *J. Polym. Sci., Part B: Polym. Phys.* **2016**, *54* (14), 1365-1380.

(16) Chen, S., Hu, J., Zhuo, H., Zhu, Y., Two-Way Shape Memory Effect in Polymer Laminates. *Mater. Lett.* **2008**, *62* (25), 4088-4090.

(17) Li, M. H., Keller, P., Artificial Muscles Based On Liquid Crystal Elastomers. *Philos. Trans. R. Soc., A* **2006**, *364* (1847), 2763-2777.

(18) Chung, T., Romo-Uribe, A., Mather, P. T., Two-Way Reversible Shape Memory in a Semicrystalline Network. *Macromolecules* **2008**, *41* (1), 184-192.

(19) Behl, M., Kratz, K., Zotzmann, J., Nöchel, U., Lendlein, A., Reversible Bidirectional Shape-Memory Polymers. *Adv. Mater.* **2013**, *25* (32), 4466-4469.

(20) Li, J., Rodgers, W. R., Xie, T., Semi-Crystalline Two-Way Shape Memory Elastomer. *Polymer* **2011**, *52* (23), 5320-5325.

(21) Zotzmann, J., Behl, M., Hofmann, D., Lendlein, A., Reversible Triple-Shape Effect of Polymer Networks Containing Polypentadecalactone- and Poly(ϵ-caprolactone)-Segments. *Adv. Mater.* **2010**, *22* (31), 3424-3429.

(22) Bai, Y., Zhang, X., Wang, Q., Wang, T., A Tough Shape Memory Polymer with Triple-Shape Memory and Two-Way Shape Memory Properties. *J. Mater. Chem. A* **2014**, *2* (13), 4771-4778.

(23) Huang, M., Dong, X., Wang, L., Zhao, J., Liu, G., Wang, D., Two-Way Shape Memory Property and its Structural Origin of Cross-Linked Poly(Epsilon-Caprolactone). *RSC Adv.* **2014**, *4* (98), 55483-55494.

(24) Behl, M., Zotzmann, J., Lendlein, A., One-Way and Reversible Dual-Shape Effect of Polymer Networks Based On Polypentadecalactone Segments. *Int. J. Artif. Organs* **2011**, *34* (2), 231-237.

(25) Saatchi, M., Behl, M., Nöchel, U., Lendlein, A., Copolymer Networks From Oligo(ϵ-Caprolactone) and n-Butyl Acrylate Enable a Reversible Bidirectional Shape-Memory Effect at Human Body Temperature. *Macromol. Rapid Comm.* **2015**, *36* (10), 880-884.

(26) Fang, L., Fang, T., Fang, Z., Lu, C., Xu, Z., Solar Light Responsive Polymer Composites with Three Shape-Memory Effects. *Macromol. Mater. Eng.* **2016**, *301* (3), 267-273.

(27) Farhan, M., Chaganti, S. R., Nöchel, U., Kratz, K., Lendlein, A., Reversible Shape-Memory Properties of Surface Functionalizable, Crystallizable Crosslinked Terpolymers. *Polym. Adv. Technol.* **2015**, *26* (12), 1421-1427.

(28) Behl, M., Kratz, K., Noechel, U., Sauter, T., Lendlein, A., Temperature-Memory Polymer Actuators. *Proc. Natl. Acad. Sci. U. S. A.* **2013**, *110* (31), 12555-12559.

(29) Zhou, J., Turner, S. A., Brosnan, S. M., Li, Q., Carrillo, J. Y., Nykypanchuk, D., Gang, O., Ashby, V. S., Dobrynin, A. V., Sheiko, S. S., Shapeshifting: Reversible Shape Memory in Semicrystalline Elastomers. *Macromolecules* **2014**, *47* (5), 1768-1776.

(30) Li, Q., Zhou, J., Vatankhah-Varnoosfaderani, M., Nykypanchuk, D., Gang, O., Sheiko, S. S., Advancing Reversible Shape Memory by Tuning the Polymer Network Architecture. *Macromolecules* **2016**, *49* (4), 1383-1391.

(31) Turner, S. A., Zhou, J., Sheiko, S. S., Ashby, V. S., Switchable Micropatterned Surface Topographies Mediated by Reversible Shape Memory. *ACS Appl. Mater. Interfaces* **2014**, *6* (11), 8017-8021.

(32) Tippets, C. A., Li, Q., Fu, Y., Donev, E. U., Zhou, J., Turner, S. A., Jackson, A. S., Ashby, V. S., Sheiko, S. S., Lopez, R., Dynamic Optical Gratings Accessed by Reversible Shape Memory. *ACS Appl. Mater. Interfaces* **2015**, *7* (26), 14288-14293.

(33) Meng, Y., Jiang, J., Anthamatten, M., Shape Actuation via Internal Stress-Induced Crystallization of Dual-Cure Networks. *ACS Macro Lett.* **2015**, *4* (1), 115-118.

(34) Lu, L., Li, G., One-Way Multishape-Memory Effect and Tunable Two-Way Shape Memory Effect of Ionomer Poly(Ethylene-Co-Methacrylic acid). *ACS Appl. Mater. Interfaces* **2016**, *8* (23), 14812-14823.

(35) Biswas, A., Aswal, V. K., Sastry, P. U., Rana, D., Maiti, P., Reversible Bidirectional Shape Memory Effect in Polyurethanes through Molecular Flipping. *Macromolecules* **2016**, *49* (13), 4889-4897.

(36) Kolesov, I. S., Multiple Shape-Memory Behavior and Thermal-Mechanical Properties of Peroxide Cross-Linked Blends of Linear and Short-Chain Branched Polyethylenes. *Express Polym. Lett.* **2008**, *2* (7), 461-473.

(37) Zhao, J., Chen, M., Wang, X., Zhao, X., Wang, Z., Dang, Z., Ma, L., Hu, G., Chen, F., Triple Shape Memory Effects of Cross-Linked Polyethylene/Polypropylene Blends with Cocontinuous Architecture. *ACS Appl. Mater. Interfaces* **2013**, *5* (12), 5550-5556.

(38) Zhang, Q., Feng, J., Difunctional Olefin Block Copolymer/Paraffin Form-Stable Phase Change Materials with Simultaneous Shape Memory Property. *Sol. Energy Mater. Sol. Cells.* **2013**, *117*, 259-266.

(39) Kresge, E. N., In *Thermoplastic Elastomers 3rd Edition*, G. Holden, H. Kricheldorf and R. Quirk, ''Eds.' Hanser Publications: **2004**; 'Chapter' 5, p 93.

(40) Kolesov, I., Dolynchuk, O., Jehnichen, D., Reuter, U., Stamm, M., Radusch, H., Changes of Crystal Structure and Morphology during Two-Way

Shape-Memory Cycles in Cross-Linked Linear and Short-Chain Branched Polyethylenes. *Macromolecules* **2015**, *48* (13), 4438-4450.

(41) Kolesov, I., Dolynchuk, O., Borreck, S., Radusch, H., Morphology-Controlled Multiple One- and Two-Way Shape-Memory Behavior of Cross-Linked Polyethylene/Poly(ϵ-Caprolactone) Blends. *Polym. Adv. Technol.* **2014**, *25* (11), 1315-1322.

(42) Dolynchuk, O., Kolesov, I., Radusch, H., Theoretical Description of an Anomalous Elongation During Two-Way Shape-Memory Effect in Crosslinked Semicrystalline Polymers. *Macromol. Symp.* **2014**, *346* (1), 48-58.

(43) Ma, L., Zhao, J., Wang, X., Chen, M., Liang, Y., Wang, Z., Yu, Z., Hedden, R. C., Effects of Carbon Black Nanoparticles On Two-Way Reversible Shape Memory in Crosslinked Polyethylene. *Polymer* **2015**, *56*, 490-497.

(44) Liu, W., Ojo, A. T., Wang, W., Fan, H., Li, B., Zhu, S., Preparation of Ultrahigh Molecular Weight Ethylene/1-Octene Block Copolymers Using Ethylene Pressure Pulse Feeding Policies. *Polym. Chem.* **2015**, *6* (20), 3800-3806.

(45) Zhao, Q., Zou, W., Luo, Y., Xie, T., Shape Memory Polymer Network with Thermally Distinct Elasticity and Plasticity. *Sci. Adv.* **2016**, *2* (1), e1501297.

§ 3.7 Supporting Information

Table S3.1. Basic characterization data for the diblock copolymers used in this work.

	F_2 (mol%)	M_w (10^4g/mol)	PDI	T_m (°C)	T_c (°C)	T_g (°C)	ΔH_m (J/g)
Sample1	12.3	42.45	1.16	78.7	60.6	-61.6	47.0
Sample2	13.1	57.04	1.58	85.8	67.3	-61.3	43.0
Sample3	13.6	83.54	1.17	82.4	64.2	-61.2	47.2

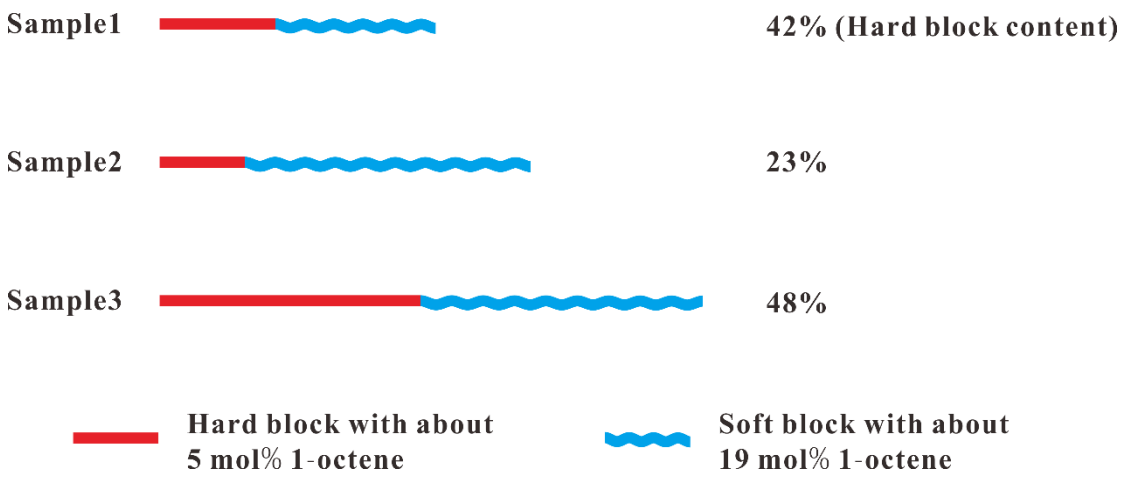

Scheme S3.1. Schematic structures of the diblock copolymers used in this work.

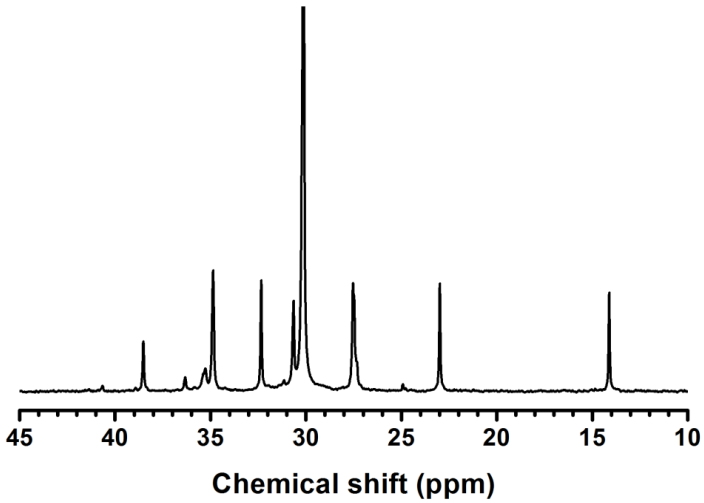

Figure S3.1. ^{13}C NMR spectra of the ethylene/1-octene diblock copolymer Sample1

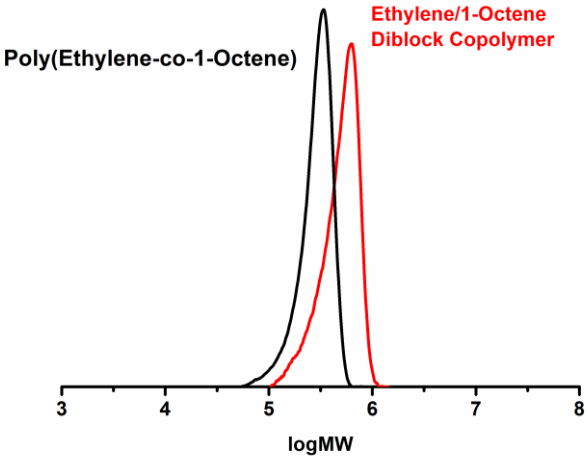

Figure S3.2. GPC curves of ethylene/1-octene diblock copolymer Sample1 and poly(ethylene-co-1-octene) soft block.

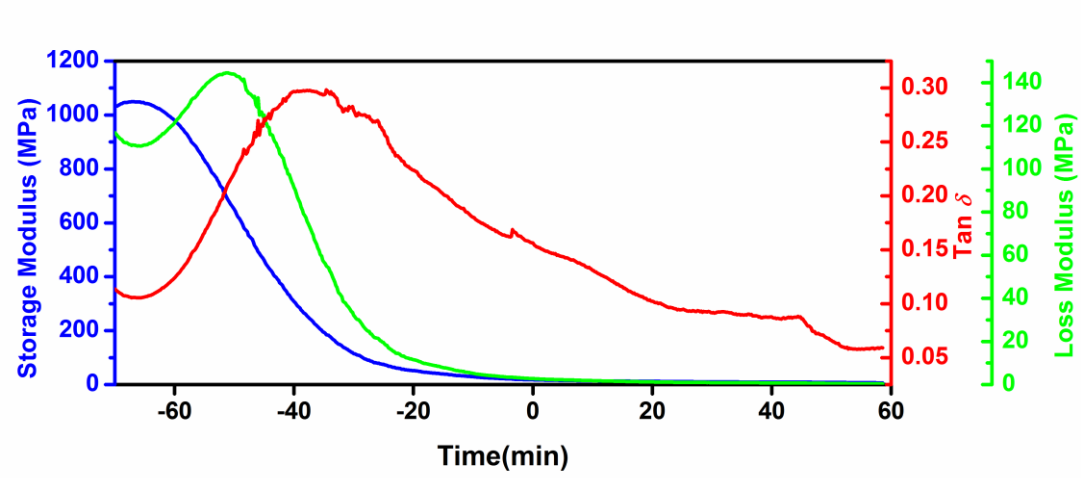

Figure S3.3. Temperature dependent modulus curves of ethylene/1-octene diblock copolymer Sample1 from -70 °C to 60 °C at a rate of 3 °C/min.

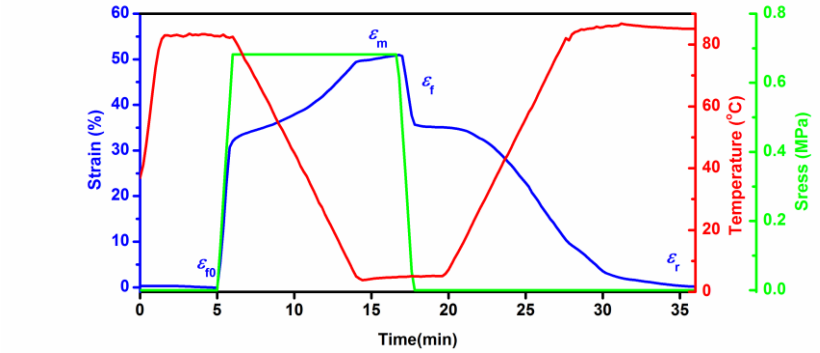

(a)

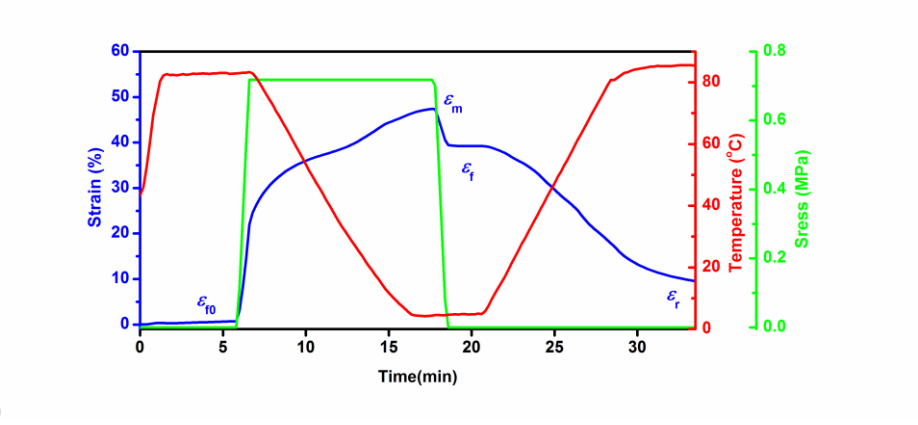

(b)

Figure S3.4. One-way dual-shape memory effect of ethylene/1-octene diblock copolymers[1] by DMA. T_p = 82 °C, T_{low} = 5 °C, (a) Sample2 with lower hard segment content (23%) R_f = 69.1%, R_r = 99.9%. (b) Sample3 with higher hard segment content (48%). R_f = 82.5%, R_r = 76.6%.

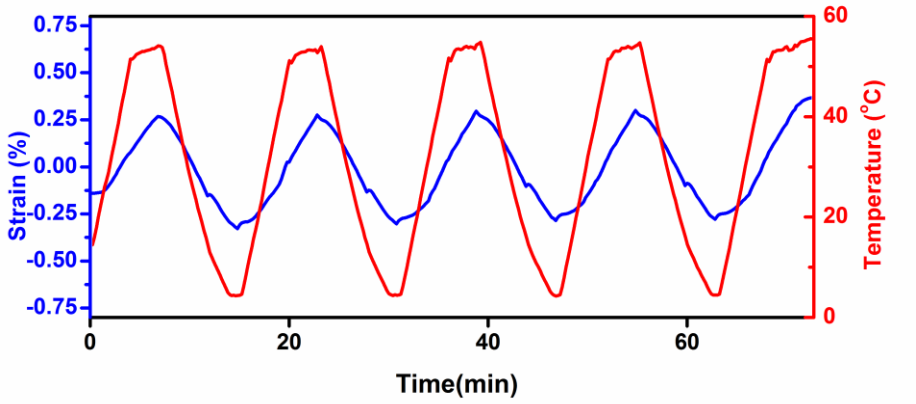

Figure S3.5. Thermal extension effect of Sample1 upon heating and cooling cycles between 5 °C and 53 °C under stress-free condition. The first cycle was removed for eliminating the thermal history.

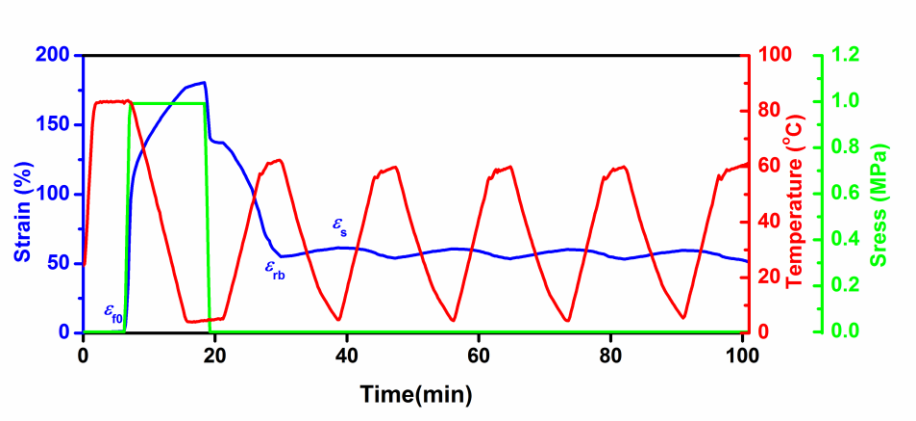

Figure S3.6. Reversible shape memory effect of ethylene/1-octene diblock copolymer Sample1 by DMA with large pre-strain under stress-free condition. T_p = 82 °C, T_{low} = 5 °C, and T_{high} = 60 °C. The reversible strain is 5.5%, reversible ratio is 8.9%. The reversible strain can be obviously increased if the pre-strain was further increased. But the pre-strain was limited to less than 200% because of the range limit of our DMA instrument.

Video S3.1: demonstration of reversible shape memory effect of the ethylene/1-ocetene diblock copolymer.

3.7.1 References

(1) Liu, W., Ojo, A. T., Wang, W., Fan, H., Li, B., Zhu, S., Preparation of Ultrahigh Molecular Weight Ethylene/1-Octene Block Copolymers Using Ethylene Pressure Pulse Feeding Policies. *Polym. Chem.* **2015**, *6* (20), 3800-3806.

4 THERMOPLASTIC POLYOLEFIN ELASTOMER BLENDS FOR MULTIPLE AND REVERSIBLE SHAPE MEMORY POLYMER

In this chapter, the multiple and reversible shape memory effect of the commercial thermoplastic polyolefin elastomer blends is demonstrated and represented. This chapter is based on the peer-reviewed published journal paper as follows: “Gao, Y.; Liu, W.; Zhu, S., Thermoplastic Polyolefin Elastomer Blends for Multiple and Reversible Shape Memory Polymer”, *Industrial & Engineering Chemistry Research*, **2019**, *58(42)*, 19495-19502. Reprinted with permission from *Industrial & Engineering Chemistry Research*, **2019**, *58(42)*, 19495-19502.

Author contributions

Yuan Gao conducted the experiments and wrote the first draft of the manuscript under the guidance of Dr. Shiping Zhu and Dr. Weifeng Liu. Dr. Weifeng Liu provided the first revision of the manuscript. The final revision was provided by Dr. Zhu.

§ 4.1 Abstract

This work reports a novel type of reversible shape memory polymers (RSMPs) from commercially available thermoplastic polyolefin elastomers (POEs). Two RSMPs based on Dow Chemical's POE Engage 8003, Engage 8137, Engage 8180, olefin block copolymer elastomer (OBC) Infuse 9007 were prepared by simple blending of the commercial products having different melting temperatures. The multiple and reversible shape memory performances of the as-prepared blends were clearly demonstrated. This work provides a facile and low-cost method for the large-scale preparation of the reversible shape memory materials. It broadens the source of the materials for the design and development of RSMPs.

§ 4.2 Introduction

Shape memory polymers (SMPs) are representative of stimuli-responsive materials, which can memorize one or several different temporary shapes and recover to their original shapes with external triggers, such as heat, light, electromagnetic field, etc. SMP usually contain a stable network to maintain its permanent shape, and switch phases to fix the temporary shape(s). This delicate structure endows SMPs with the ability to switch their shape based on environmental conditions. Various SMPs have been synthesized and showed great potential in the areas of textiles, aerospace facilities and biomedical devices.[1-7]

Recently, soft actuators based on SMPs have attracted the attention of many because of their potential applications in microrobots and artificial muscles, etc.[8] These actuators could shift between different temporary shapes when exposed to external stimuli without the need for additional programming steps. This type of SMPs is termed as two-way shape memory polymer or reversible shape memory polymer (RSMP). Up to now, liquid crystalline elastomers (LCE),[9] polymer laminates,[10] and semicrystalline polymers[11] have been found to exhibit the reversible shape memory effect (RSME). Among these materials, semicrystalline polymers are best suited as RSMPs, because of their variable polymer chain structures and comparably easy synthesis route. Since the first semicrystalline RSMP demonstrated by Mather et al. in 2008,[11] who examined a crosslinked

poly(cyclooctene) (PCO), a large variety of RSMPs have been synthesized and studied, such as poly(octylene adipate),[12] polycaprolactone (PCL),[13] poly(ethylene-co-vinyl acetate) (PEVA),[14,15] polycaprolactone and polypentadecalactone system,[16,17] poly(tetramethylene oxide) glycol,[18] and polyolefins.[19, 20]

Reportedly, semicrystalline RSMPs are all based on the same mechanism of crystallization-induced elongation (CIE) and melting-induced contraction (MIC) of the crystal actuator domains. A RSMP system usually contains several switch phases with distinguished melting transitions, or a continuous phase with a broad range of melting transitions. Upon cooling, a switch phase composed of large crystals with relatively higher melting temperatures is first to crystallize, and acts as the skeletal domain in the direction of applied stress. A switch phase composed of small crystals with relatively lower melting temperatures crystallizes along the oriented skeletal domain, which induces an elongation. Upon heating, the small crystal domains melt and induce a contraction. The elongation and contraction induced by this oriented crystallization and related crystal melting achieves actuation during the cooling and heating cycles. Besides the CIE/MIC mechanism, entropic elasticity above the melting temperature of the semicrystalline RSMP was also considered to be a contributing factor to the reversible actuation.[21, 22]

It should be noted that most of the reported RSMPs are thermoset polymers, in which chemical crosslinks are essential in maintaining their permanent shapes.

Dependency on chemical crosslinking is a clear drawback when the area of application expects reprocessing and recycling. In recent years, there have been a few studies demonstrating thermoplastic polymers as exhibiting RSME, such as poly(ethylene-co-methacrylic acid),[23] polyurethane,[24,25] ethylene/1-octene diblock copolymer,[26] and poly(3*S*-isobutylmorpholin-2,5-dione) -polycaprolactone copolymer.[27] The physical crosslinks in these thermoplastic polymers helped to keep their permanent shapes, instead of the chemical crosslinks in the thermoset polymers. Xie et al.[28] reported a PCL-based polymer containing thermo- and photo-reversible bonds, which could gain thermally induced plasticity at high temperature and give solid-state reprocessability to a covalent crosslink network. However, it is challenging to expand raw material sources of such thermoplastic RSMPs and their preparation are costly and lab intensive.

As the world's number one polymer type in production and consumption, polyolefins are defined as commodity polymers but that does not detract from their potential as SMP material due to their good crystallizability and various chain microstructures.[29-32] Their excellent weatherability, chemical resistance, and low costs are clearly advantageous. In fact, the elongation phenomenon of polyolefins induced by oriented crystallization was studied as early as in the 1950's,[33,34] though the development of polyolefin-based RSME was only reported very recently. Kolesov et al. investigated RSME of crosslinked linear and short-chain branched polyethylenes theoretically.[19, 20, 35, 36] Hedden et al. reported an enhanced RSME of crosslinked polyethylene through the addition of carbon black

nanoparticles.[37] Nowadays, the development of novel high-performance thermoplastic polyolefin elastomers has provided an opportunity for the preparation of RSMPs. Our previous work on tailor-designed ethylene/1-octene diblock copolymers[38] has demonstrated free-standing RSME over a broad melting transition, arising from a precisely controlled chain structure with blocky connected hard and soft segments.[26] However, this kind of polyolefin block copolymer-based RSMPs is difficult to prepare on a large scale.

Polymer blending of commercial polymers provides a unique approach for the simple preparation of RSMPs. Blending is a common practice in the preparation of polymer materials for seeking synergy among the combined components for improved application properties. Some commercial thermoplastic polyethylene elastomers contain alternative hard and soft segments, in which the hard ethylene segments could crystallize to form physical crosslinks while the soft α-olefin-rich segments form an amorphous phase. A single polyethylene elastomer product usually has a narrow melting transition. It is hypothesized that blending of several polyethylene elastomers having different melting temperatures would result in a broad melting transition and could serve as a good candidate for RSMPs. This work explores the possible facile approach for upgrading commercially available commodity polyolefins into smart materials.

§ 4.3 Experimental Section

4.3.1 Materials

Polyolefin elastomers (POE) Engage™ 8003, Engage™ 8137 and Engage™ 8180, olefin block copolymer elastomer (OBC) Infuse™ 9007 were supplied by the Dow Chemical Company and were used without further treatments. The elastomer blends were prepared using a Thermo Haake Rheometer at 160 °C for 6 min. Table 1 and Table 2 summarizes the physical properties and recipes of the prepared elastomer blends. The resulting polyolefin blends were molded in a hot press at 13.8 MPa and 160 °C for 10 min to form flat specimens with dimensions of 120 × 120 × 0.5 mm^3. The requirements for selecting the POE components in preparing polymer blends include similar chain structures and partly overlapped melting transitions, which ensured the formation of interfacial crystal domains of various sizes.

Table 4.1. Melting and crystallization temperatures of commercial POEs and OBC for blending.

	Name	T_m(°C)	T_c (°C)
POE1	Engage™ 8003	85.1	58.6
POE2	Engage™ 8137	60.9	38.4
POE3	Engage™ 8180	52.1	28.9
OBC	Infuse™ 9007	122.0	83.8

Table 4.2. Recipes of the elastomer blends.

	E1	E2
POE1	30%	30%
POE2	/	30%
POE3	40%	40%
OBC	30%	/

4.3.2 Polymer Characterization

Modulated DSC 2910 (TA instruments) was used to measure melting temperature T_m and crystallization temperature T_c of the raw materials and blends. About 6.0 mg of each sample was prepared and the thermal history was first removed by heating the sample to 160 °C and keeping isothermal for 5 min. It was then cooled to -20 °C at a rate of 10 °C/min and maintained at the temperature for 5 min, before finally being reheated to 160 °C at 10 °C/min.

The shape memory effects were measured by DMA 2980 (TA instruments). The samples were cut into pieces of 20 × 2 × 0.5 mm. In the one-way dual-shape memory effect measurement, a sample (e.g. E1) was preheated to 85 °C under a preload of 0.004 N for 4 min. The strain was recorded as ε_{f0}. It was then stretched by a stress around 0.15 MPa, cooled from 85 to 5 °C at a rate of 10 °C/min and stayed isothermal at 5 °C under stress for 3 min to obtain the maximum elongated strain ε_m. After removal of the stress, the sample was kept at the same

temperature for another 2 min to obtain the fixed strain ε_f. It was finally heated back to 85 °C at a rate of 10 °C/min and stayed isothermal for 10 min, with the recovery strain recorded as ε_r. The fixing ratio R_f and the recovery ratio R_r were calculated from:

$$R_f = \frac{\varepsilon_f - \varepsilon_{f0}}{\varepsilon_m - \varepsilon_{f0}} \text{ and } R_r = \frac{\varepsilon_f - \varepsilon_r}{\varepsilon_f - \varepsilon_{f0}}$$

In the one-way triple-shape memory test, a sample (e.g. E1) was heated to 85 °C under a preload of 0.004 N for 4 min. The strain was recorded as ε_{f0}. It was then stretched by a stress around 0.2 MPa, cooled from 85 to 50 °C at a rate of 10 °C/min and kept isothermal at 50 °C under stress for 3 min to obtain the first maximum elongated strain ε_{m1}. The stress was removed and the sample was maintained at 50 °C for 2 min to obtain the first fixed strain ε_{f1}. The sample was then stretched under 0.4 MPa, cooled from 50 to 5 °C at a rate of 10 °C/min, and kept isothermal at 5 °C under stress for 3 min to obtain the second maximum elongated strain ε_{m2}. After the stress was removed, the sample was maintained at 5 °C for 2 min to obtain the second fixed strain ε_{f2}. The sample was reheated to 50 °C at a rate of 10 °C/min and maintained at 50 °C for 10 min to obtain the recovery strain ε_{r1}. Finally, the sample was heated back to 85 °C to obtain the recovery strain ε_{r0}. The fixing ratio R_f and the recovery ratio R_r were calculated from:

$$R_{fi} = \frac{\varepsilon_{fi} - \varepsilon_{f(i-1)}}{\varepsilon_{mi} - \varepsilon_{f(i-1)}} \text{ and } R_{ri} = \frac{\varepsilon_{fi} - \varepsilon_{r(i-1)}}{\varepsilon_{fi} - \varepsilon_{f(i-1)}}$$

In the one-way quadruple-shape memory test, the method and the calculation of fixing/recovery ratios were similar to the procedures described above.

To test RSME, a typical process is as follows: a sample (e.g. E1) was heated to 85 °C for 4 min, and the strain was recorded as ε_{f0}. It was then stretched by a stress around 0.2 MPa, cooled from 85 to 5 °C at a rate of 10 °C/min, and annealed under stress at 5 °C for 3 min. The sample was heated to 50 °C and annealed for 3 min to obtain the reversible strain ε_{rb}. After another cooling process to 5 °C, a stable strain ε_s was obtained. The cooling-heating segments between 5 °C and 50 °C were repeated for 5 cycles. The reversible ratio R_{rb} was calculated from:

$$R_{\mathrm{rb}} = \frac{\varepsilon_{\mathrm{s}} - \varepsilon_{\mathrm{rb}}}{\varepsilon_{\mathrm{s}} - \varepsilon_{\mathrm{f0}}}$$

X-ray diffraction (XRD) analysis was performed on a Bruker D8 DISCOVER with DAVINCI.DESIGN diffractometer. Co was used as the anode material. The sample was scanned from 10° to 35° with a scanning increment of 0.02° at 35 kV generator voltage and 45 mA current.

§ 4.4 Results and Discussion

A series of commercial polyolefin elastomers having different ethylene contents and ethylene sequence lengths were selected as the raw materials.

Figure 4.1 shows the DSC curves of the raw materials and their corresponding blends. Each POE or OBC sample had a relatively narrow melting transition. The different melting temperatures corresponded to the different sized crystal domains. Typically, larger crystals require more heat to melt and thus have a higher melting temperature. In Figure 4.1, the OBC sample has the highest melting temperature of 120 °C due to its largest crystalline domains resulted from the longest crystalline ethylene sequence length. The POE samples of T_m = 85.1 °C, 60.9 °C and 52.1 °C indicate that the crystalline ethylene sequence length decreased in the order of POE1>POE2>POE3.

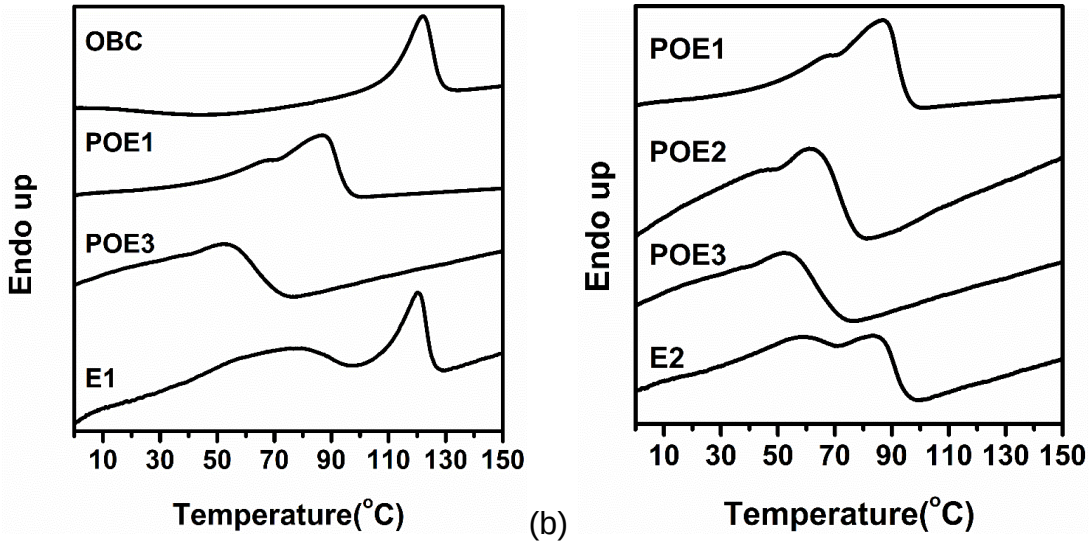

Figure 4.1. DSC curves of the pure POEs and OBC samples and their blends: (a) E1 and (b) E2.

According to the mechanism of one-way multi-shape memory and that of reversible shape memory, either several distinguished melting transitions or a

broad range of melting transitions is required. Therefore, we blended several POE and OBC materials as the model composites, to prepare RSMPs from the thermoplastic polyolefin elastomers. Elastomer blends E1 and E2 were prepared and characterized. E1 was blended from OBC, POE1, and POE3 with the mass ratio of 30:30:40. E2 was blended from POE1, POE2, and POE3 with the mass ratio of 30:30:40. In Figure 4.1a, E1 exhibited a typical bimodal melting behavior, including a broad melting transition from 10 °C to 100 °C and a sharp melting peak at 120 °C, suggesting a discontinuous crystal size distribution in the blend of OBC with POEs. In Figure 4.1b, E2 exhibited a continuous broad melting transition from 10 °C to 100 °C, resulting from an increased diversity in the crystal sizes in the blend of three POE. For both blends, the melting peak of the blend sample showed some shift compared to each POE component, suggesting that the polymer chains from each POE component were mixed to form new interfacial crystal domains of various sizes, which facilitated stress transfer and reduced chain slippage in the shape memory cycles.

4.4.1 One-way shape memory effect

The conventional one-way shape memory effects of E1 and E2 were measured by dynamic mechanical analysis (DMA). According to the melting transitions of E1 and E2 shown in Figure 4.1, the memorable temperature range of E1 could be from 10 °C to 90 °C, and E2 could be from 10 °C to 80 °C. Theoretically speaking, any temperature(s) in this range could serve as the

programming temperature(s) (T_p). For better observation, 85 °C and 75°C were selected as T_p for E1 and E2, respectively, as demonstration of the conventional one-way dual-shape and multi-shape memory effects.

In Figure 4.2a, E1 was first heated to 85 °C for 4 min, stretched under a pre-stress of 0.15 MPa, and cooled from 85 °C to 5 °C with the rate of 10 °C/min. After 3 min isothermal at the fixing temperature of 5 °C (T_{low}), the external stress was removed. A temporary strain of 76% was fixed at 5 °C with a fixing ratio of 95.6%. The sample was heated back to 85 °C with a heating rate of 10 °C/min, during which it contracted to its permanent strain with a recovery ratio of 95.6%, demonstrating a perfect dual-shape memory effect. E2 also exhibited an excellent dual-shape memory effect by the same method, using T_p of 75 °C, with a fixing ratio of 94.3% and a recovery ratio of 95.3% (Figure 4.2b).

The triple and quadruple shape memory effects of E1 and E2 were measured in a similar way. In the triple shape memory effect test of E1 as shown in Figure 4.2c, 85 °C and 50 °C were selected as the two programming temperatures, while the pre-stress in the two programming steps were 0.2 MPa and 0.4 MPa, respectively. The fixing ratios R_{f1} and R_{f2} of E1 in the two steps were 55.2% and 74.3%, while the recovery ratio R_{r2} and R_{r1} were 82.3% and 79.0%, respectively. E2 also showed a triple shape memory effect with the fixing ratios of 52.0% and 77.0%, and the recovery ratios of 85.9% and 75.3% under the programming temperatures of 75 °C and 50 °C, respectively (Figure 4.2d). Furthermore, the quadruple shape memory effects of E1 and E2 were demonstrated, with 85 °C,

50 °C, and 30 °C set as the programming temperatures and 5 °C as the fixing temperature for E1 measurement. In Figure 4.2e, E1 showed an obvious quadruple-shape memory effect with the fixing ratios R_{f1}, R_{f2} and R_{f3} as 47.3%, 49.7%, and 60.5%, respectively, and the recovery ratios R_{r3}, R_{r2} and R_{r1} as 59.8%, 66.2%, and 78.1%, respectively. Similarly, the fixing ratios of quadruple-shape memory effect for E2 were 47.1%, 40.1%, and 62.8%. The recovery ratios were 59.4%, 64.6% and 70.7% at the programming temperatures of 70 °C, 50 °C, and 30 °C, respectively (See Figure 4.2f).

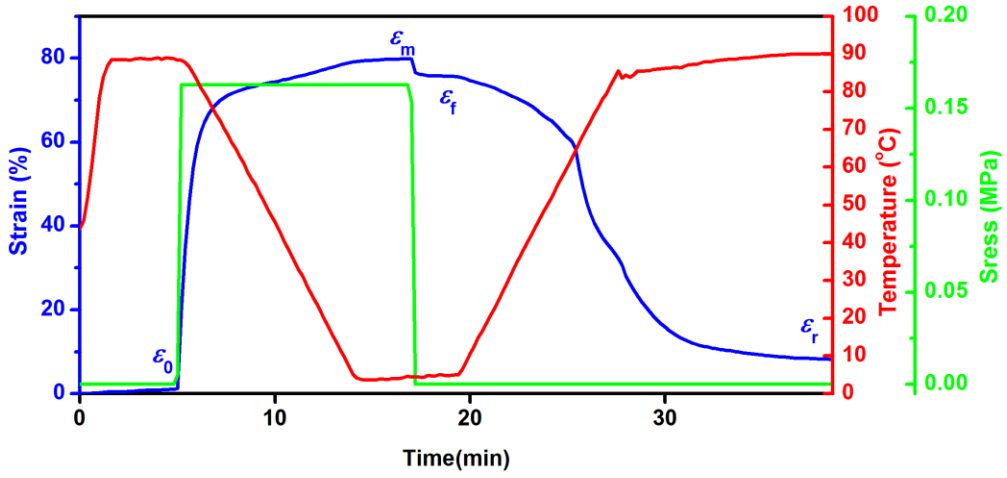

(a)

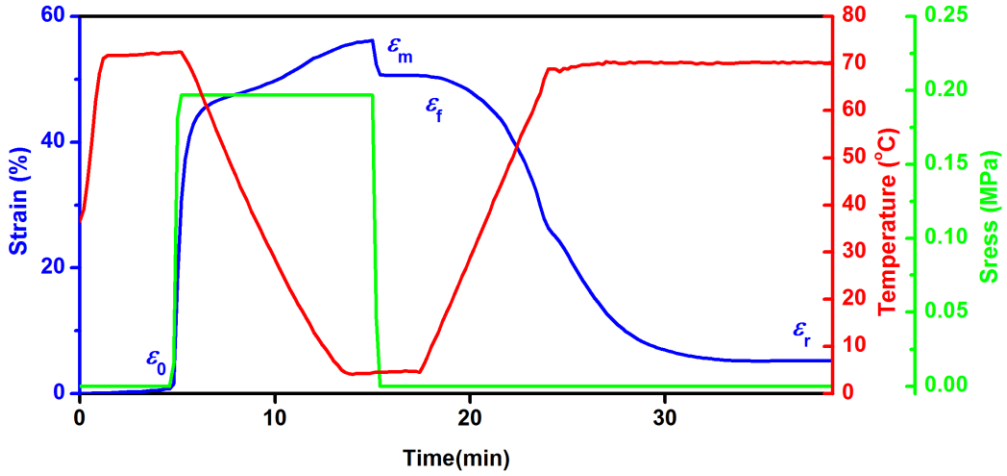
Strain (%)
Temperature (°C)
Sress (MPa)
Time(min)
ε_m
ε_f
ε_0
ε_r

(b)

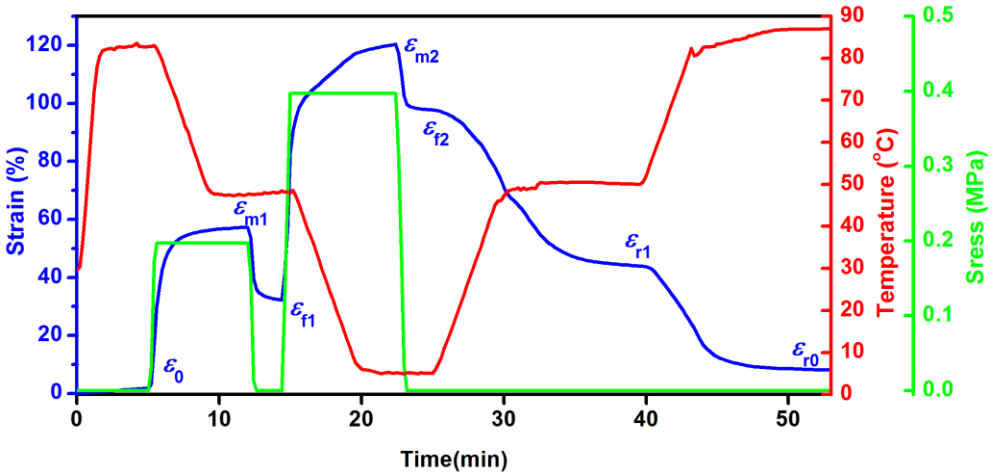
Strain (%)
Temperature (°C)
Sress (MPa)
Time(min)
ε_{m2}
ε_{f2}
ε_{m1}
ε_{f1}
ε_{r1}
ε_0
ε_{r0}

(c)

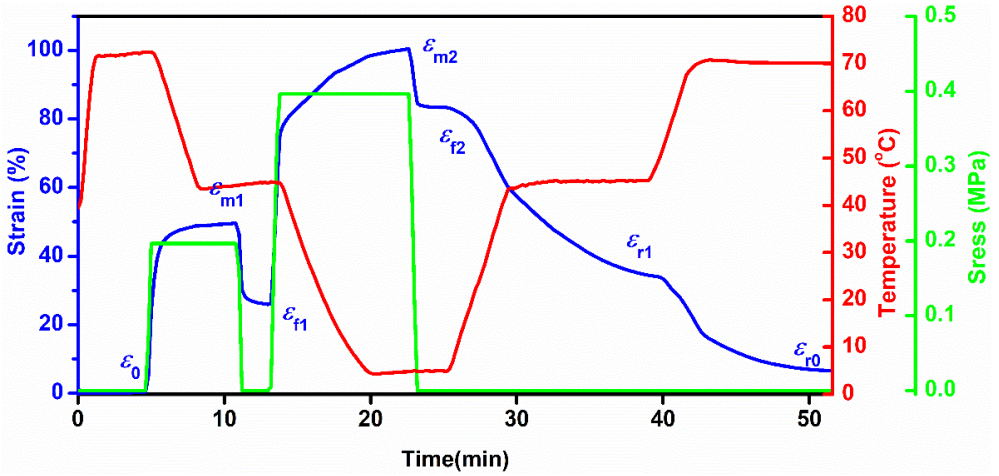
Strain (%)
Temperature (°C)
Sress (MPa)
Time(min)
ε_{m2}
ε_{f2}
ε_{m1}
ε_{f1}
ε_{r1}
ε_0
ε_{r0}

(d)

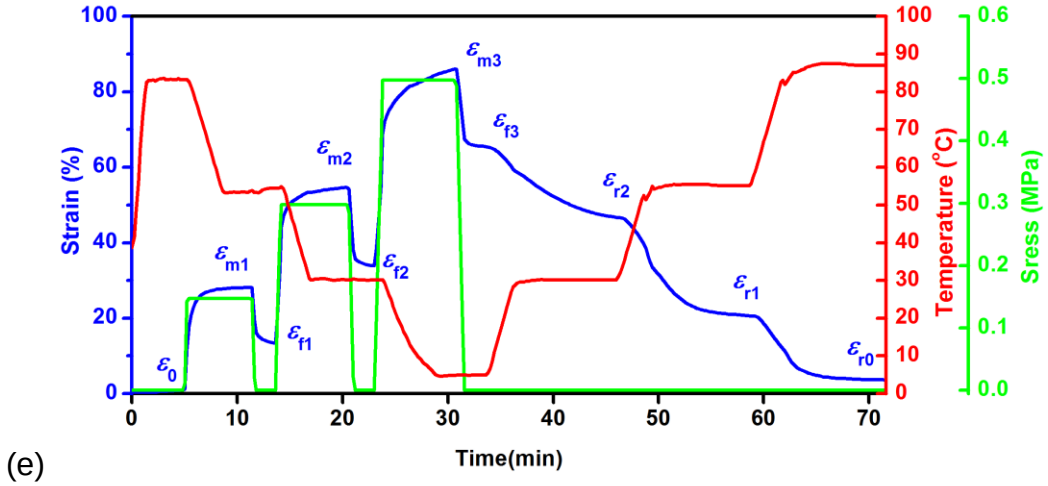

(e)

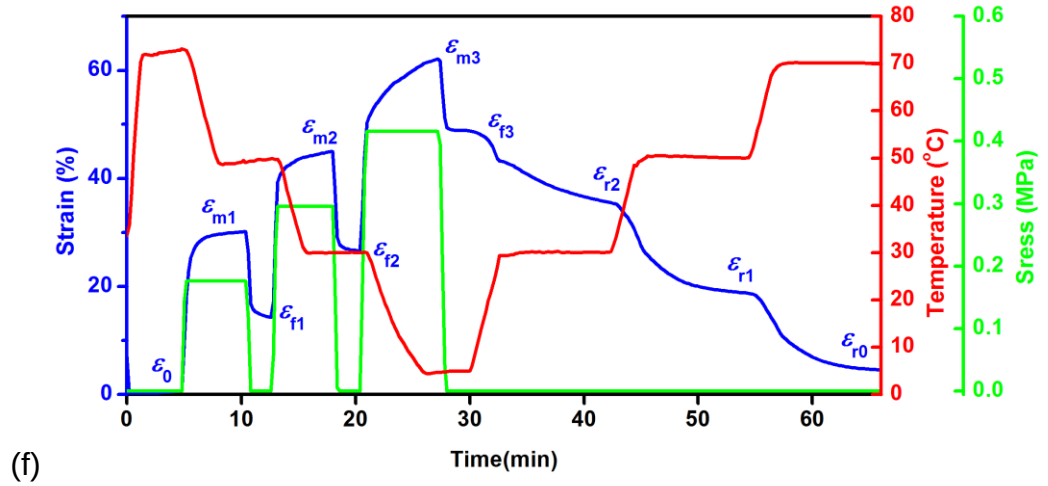

(f)

Figure 4.2. One-way shape memory effect of the polyolefin thermoplastic elastomer blends E1 and E2 samples. (a) Dual-shape memory effect of E1; (b) Dual-shape memory effect of E2; (c) Triple-shape memory effect of E1; (d) Triple-shape memory effect of E2; (e) Quadruple-shape memory effect of E1; (f) Quadruple-shape memory effect of E2.

Figure 4.3 shows a visual illustration of the one-way shape memory effect. The flat specimens of E1 and E2 were prepared, with the edge of E1 sample painted in red and that of E2 in green for the convenience of observation. As shown in Figure 4.3a, the E1 sample with permanent flat shape was first heated to 85 °C and programmed to a temporary Shape 1 (C type). The sample was cooled to 50 °C. After the external force was removed, Shape 1 was fixed. In the second step, E1 with Shape 1 was further programmed to a temporary Shape 2 (helix) at 50 °C, and it was then cooled to 0 °C. The new temporary Shape 2 was thus fixed at 0 °C. E1 with Shape 2 at 0 °C was then heated back to 50 °C and 85 °C, the sample was first recovered to Shape 1 and then to the permanent flat shape. For each step of recovery, the shape switched over a span of seconds. Similarly, an E2 sample could also fix a temporary Shape 3 at 50 °C and an additional temporary Shape 4 at 0 °C. Upon heating, the sample in Shape 4 recovered to Shape 3 at 50 °C and to the permanent flat shape at 75 °C. The one-way multi-shape memory effects of E1 and E2 were clearly demonstrated.

It becomes evident that the different sized crystal domains having different melting temperatures could fix multiple shapes. At a high temperature, small crystals melt and large crystals maintain a permanent shape. When the sample is programmed to a temporary shape and the temperature decreases to a medium level, e.g. 50 °C, the medium-size crystal domains crystallize and fix a temporary shape. When programmed to an additional temporary shape with temperature further decreased to a lower level, e.g. 5 °C, small crystals fix the second

temporary shape. Finally, upon heating, the different sized crystals melted one after another and the sample quickly recovered its shape to these temporary shapes one by one, and finally back to its permanent shape.

(a)

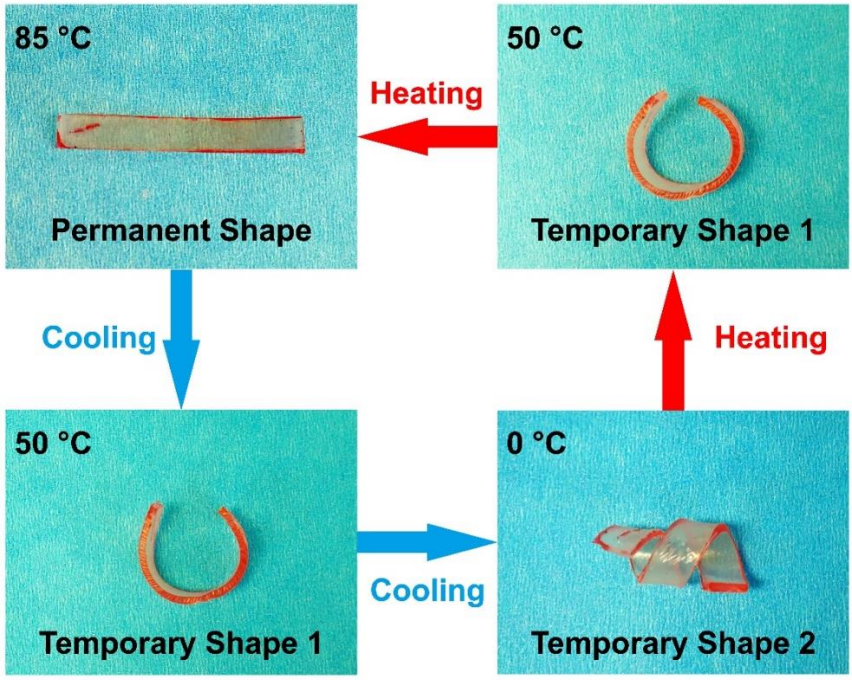

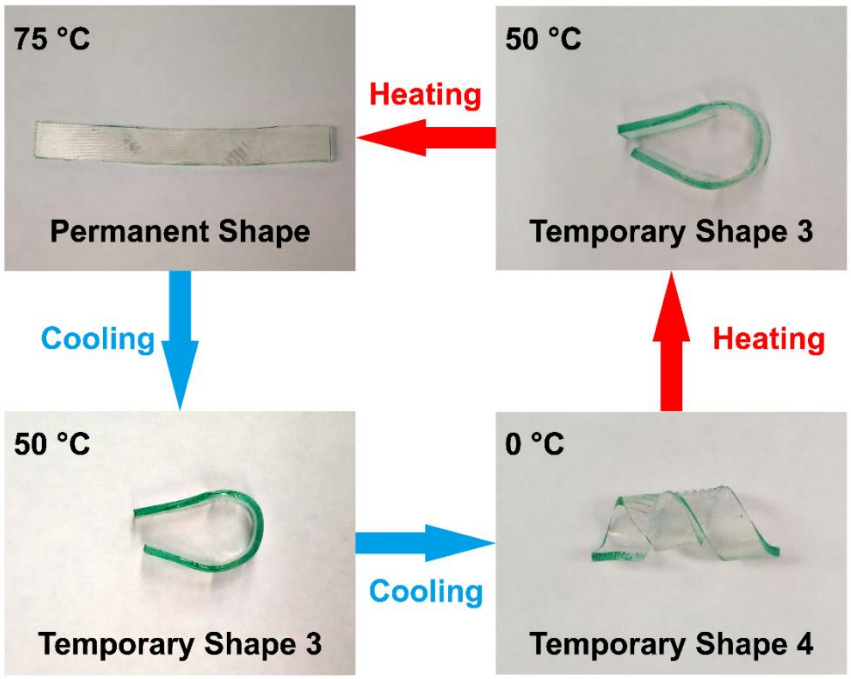

(b)

Figure 4.3. Multi-shape memory effects of (a) E1 at 0 °C, 50 °C and 85 °C; (b) E2 at 0 °C, 50 °C and 75 °C.

4.4.2 Reversible Shape Memory Effect

It should be noted that almost all the previously reported thermoplastic RSMPs were designed and synthesized in the lab, which is costly and labor intensive. It is therefore desirable to broaden material sources and to simplify synthesis methods, to facilitate easy large-scale preparation of RSMPs. The RSMEs of the as-prepared thermoplastic polyolefin elastomer blends were thus investigated. The E1 and E2 samples were measured to explore their possible applications as RSMPs.

RSME was first measured under certain external stress conditions. As shown in Figure 4.4a, E1 was heated to the programming temperature of 82 °C. After stretched under 0.25 MPa, the temperature was reduced from 82 °C to 5 °C at the rate of 10 °C/min. With the constant external stress of 0.25 MPa, the sample was then heated to 50 °C at the rate of 10 °C/min and remained isothermal for 3 min. Upon heating, it was partially contracted and the reversible strain ε_{rb} was recorded. The sample was cooled down again to 5 °C, during which it was elongated to the stable strain ε_s. Figure 4.4a shows five cycles of cooling and heating E1. The reversible ratio was calculated as 10.0%, demonstrating RSME under certain stress. When the constant external stress decreased to 0.2 MPa (Figure 4.4b), the resulted reversible ratio decreased to 8.2%, suggesting that the polymer chains were more easily oriented uniaxially with more crystals formed along the stretching direction while under larger external stress. Figure 4.4c shows that E1 had no RSME under the free-standing condition. The RSME of E2 was also measured. In Figure 4.4d and Figure 4.4e, E2 yielded reversible ratios of 15.9% and 10.7% under 0.25 MPa and 0.2 MPa, respectively, which were higher than those of E1 under the same external stress. In particular, E2 still possessed the reversible ratio of 4.2% under the stress-free condition, suggesting a better RSME of E2 than E1.

The E2 sample contained three POE components having similar chain structures but slightly different crystalline ethylene sequence lengths, which resulted in a continuous broad distribution of crystal sizes, as shown in Figure

4.1b. This would be advantageous for an oriented crystallization of the small crystals along the direction constrained by comparably larger oriented crystal domains. In contrast, the E1 sample contained two POE components having relatively short crystalline ethylene sequence lengths and one OBC component with much longer crystalline ethylene sequence length, which resulted in a discontinuous crystal size distribution, evident from the separated melting transitions in Figure 4.1a. The large crystals in E1 might not be able to constrain crystallization behavior of the short crystalline ethylene segments, as illustrated in Scheme 1. In the range of experimental temperatures, the large crystal domains with high melting temperature in E1 could only fix the permanent shape but could not induce the oriented crystallization found with the small crystals. There were not adequate crystal domains to act as the skeleton to keep a uniaxially oriented chain conformation. This eventually resulted in the RSME of E1 being weaker than that of E2, under either external force or free-standing conditions.

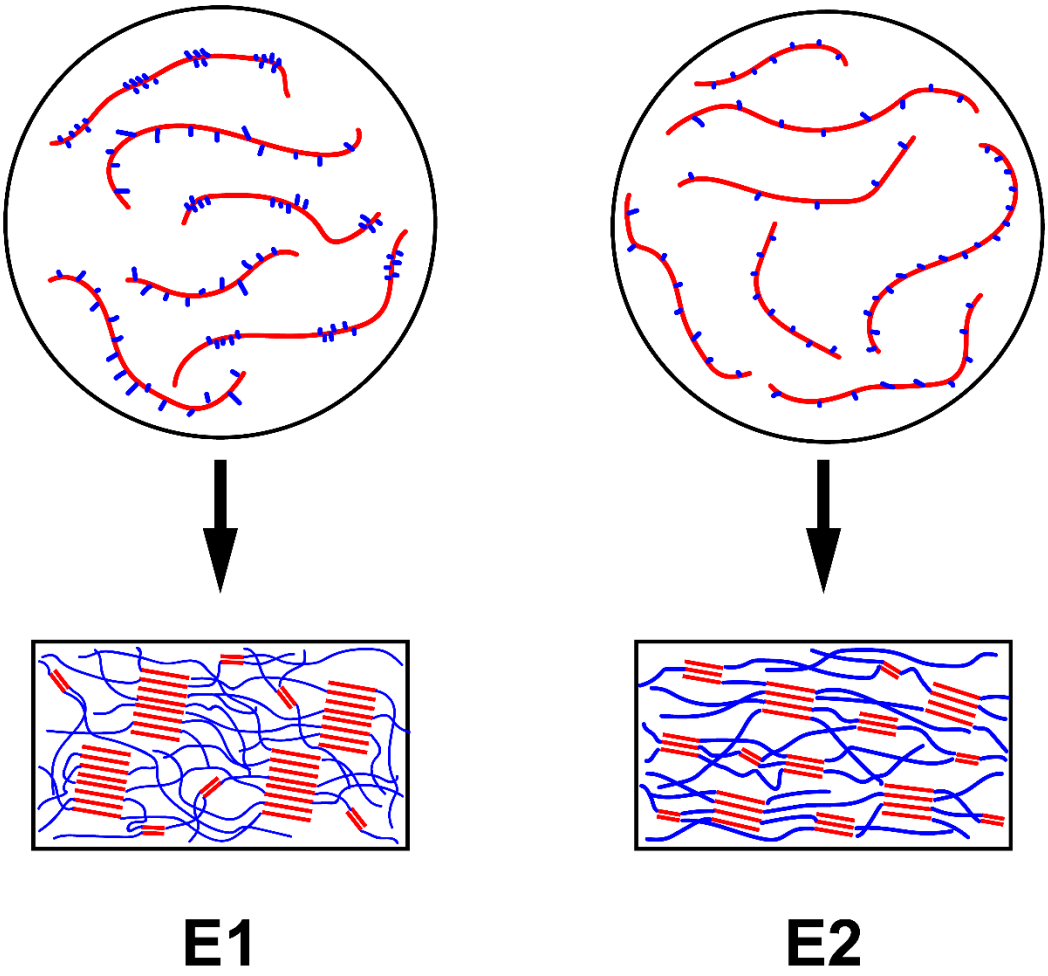

Scheme 4.1. Illustration of the chain structures and crystallization mechanism of E1 and E2

The RSME of the thermoplastic polyolefin elastomer blends was successfully demonstrated. Compared to the thermoset RSMP, the as-prepared E1 and E2 blends showed smaller reversible ratios, which was reasonable due to their lower mechanical strength and less chain orientation ability, caused by higher chain mobility. The reversible shape memory performance of the polyolefin blends

could be further improved by optimizing the material sources and structures. The purpose for this work was to explore a possible route via facile compounding of commercially available polymers for a large-scale preparation of the reversible shape memory materials.

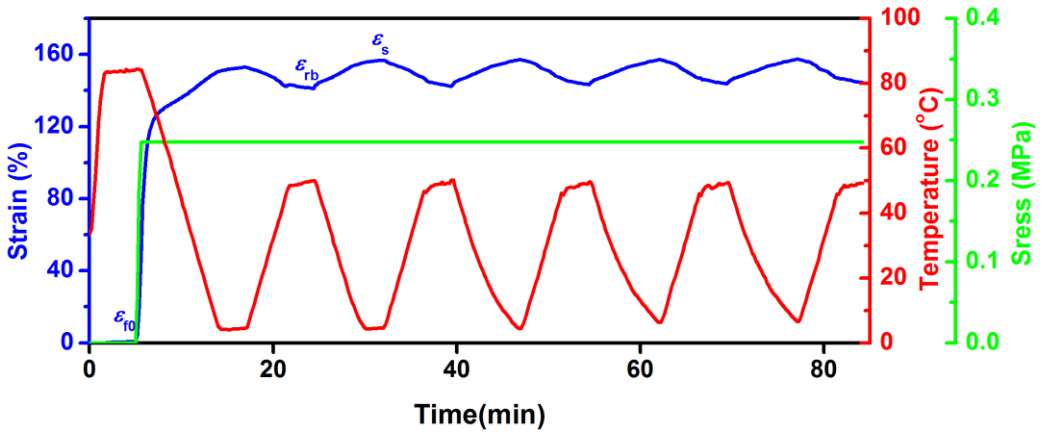

(a)

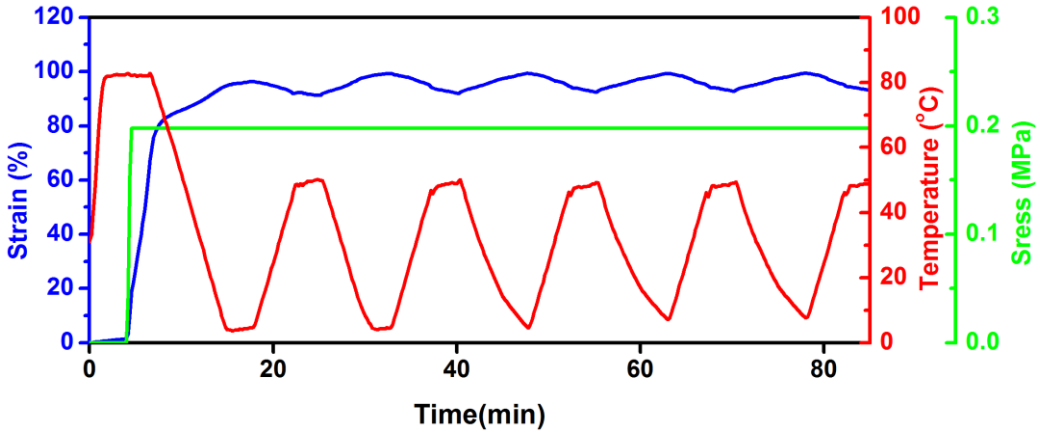

(b)

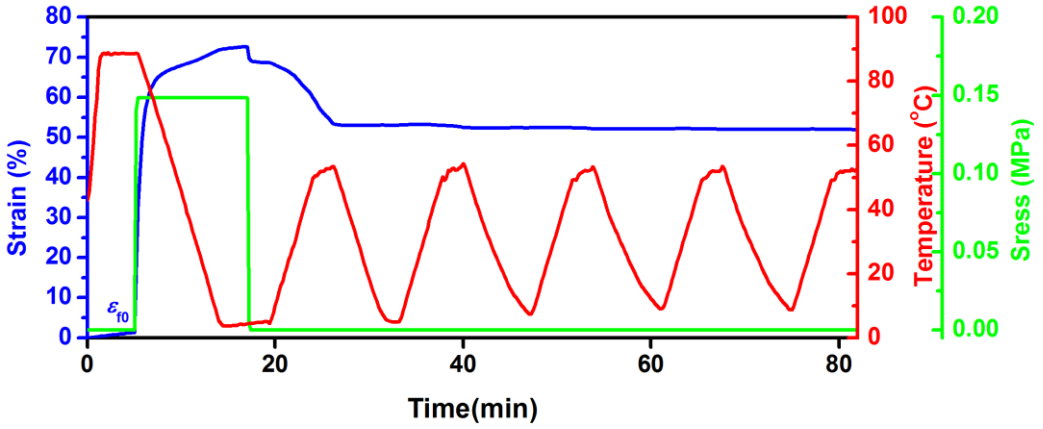
Strain (%)
Temperature (°C)
Sress (MPa)
Time(min)
ε_{f0}

(c)

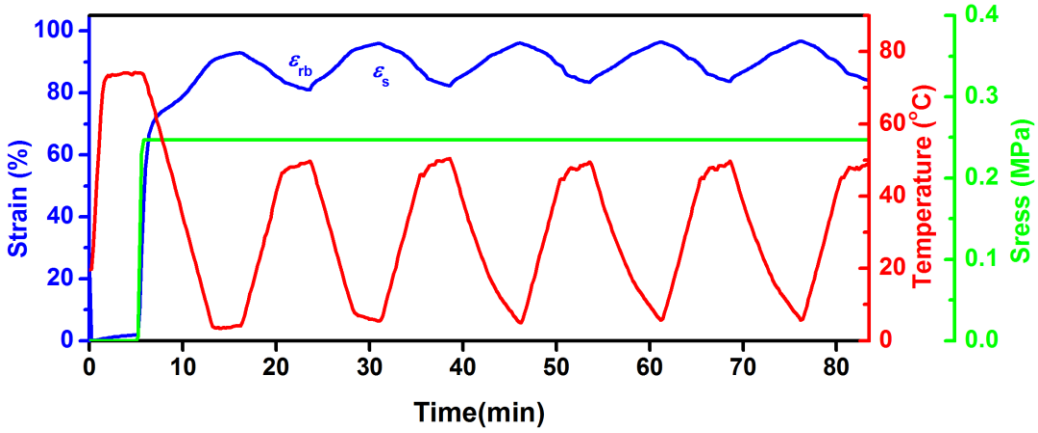
Strain (%)
Temperature (°C)
Sress (MPa)
Time(min)
ε_{rb}
ε_{s}

(d)

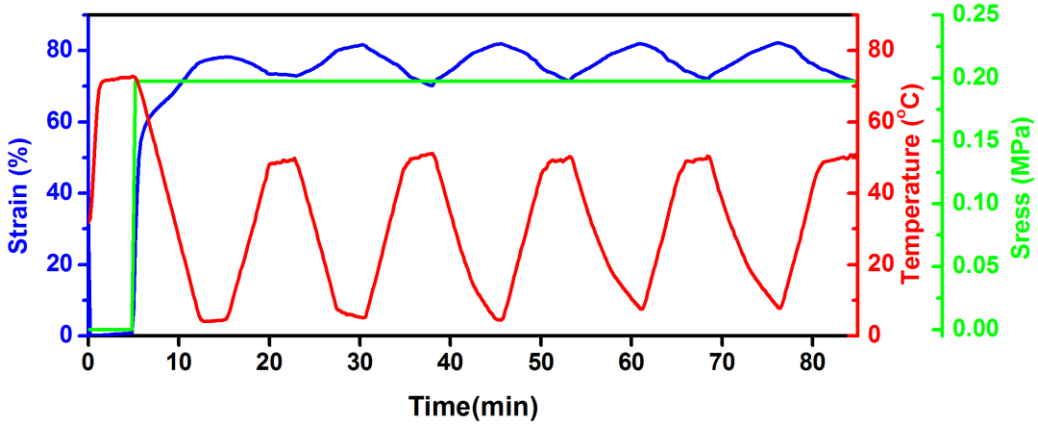
Strain (%)
Temperature (°C)
Sress (MPa)
Time(min)

(e)

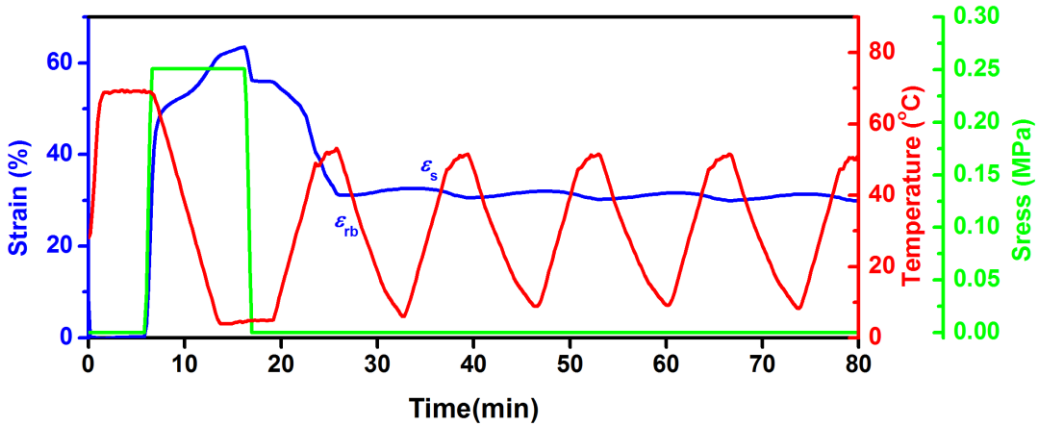

(f)

Figure 4.4. RSMEs of E1 (a, b, and c) and E2 (d, e, and f) under stress and stress-free conditions.

The oriented crystallization phenomena were confirmed by an XRD analysis. The E1 and E2 films were heated at 80 °C for 4 min. Some samples were stretched to 100% strain and quenched to 5 °C to fix the pre-strain state, while the others were quenched to 5 °C without pre-stretching. The samples were then measured by XRD at room temperature. Figure 4.5a and 5b show XRD spectra of the E1 and E2 samples with 0% and 100% pre-strain, respectively. The peak near 25° was attributed to the reflection of (110) crystallographic plane, while the peak near 27° was attributed to the reflection of (200) crystallographic plane. The broad peak near 23° was attributed to the amorphous phase. In Figure 4.5a, the E1 samples with 0% and 100% pre-strain showed little difference in the reflection intensity at (100) plane. There was no significant difference in the crystal domains of the two samples. The polymer chains oriented by stretching at 80 °C had no contribution to induce the formation of new crystal domains under stress-free

condition, corresponding to the results shown in Figure 4.4c. On the other hand, Figure 4.5b shows that E2 with 100% pre-strain had a higher reflection intensity for the (110) and (200) planes than the corresponding samples without pre-strain. Pre-stretching yielded a higher crystallinity in E2. The oriented crystallization along the stretched polymer chains in E2 could occur at 80 °C. The XRD curves of the pre-stretched E1 and E2 samples at various temperatures were also provided in Figure S4.1, as supporting information. Both E1 and E2 maintained obvious crystalline reflections at 50 °C, explaining the good ability of shape fixation at 50 °C in the multi-shape memory exhibition.

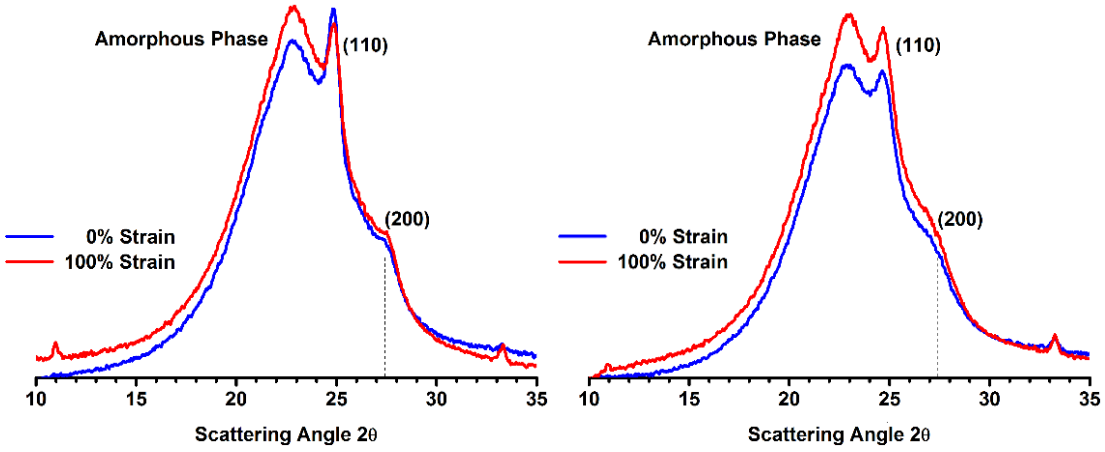

(a) (b)

Figure 4.5. XRD curves of (a) E1 and (b) E2 samples with 0% and 100% strain at room temperature.

The RSME of E2 under the free-standing condition was also confirmed in Figure 4.6. The E2 sample was hot-pressed and cut into a dimension of 40×5×1 mm. The sample was first heated to 75 °C for 4 min. It was then programmed to a V shape and quenched to 0 °C. After the temporary V shape with 36.1° was fixed, the external force was removed. It was then heated to 50 °C. A shape change was clearly observed with the angle opened up to 44.5°. Repeated cooling and heating cycles between 0 °C and 50 °C led to the angle actuation, as recorded in Figure 4.6b, demonstrating a good RSME of the E2 sample under the stress-free condition.

(a)

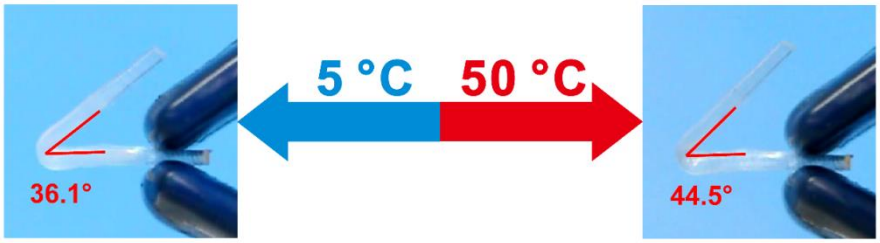

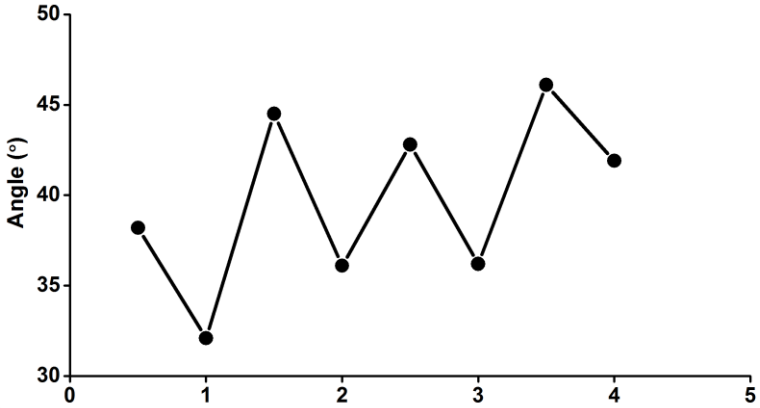

Figure 4.6. (a) RSME of E2 in a free-standing condition between 5 °C and 50 °C. (b) angle actuation of a V-shape sample versus cooling and heating cycles.

4.4.3 The mechanism for the reversible shape memory effect of thermoplastic polyolefin elastomer blends

Based on the above experimental observations, we provide the following mechanistic explanation to RSME of the as-prepared thermoplastic polyolefin elastomer blends, as illustrated in Scheme 2. A wide continuous melting transition was realized through the simple blending of several commercial thermoplastic polyolefin elastomer components in an appropriate ratio. The blending yielded a wide and continuous size distribution of crystal domains in the blends. The largest crystals had the highest melting temperatures, and acted as physical crosslinks to keep the permanent shape in the range of experimental temperature. At the programming temperature T_p, the sample was programmed

and subsequently cooled to the low temperature T_{low}, during which the polymer chains were oriented by the external programming force. All the crystals having medium and small sizes crystallized along the direction of chain orientation and the oriented crystallization induced an elongation. When the external force was removed at T_{low}, a temporary shape A was fixed. Upon heating to the temperature T_{high}, the small crystals would melt, while the large and medium crystals maintained the chain orientation and fixed a temporary shape B, which was contracted from the temporary shape A. Upon cooling to T_{low}, the oriented chains crystallized again and induced an elongation back to the temporary shape A. The RSME was thus achieved. With a remaining external force during the experiment, the chain orientation would be more significant, resulting in a higher RSME.

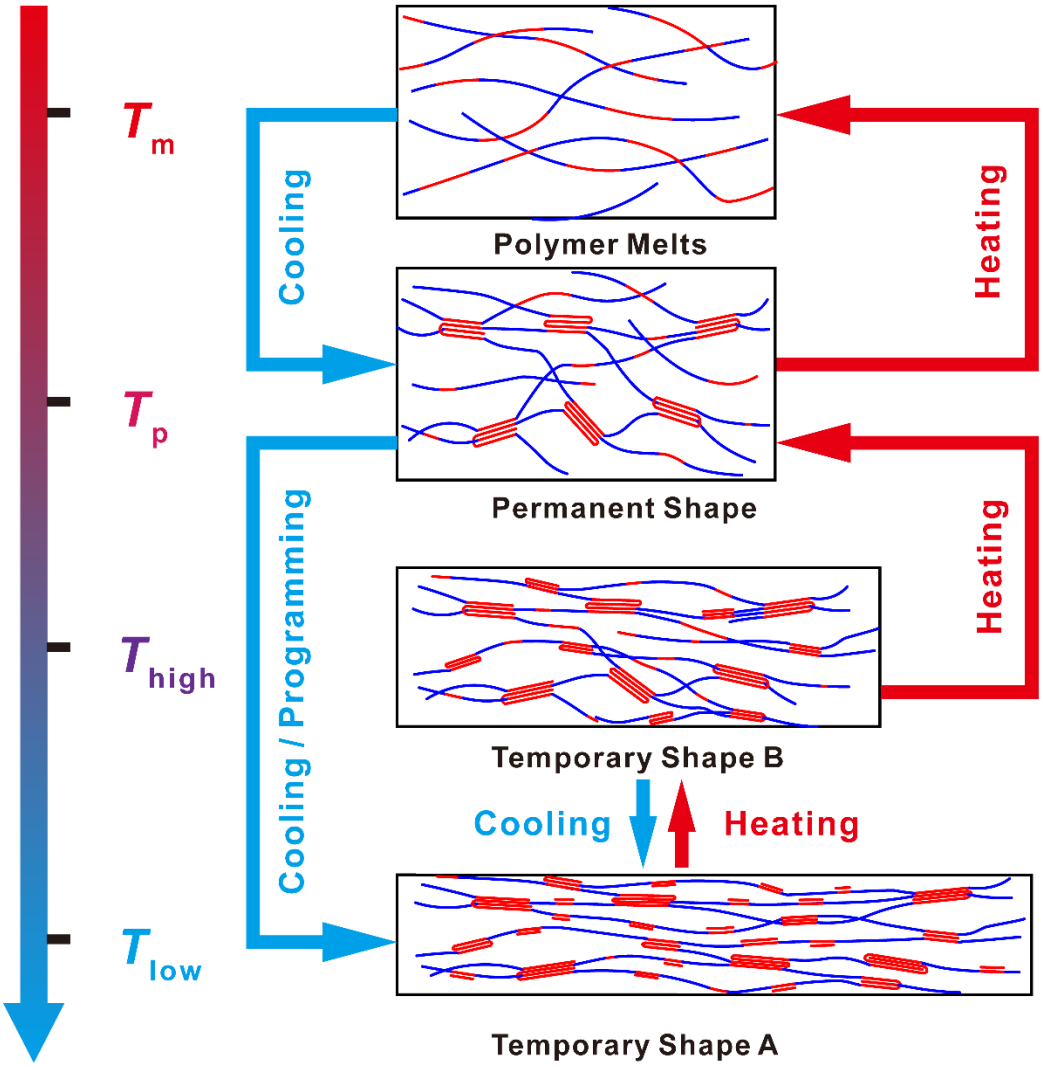

Scheme 4.2. The mechanistic explanation for RSME of the thermoplastic polyolefin elastomer blends.

§ 4.5 Conclusions

In summary, the multiple and reversible shape memory performance of polyolefin thermoplastic elastomer blends has been successfully demonstrated. Two types of thermoplastic polyolefin elastomer blends were prepared by simply blending of several commercial components having different melting temperatures. The resulted elastomers E1 and E2 contained a wide range of melting transitions from 10 °C to 100 °C. The one-way multiple shape memory effect was demonstrated in both E1 and E2 samples at the proper programming temperatures. Both E1 and E2 exhibited reversible shape memory effects under an external force through the mechanism of crystallization-induced elongation (CIE) and melting-induced contraction (MIC). However, only E2 possessed a reversible shape memory effect under the free-standing condition due to its broad melting transition and sufficient amount of the remained crystal domains with the melting temperature around the selected T_{high} temperature in the experiments. This work reported on the first reversible shape memory polymer prepared from commercially available thermoplastic polyolefin elastomers. It significantly broadened the source of the materials for designing reversible shape memory polymers. The simple method through blending of the commercially available polymers facilitates easy and inexpensive preparation of thermoplastic reversible shape memory polymers on a large scale, and thus provides great opportunities for the development of reversible shape memory polymers.

§ 4.6 References

(1) Mather, P. T.; Luo, X.; Rousseau, I. A., Shape Memory Polymer Research. In *Annu. Rev. Mater. Res.*, **2009**, *39*, 445.

(2) Xie, T., Recent advances in polymer shape memory. *Polymer* **2011**, *52*, 4985.

(3) Hu, J.; Zhu, Y.; Huang, H.; Lu, J., Recent advances in shape‐memory polymers: Structure, mechanism, functionality, modeling and applications. *Prog. Polym. Sci.* **2012**, *37*, 1720.

(4) Meng, H.; Li, G., Reversible switching transitions of stimuli-responsive shape changing polymers. *J. Mater. Chem. A* **2013**, *1*, 7838.

(5) Berg, G. J.; McBride, M. K.; Wang, C.; Bowman, C. N., New directions in the chemistry of shape memory polymers. *Polymer* **2014**, *55*, 5849.

(6) Zhao, Q.; Qi, H. J.; Xie, T., Recent progress in shape memory polymer: New behavior, enabling materials, and mechanistic understanding. *Prog. Polym. Sci.* **2015**, *49-50*, 79.

(7) Hager, M. D.; Bode, S.; Weber, C.; Schubert, U. S., Shape memory polymers: Past, present and future developments. *Prog. Polym. Sci.* **2015**, *49-50*, 3.

(8) Zhou, J.; Sheiko, S. S., Reversible shape-shifting in polymeric materials. *J. Polym. Sci., Part B: Polym. Phys.* **2016**, *54*, 1365.

(9) Ahir, S. V.; Tajbakhsh, A. R.; Terentjev, E. M., Self-Assembled Shape-Memory Fibers of Triblock Liquid-Crystal Polymers. *Adv. Funct. Mater.* **2006**, *16*, 556.

(10) Chen, S.; Hu, J.; Zhuo, H.; Zhu, Y., Two-way shape memory effect in polymer laminates. *Mater. Lett.* **2008**, *62*, 4088.

(11) Chung, T.; Romo-Uribe, A.; Mather, P. T., Two-Way Reversible Shape Memory in a Semicrystalline Network. *Macromolecules* **2008**, *41*, 184.

(12) Zhou, J.; Turner, S. A.; Brosnan, S. M.; Li, Q.; Carrillo, J. Y.; Nykypanchuk, D.; Gang, O.; Ashby, V. S.; Dobrynin, A. V.; Sheiko, S. S., Shapeshifting: Reversible Shape Memory in Semicrystalline Elastomers. *Macromolecules* **2014**, *47*, 1768.

(13) Huang, M.; Dong, X.; Wang, L.; Zhao, J.; Liu, G.; Wang, D., Two-way shape memory property and its structural origin of cross-linked poly(epsilon-caprolactone). *RSC Adv.* **2014**, *4*, 55483.

(14) Behl, M.; Kratz, K.; Noechel, U.; Sauter, T.; Lendlein, A., Temperature-memory polymer actuators. *Proc. Natl. Acad. Sci. U. S. A.* **2013**, *110*, 12555.

(15) Li, J.; Rodgers, W. R.; Xie, T., Semi-crystalline two-way shape memory elastomer. *Polymer* **2011**, *52*, 5320.

(16) Zotzmann, J.; Behl, M.; Hofmann, D.; Lendlein, A., Reversible Triple-Shape Effect of Polymer Networks Containing Polypentadecalactone- and Poly(ε-caprolactone)-Segments. *Adv. Mater.* **2010**, *22*, 3424.

(17) Behl, M.; Kratz, K.; Zotzmann, J.; Nöchel, U.; Lendlein, A., Reversible Bidirectional Shape-Memory Polymers. *Adv. Mater.* **2013**, *25*, 4466.

(18) Xie, H.; Cheng, C.; Deng, X.; Fan, C.; Du, L.; Yang, K.; Wang, Y., Creating Poly(tetramethylene oxide) Glycol-Based Networks with Tunable Two-Way Shape Memory Effects via Temperature-Switched Netpoints. *Macromolecules* **2017**, *50*, 5155.

(19) Kolesov, I.; Dolynchuk, O.; Borreck, S.; Radusch, H., Morphology-controlled multiple one- and two-way shape-memory behavior of cross-linked polyethylene/poly(ε-caprolactone) blends. *Polym. Adv. Technol.* **2014**, *25*, 1315.

(20) Dolynchuk, O.; Kolesov, I.; Radusch, H., Theoretical Description of an Anomalous Elongation During Two-Way Shape-Memory Effect in Crosslinked Semicrystalline Polymers. *Macromol. Symp.* **2014**, *346*, 48.

(21) Westbrook, K. K.; Parakh, V.; Chung, T.; Mather, P. T.; Wan, L. C.; Dunn, M. L.; Qi, H. J., Constitutive Modeling of Shape Memory Effects in Semicrystalline Polymers with Stretch Induced Crystallization. *J. Eng. Mater. Technol.* **2010**, *132*, 041010.

(22) Lu, L.; Cao, J.; Li, G., Giant reversible elongation upon cooling and contraction upon heating for a crosslinked cis poly(1,4-butadiene) system at temperatures below zero Celsius. *Sci. Rep.* **2018**, *8*, 14233.

(23) Lu, L.; Li, G., One-Way Multishape-Memory Effect and Tunable Two-Way Shape Memory Effect of Ionomer Poly(ethylene-co-methacrylic acid). *ACS Appl. Mater. Interfaces* **2016**, *8*, 14812.

(24) Bothe, M.; Pretsch, T., Bidirectional actuation of a thermoplastic polyurethane elastomer. *J. Mater. Chem. A* **2013**, *1*, 14491.

(25) Biswas, A.; Aswal, V. K.; Sastry, P. U.; Rana, D.; Maiti, P., Reversible Bidirectional Shape Memory Effect in Polyurethanes through Molecular Flipping. *Macromolecules* **2016**, *49*, 4889.

(26) Gao, Y.; Liu, W.; Zhu, S., Polyolefin Thermoplastics for Multiple Shape and Reversible Shape Memory. *ACS Appl. Mater. Interfaces* **2017**, *9*, 4882.

(27) Yan, W.; Rudolph, T.; Noechel, U.; Gould, O.; Behl, M.; Kratz, K.; Lendlein, A., Reversible Actuation of Thermoplastic Multiblock Copolymers with Overlapping Thermal Transitions of Crystalline and Glassy Domains. *Macromolecules* **2018**, *51*, 4624.

(28) Jin, B.; Song, H.; Jiang, R.; Song, J.; Zhao, Q.; Xie, T., Programming a crystalline shape memory polymer network with thermo- and photo-reversible bonds toward a single-component soft robot. *Sci. Adv.* **2018**, *4*, o3865.

(29) Luo, Y.; Guo, Y.; Gao, X.; Li, B.; Xie, T., A General Approach Towards Thermoplastic Multishape-Memory Polymers via Sequence Structure Design. *Adv. Mater.* **2013**, *25*, 743.

(30) Kolesov, I. S., Multiple shape-memory behavior and thermal-mechanical properties of peroxide cross-linked blends of linear and short-chain branched polyethylenes. *eXPRESS Polym. Lett.* **2008**, *2*, 461.

(31) Zhao, J.; Chen, M.; Wang, X.; Zhao, X.; Wang, Z.; Dang, Z.; Ma, L.; Hu, G.; Chen, F., Triple Shape Memory Effects of Cross-Linked Polyethylene/Polypropylene Blends with Cocontinuous Architecture. *ACS Appl. Mater. Interfaces* **2013**, *5*, 5550.

(32) Zhang, Q.; Feng, J., Difunctional olefin block copolymer/paraffin form-stable phase change materials with simultaneous shape memory property. *Sol. Energy Mater. Sol. Cells* **2013**, *117*, 259.

(33) Flory, P. J., Role of Crystallization in Polymers and Proteins. *Science* **1956**, *124*, 53.

(34) Mandelkern, L.; Roberts, D. E.; Diorio, A. F.; Posner, A. S., Dimensional Changes in Systems of Fibrous Macromolecules: Polyethylene1. *J. Am. Chem. Soc.* **1959**, *81*, 4148.

(35) Kolesov, I.; Dolynchuk, O.; Jehnichen, D.; Reuter, U.; Stamm, M.; Radusch, H., Changes of Crystal Structure and Morphology during Two-Way

Shape-Memory Cycles in Cross-Linked Linear and Short-Chain Branched Polyethylenes. *Macromolecules* **2015**, *48*, 4438.

(36) Dolynchuk, O.; Kolesov, I.; Androsch, R.; Radusch, H., Kinetics and dynamics of two-way shape-memory behavior of crosslinked linear high-density and short-chain branched polyethylenes with regard to crystal orientation. *Polymer* **2015**, *79*, 146.

(37) Ma, L.; Zhao, J.; Wang, X.; Chen, M.; Liang, Y.; Wang, Z.; Yu, Z.; Hedden, R. C., Effects of carbon black nanoparticles on two-way reversible shape memory in crosslinked polyethylene. *Polymer* **2015**, *56*, 490.

(38) Liu, W.; Ojo, A. T.; Wang, W.; Fan, H.; Li, B.; Zhu, S., Preparation of ultrahigh molecular weight ethylene/1-octene block copolymers using ethylene pressure pulse feeding policies. *Polym. Chem.* **2015**, *6*, 3800.

§ 4.7 Supporting information

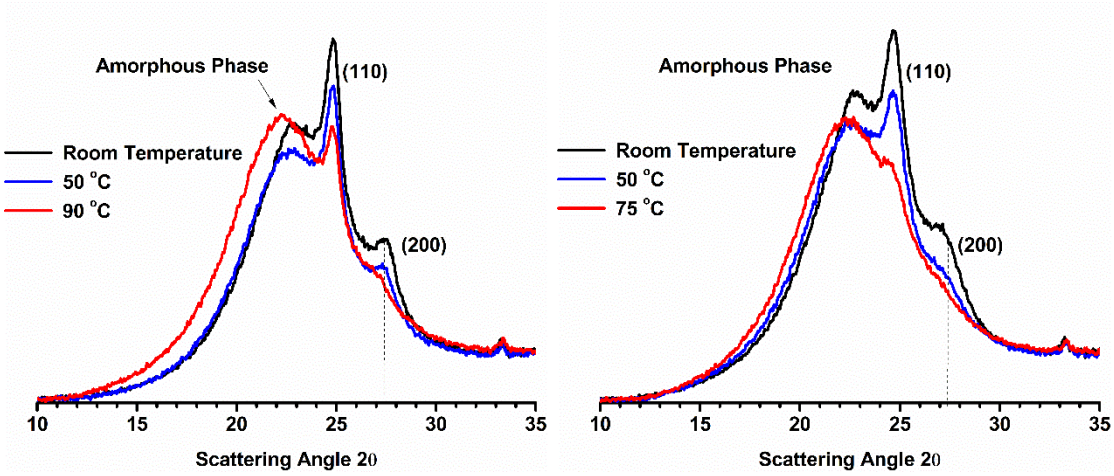

A) B)

Figure S4.1. In situ XRD curves of A) E1 sample with 100% strain at room temperature, 50 °C, and 90 °C. And B) E2 sample with 100% strain at room temperature, 50 °C, and 75 °C. Both E1 and E2 samples were first heated to 80 °C and kept for 4 min, then the sample was stretched to 100% strain and cooled to 5 °C at the rate of 5 °C/min and kept at 5 °C until measurement.

5 REVERSIBLE SHAPE MEMORY POLYMER FROM SEMICRYSTALLINE POLY(ETHYLENE-CO-VINYL ACETATE) WITH DYNAMIC COVALENT POLYMER NETWORKS

In this chapter, the combination of a reconfigurable covalent polymer network and a reversible shape memory polymer based on poly(ethylene-co-vinyl acetate) is presented. This chapter is based on the paper published in the peer-reviewed journal, as follows: “Gao, Y.; Liu, W.; Zhu, S., Reversible Shape Memory Polymer from Semicrystalline Poly(ethylene-co-vinyl acetate) with Dynamic Covalent Polymer Networks, Macromolecules, 2018, 51(28), 8956-8963. (DOI: 10.1021/acs.macromol.8b01724). Reprinted with permission from

Macromolecules, 2018, 51(28), 8956-8963.

Author contributions

Yuan Gao conducted the experiments and wrote the first draft of the manuscript under the guidance of Dr. Shiping Zhu and Dr. Weifeng Liu. Dr. Weifeng Liu provided the first revision of the manuscript. The final revision was provided by Dr. Zhu.

§ 5.1 Abstract

This work reports the reversible shape memory polymer (RSMP) by semicrystalline poly(ethylene-*co*-vinyl acetate) (PEVA) with dynamic covalent polymer networks. The ester linkages in the cross-linked PEVA acted as dynamic covalent bonds in the presence of a transesterification catalyst. This dynamic covalent network imparted the material with good thermal plasticity in a non-flow state at high temperature. The resulting PEVA possessed both the reversible shape memory effect (RSME) and thermadapt property. The thermadapt performance gave little adverse effect on the RSME. This work provides an approach to improve the reprocessability/recyclability of thermoset RSMPs through simple modification of commercially available polymers.

§ 5.2 Introduction

Recently, shape memory polymers (SMPs) as an emerging type stimuli-responsive material have attracted great attention in both academia and industry, especially in the areas of textiles, biomedicine and aerospace, due to their abilities that could memorize different shapes under certain external stimuli such as heat, light, redox, electromagnetic field, pH, and so forth.[1-6]

Besides the remarkable progress in the conventional one-way shape memory polymers, the reversible shape memory polymers (RSMP), which could shift between two different temporary shapes back and forth without new programming, have become a focus in the shape memory polymer research.[7] Several types of shape memory polymers with reversible or two-way actuating property have been reported, such as polymer laminates,[8] liquid crystalline elastomers (LCE),[9] and semicrystalline polymers.[10] Among them, the semicrystalline RSMPs are most interesting due to the abundance of their polymer structures and the relatively easy fabrication.

Since the first attempt of Mather et al.[10] who employed poly(cyclooctene) (PCO) as a RSMP under external stress, a series of semicrystalline polymers have been demonstrated to perform the reversible shape memory effect (RSME). So far, poly(caprolactone) (PCL),[11] the poly(caprolactone) and poly(pentadecalactone) system,[12,13] poly(octylene adipate),[14] poly(tetramethylene

oxide) glycol,[15] poly(ethylene-*co*-vinyl acetate) (PEVA),[16-18] and polyolefins,[19] have been reported to have good reversible shape memory performance under tensile load or at free-standing conditions. Despite the diversity of semicrystalline RSMPs, the mechanisms of the RSME are identical. The semicrystalline RSMPs usually contain crystal domains having several levels of sizes. The large crystal domains act as “skeletons” and fix a first temporary shape at a relatively high temperature during programming. The small crystal domains would be oriented and crystallized along the “skeletons” upon cooling, resulting in a crystallization-induced elongation (CIE) to fix a second temporary shape. The small crystal domains would melt upon heating and contract back to the first temporary shape, which is fixed by the large crystal domains. The so-called melting-induced contraction (MIC) upon heating and crystallization-induced elongation (CIE) upon cooling of the small crystal domains result in the reversible shape memory effect.[2,7]

However, the majority of the reported RSMPs are thermosets, which is disadvantageous in recycle utilization. It represents a great challenge for material researchers to develop novel RSMP structures having improved processing performance for a wide range of potential applications. A feasible approach is to develop thermoplastic RSMPs. Li et al.[20] demonstrated a thermoplastic poly(ethylene-co-methacrylic acid) and Maiti et al.[21] demonstrated a thermoplastic polyurethane, that showed RSME. Gao et al.[22] showed that the ethylene/1-octene diblock copolymer, a kind of polyolefin thermoplastic elastomer,

gave good RSME.[23] These thermoplastic RSMPs could be melted at high temperature and remolded for resetting the permanent shapes. However, complicated molds were required in the fabrication of sophisticated shapes, which is a time- and resource-consuming process. In addition, compared with thermoset RSMPs, thermoplastic RSMPs usually exhibit poorer mechanical strength and weaker reversibility.[6]

As a brand-new concept in polymer chemistry, the dynamic covalent polymer network has been introduced into polymer material design over the past few years.[24,25] The dynamic covalent polymer network is composed of exchangeable covalent bonds such as ester bonds,[26] carbamoyl bonds,[27] and ally sulfide bonds.[28] These bonds could break and form new connections under external stimuli or in the presence of catalysts. The dynamic covalent polymer networks are thus reconfigurable at a certain condition and the material maintains its original 3D shape. On the other hand, it is also very plausible that the polymers with dynamic covalent networks could be reprocessed and reshaped when the networks are rearranged, during which the polymers show a significant stress relaxation phenomenon. This unique feature of neither thermoplastic nor thermoset facilitates the design of novel polymer materials, which could be reshaped from a simple molded shape to a relatively more sophisticated shape.

Recently, a variety of dynamic covalent bonds have been employed in the design and fabrication of shape memory polymers to improve their

reprocessability. Mather et al.[29] reported a PCL network with anhydride linkages as the dynamic covalent bonds. Xie's group demonstrated a series of reversible reactions and established different dynamic covalent networks in SMPs, such as transesterification,[30] Diels-Alder reaction,[31] and transcarbamoylation.[32-34] They also coined the novel type of SMPs as "thermadapt" SMP. The "thermadapt" concept recognizes the unique material behaviors of thermal adaptability in reprocessing, and it also reflects the fact that such materials combine the processability of "thermoplastics" (linear chains) and the mechanical strength and thermostability of "thermosets" (three dimensional network).[24] However, until now, the SMP with dynamic covalent network has been rarely reported for reversible shape memory effect (RSME). Only a few pioneering works on liquid crystalline elastomers with epoxy and ester groups as the dynamic covalent bonds were reported by Ji et al.[35, 36] Anthamatten et al.[37] introduced photoreactive ally sulfide groups into the PCL-based network to achieve the dynamic reactions. However, the photoirradiation could only reach surface areas and it is not effective for thick polymer devices. As thermoplastic RSMPs usually have poor mechanical strength and reversibility, and thermoset RSMPs are not recyclable, the thermadapt RSMPs provide a good opportunity for the design and synthesis of SMPs having good recycling, as well as mechanical and reversible shape memory properties.

Very recently, Xie et al.[38] reported a type of crystalline shape memory polymer with thermo- and photoreversible bonds, which combined the

"thermadapt" concept with the reversible shape memory effect (RSME). However, the introduced additional photoactive bonds may limit potential application conditions and result in a relatively complicated synthesis route. Poly(ethylene-*co*-vinyl acetate) (PEVA) is a widely used commercial polar polyolefin product. Because of its broad range of melting transition, PEVA has also been demonstrated as one of the RSMPs and it has been well studied as polymer actuators.[16-18,39,40] However, the abundant ester groups of PEVA have seldom been considered as potential reactive bonds in applications. In the present work, the PEVA polymer network is selected as the matrix RSMP. Our objective is to demonstrate that the ester bonds of PEVA could function as a type of important dynamic covalent bond, based on which novel thermadapt RSMPs could be developed.

§ 5.3 Experimental Section

5.3.1 Materials and Preparations

Poly(ethylene-co-vinyl acetate) (25 wt% vinyl acetate, melt index 19 g/min), 1,5,7-triazabicyclo[4.4.0] dec-5-ene (TBD), dicumyl peroxide (DCP), and toluene were purchased from Aldrich. All the chemicals were used without further treatment.

Thermadapt RSMP sample taPEVA was fabricated as follows. 4.8 g of PEVA pellets, 0.1 g of TBD, and 0.1 g of DCP were dissolved and mixed in 100 mL of toluene. The mixture was then poured into a mold and evaporated at room

temperature and pressure for 15 h. The resulting elastomer was put into a mold with dimensions of 40 × 40 × 1 mm^3 and molded on a hot press from Carver Inc. at 1000 6.9 MPa and 160 °C for 20 min. It was then cooled to room temperature to form a flat film. The counterpart thermoset RSMP sample tsPEVA was fabricated using the same method with 4.9 g of PEVA pellets and 0.1 g of DCP.

5.3.2 Polymer Characterization

The melting temperature (T_m) and crystallization temperature (T_c) were measured by a 2910 Modulated DSC (TA Instruments). Each sample was first heated to 160 °C at a heating rate of 50 °C/min, and kept at 160 °C for 3 min. The heating and cooling rates were 10 °C/min between 160 °C and −20 °C. The thermal data were obtained from the second heat segment.

The gel content was measured as follows. 60 mg of each sample was soaked in 10 mL of toluene for 72 h with toluene being refreshed every 24 h. The polymer sample was then dried at 60 °C in a vacuum oven overnight until the sample reached a constant weight. The gel content was calculated as the weight ratio of the sample after and before the toluene extraction. The reported gel content data were an average of three repeat experiments.

The mechanical properties and shape memory effects were measured by a 2980 Modulated DMA (TA Instruments). The temperature-dependent modulus test was performed in a tensile mode. The sample film of 20 × 2 × 1 mm^3 was first cooled to −70 °C, and then heated to 60 °C at a rate of 3 °C/min. The storage

modulus and loss modulus were measured with a frequency of 1 Hz and an amplitude of 0.3% strain.

The stress relaxation effects were measured as follows. Each sample was first cut into the dimensions of 20 × 2 × 1 mm^3 and loaded on the clamp of DMA under the stress relaxation mode. The sample was first heated to a high temperature (e.g., 80 °C) and kept for 4 min. The sample was then stretched to a constant strain of 40%. The stress relaxation curves at the temperature were then recorded.

To measure the reversible shape memory effect, a typical procedure is as follows: The sample was heated to 75 °C for 4 min at the original strain ε_{f0}. It was stretched by a stress around 0.3 MPa. The temperature was then decreased from 75 to 0 °C at a rate of 10 °C/min and the sample was annealed under the stress at 0 °C for 3 min. The stress was then removed and the sample was maintained at 0 °C for another 2 min. It was then heated to 50 °C by 10 °C/min and annealed for 3 min to obtain the reversible length ε_{rb}. After another cooling process to 0 °C, a stable length of ε_s was obtained. The cooling−heating cycles between 0 and 50 °C were repeated five times. The reversible ratio R_{rb} was calculated as

$$R_{\mathrm{rb}} = \frac{\varepsilon_{\mathrm{s}} - \varepsilon_{\mathrm{rb}}}{\varepsilon_{\mathrm{s}} - \varepsilon_{\mathrm{f0}}}$$

The FTIR measurement was performed on a Thermal NICOLET 6700 spectrophotometer. XRD analysis was performed on a Bruker D8 DISCOVER with DAVINCLDESIGN diffractometer using Co as the anode material.

§ 5.4 Results and discussion

The design of thermadapt RSMPs is to incorporate dynamic covalent bonds into a RSMP system. In this work, PEVA materials were employed for the first time as the semicrystalline RSMP with thermadapt properties. Though PEVA materials have been demonstrated as an excellent RSMP, the abundant ester linkages in the network have not been utilized as the dynamic covalent bonds. We selected the organic base 1,5,7-triazabicyclo[4.4.0]dec-5-ene (TBD) as the transesterification catalyst to transform the ester groups. The PEVA pallets, TBD and DCP were solution mixed and were then molded and cross-linked by a hot press to fabricate the elastomer films.

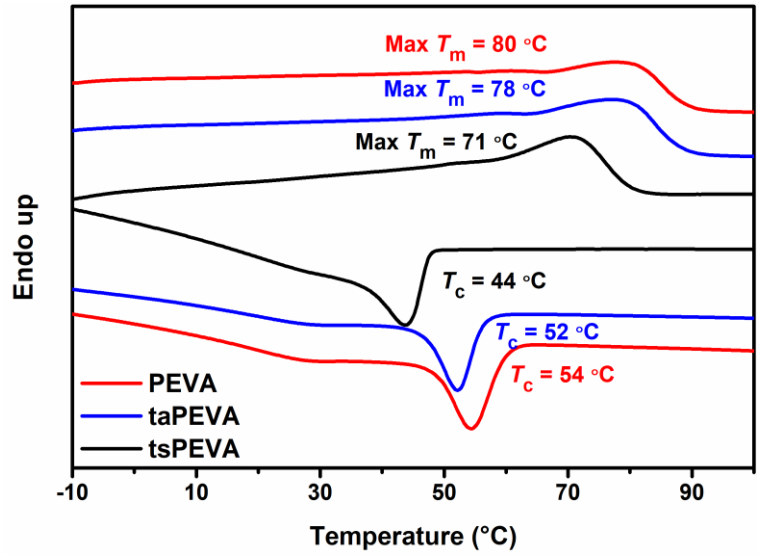

Figure 5.1. DSC heating and cooling curves of PEVA, tsPEVA and taPEVA samples.

The thermal properties of PEVA and their cross-linked counterparts tsPEVA and taPEVA were first evaluated using DSC measurements to determine their memorable temperature range. Figure 5.1 shows the DSC cooling and heating curves in the second round after removing the thermal history. Each PEVA sample exhibited broad melting transitions, indicating there were a series of crystals consisting of crystalline methylene segments with different lengths. Longer methylene segments could form larger crystal domains, which could help to maintain chain orientation as the skeletons according to the CIE/MIC mechanism of RSME. Compared to PEVA, the maximum melting temperature T_m of taPEVA shifted slightly from 80 to 78 °C, while the maximum T_m of tsPEVA shifted to 71 °C. The cooling curve showed the same shifting trend to lower

temperature with T_c shifted from 54 °C for PEVA to 52 and 44 °C for taPEVA and tsPEVA, respectively, which could be explained as the lower crystallinity caused by the poorer chain mobility after cross-linking, and it also demonstrated that tsPEVA contained a higher cross-link density than taPEVA. Based on the DSC melting curves, the PEVA samples should exhibit RSME below 80 °C. In the following measurements, the programming temperature was selected to be 75 °C, a temperature range between 0 and 50 °C was selected to measure the RSME of PEVA samples.

On the other hand, the vinyl acetate groups in PEVA may lead to an effective dynamic covalent polymer network. The cross-linking mechanism of PEVA in the presence of peroxide initiator (e.g. DCP) has been well studied a few decades ago.[41, 42] As illustrated in Scheme 1, the peroxide initiator decomposes and generates radicals at high temperature. The PEVA radicals are generated by hydrogen abstraction mainly on the tertiary CH groups in the backbones and the methyl groups in the side chains. The PEVA radicals may be coupled through termination and generate three types of cross-links, with one of which containing C−C bonds, which is well-known as chemical cross-links. The other two types contain ester groups which may act as potential dynamic cross-links if the transesterification reaction could occur.

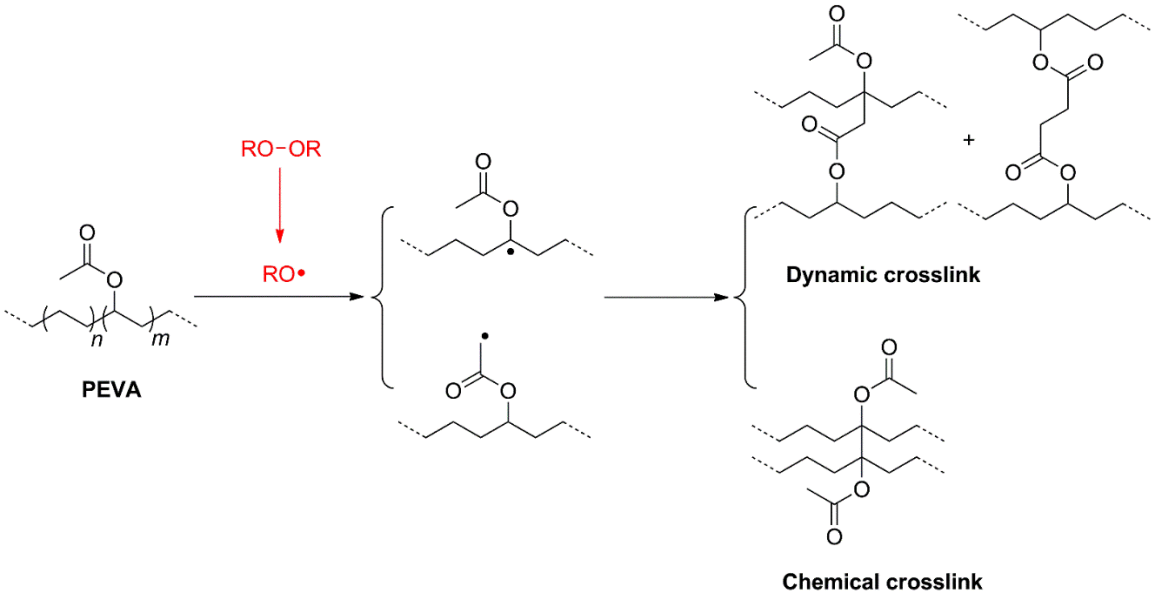

Scheme 5.1. The Mechanism of PEVA Cross-Link Reactions

5.4.1 Thermally-Induced Plasticity Measurements

It is hypothesized that the abundant ester groups in tsPEVA provide a possible rearrangement of the polymer network by transesterification reactions. However, it has not been demonstrated in the literature. The thermadapt property of PEVA was thus investigated with a transesterification catalyst. It is challenging to directly characterize breaking and re-forming of the chemical bonds in polymer films. Fortunately, the dramatic stress relaxation behavior could imply the thermally-induced plasticity.[30-34] The stress relaxation of taPEVA in the first 60 min was measured at a temperature range from 60 to 130 °C, as shown in Figure 5.2. It is shown that within 60 min, a complete stress relaxation was not achieved at the temperature below 80 °C. As the temperature increased, a shorter time

was required for a complete stress relaxation. The time needed for complete relaxation reduced from about 38 min at 90 °C to 2 min at 130 °C, which is a reasonable time frame for experiments to demonstrate an ideal thermally-induced plasticity. In comparison, the tsPEVA film gave only 20% relaxation in 60 min at 80 °C (Figure S5.2). The gel content of taPEVA was 76.2% while that without TBD was 97.8%, also demonstrating that there was a certain amount of ester-cross-linked PEVA chains degraded in the presence of TBD, which could be the potential transesterification sites. The FTIR analysis also indirectly verified the fracture of ester bonds after reheating of taPEVA in the presence of TBD (Figure S5.3). As TBD was the only difference in composition between those two cross-linked PEVA films, TBD was believed to be the reason for endowing the PEVA a dynamic covalent network through the transesterification reactions, as illustrated in Scheme 2. The taPEVA has demonstrated good plasticity at high temperature in the stress relaxation experiments. It thus became possible to remold its permanent shape at the non-flow state.

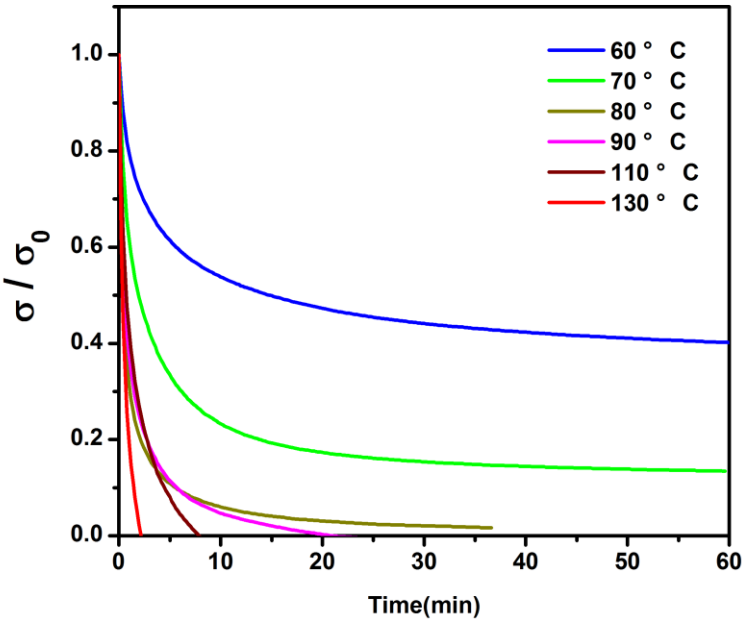

Figure 5.2. Normalized stress relaxation curves of taPEVA film at 60, 70, 80, 90, 110, and 130 °C in the first 60 min.

Based on the stress relaxation measurements, any temperature above 80 °C could be selected as the permanent shape deformation temperature (T_d). However, since the endothermic peak of taPEVA could reach 90 °C as seen in the DSC curves, a higher temperature 120 °C was selected as T_d, separating it from the T_m of PEVA. In addition, the deformation at 120 °C gave an appropriate relaxation time, allowing for convenient operation in the experiments.

In terms of visible display, the dynamic covalent polymer network was further confirmed by the manual permanent shape deformation. As shown in Scheme 2B, a film with the permanent shape I was heated to 120 °C first and kept at the

temperature for 10 min to ensure stress relaxation. The shape was then deformed manually to an S shape and maintained an isotherm for another 10 min, during which the original cross-linking network was broken, and a new polymer network was formed through the transesterification reaction. The film was cooled to room temperature, and the S shape was fixed as a new permanent shape. The dynamic nature of the covalent network was thus confirmed. This permanent S shape resulted from the rearrangement of taPEVA network at 120 °C, which had little effect on the intrinsic shape memory performance. In a normal one-way shape memory cycle, the permanent shape S was heated to the programming temperature T_p = 75 °C and deformed to a new temporary shape M. The external force was removed after the film was cooled to T_{low} = 5 °C to fix the temporary shape M. It should be noticed that when the film was heated back to 75 °C, the temporary shape M recovered to the permanent shape S, but not to the original simple shape I, suggesting that the shape S was a veritable permanent shape after the network rearrangement at 120 °C. The deformation of permanent shape induced by the transesterification reaction could be repeated to reset new shapes at the deformation temperature.[30] In contrast, tsPEVA could only perform a typical shape memory effect, but no thermal adaptability.

A)

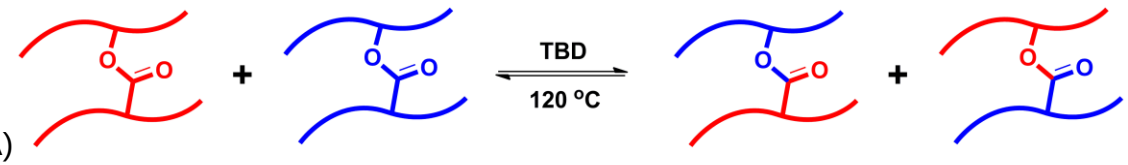

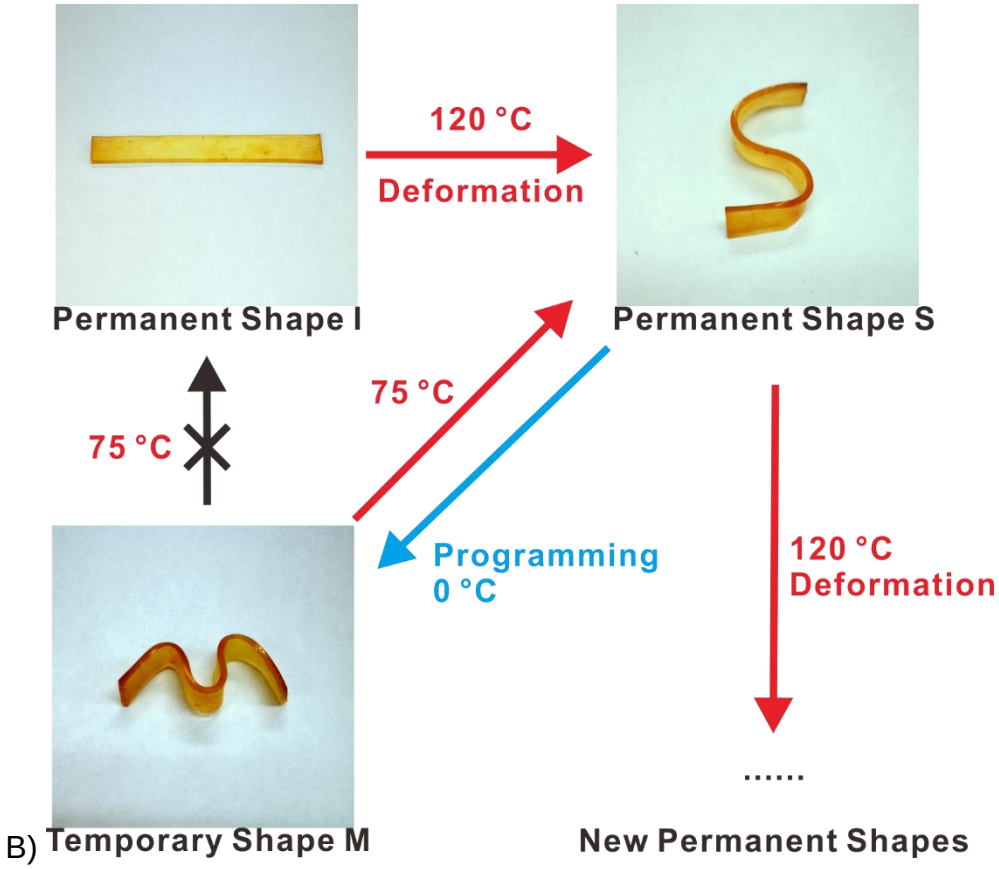

Scheme 5.2. A) Transesterification reactions in taPEVA network, B) Illustration of dynamic structure in the taPEVA system, the film size was 40 × 5 × 1 mm^3.

5.4.2 Reversible Shape Memory Effects

The reversible shape memory effect was measured in the same way as reported in the literature.[23] The detailed programming procedure for RSME was depicted in the Experimental Section. The sample was heated and cooled between 50 and 0 °C five cycles under a stress-free condition. Figure 5.3 shows the strain variation curves of taPEVA and tsPEVA. The taPEVA upon heating and

cooling yielded a reversible strain of 16.9% and a reversible ratio of 10.0%. These values were similar to the recently reported semicrystalline shape memory polymers with thermo- and photoreversible bonds under similar prestretched strains.[38] With tsPEVA, the reversible strain decreased to 10.6%, but the reversible ratio of 10.7% had little change. In the presence of TBD, the taPEVA showed a higher prestretched strain of 150%, in comparison to 50% in tsPEVA, indicating less stable ester linkages in the presence of TBD, which decreased strength of the material and increased mobility of the chains.

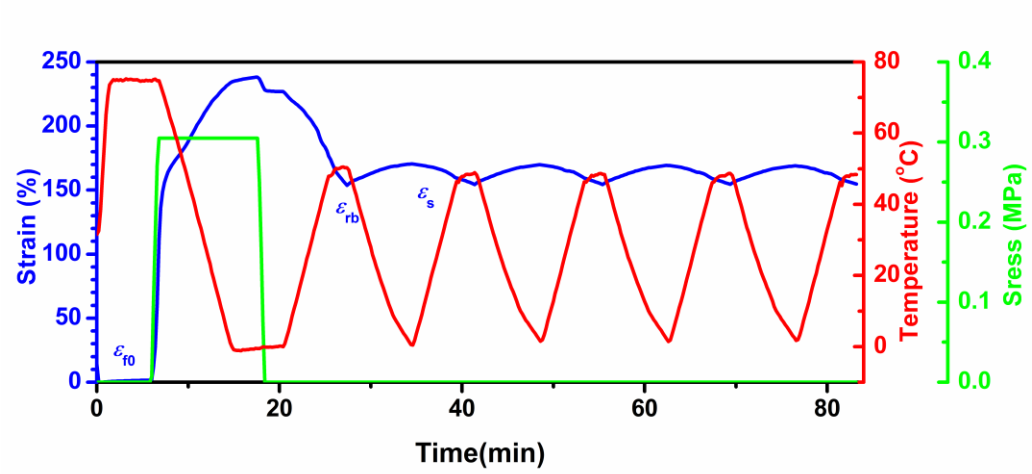

(a)

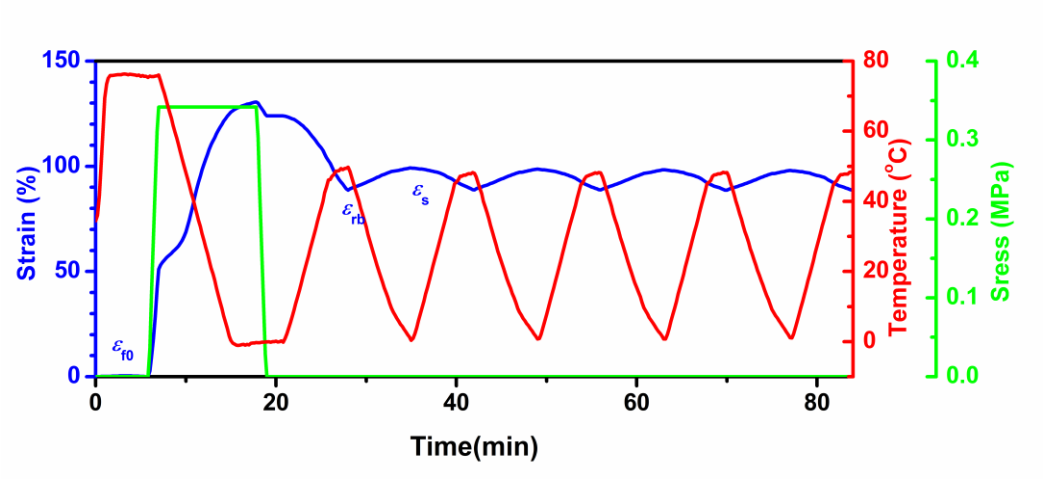

(b)

Figure 5.3. Reversible shape memory effect measurement by DMA of (a) taPEVA and (b) tsPEVA under prestress of 0.3 MPa.

5.4.3 Thermadapt Reversible Shape Memory Effects

From the above illustrations, it becomes clear that PEVA represents a type of efficient thermadapt material and a new kind of RSMP. In this part, a multistep measurement was conducted to combine the thermadapt effect with RSME. A taPEVA sample was first programmed with the prestress of 0.3 MPa under controlled force mode, as in a typical RSME measurement. The stress–strain curve upon the cooling and heating process under free-standing conditions is depicted in segment I of Figure 5.4a, yielding RSME with a reversible strain of 6.4% and a reversible ratio of 7.5%. After being annealed at 80 °C, the sample recovered to the strain of 12.3% was cooled to room temperature. The sample was then programmed with a stress relaxation process when stretched to 57.3% from 12.3% at 120 °C under a small stress in segment II. As shown in Figure 5.4b,

the sample completed the stress relaxation in 1.5 min, and it was cooled to room temperature again for a further RSME measurement. In segment III of Figure 5.4a, a prestress of 0.3 MPa under controlled force mode was again performed, and the strain value was recorded for the second RSME measurement after the stress relaxation process. The sample after the complete stress relaxation could still display RSME with a reversible strain of 7.0% and a reversible ratio of 8.8%, demonstrating that the taPEVA could still achieve RSME after the permanent shape reset. The smaller reversible strains in segment I and III in Figure 5.4a than that in Figure 5.3a were caused by the shorter prestretching time and the smaller prestrain limited by the DMA machine.[23] Similar results were also reported by Xie et al. that the reversible strain increased with the prestretch strain.[38] However, the reversible ratio did not show significant difference between segment I and III in Figure 5.4a, suggesting the orthogonality between the RSME and the thermadapt property.

(a)

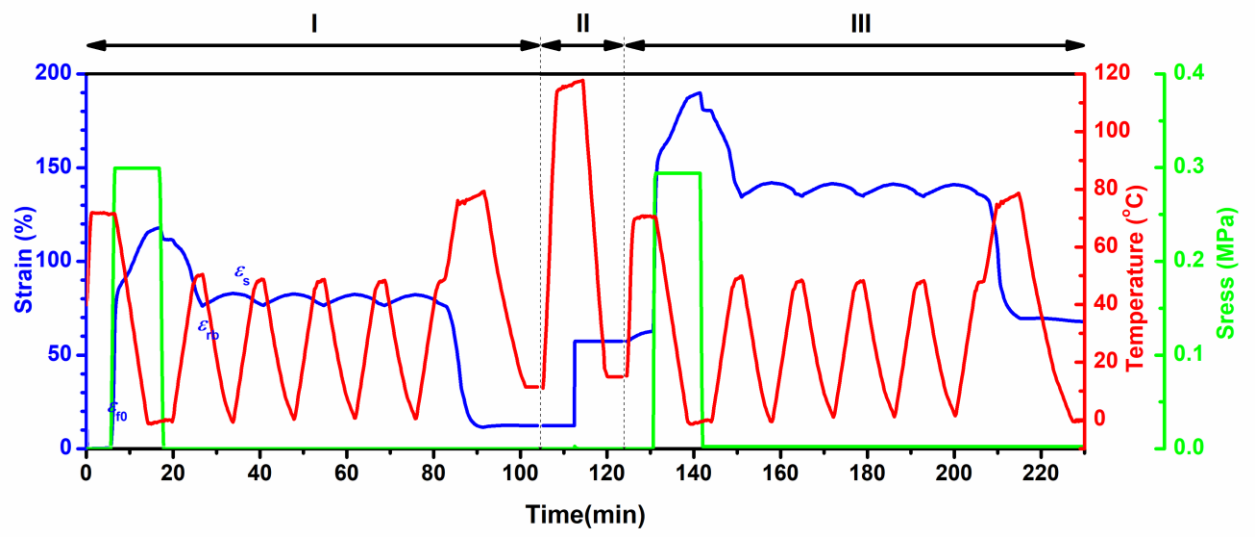

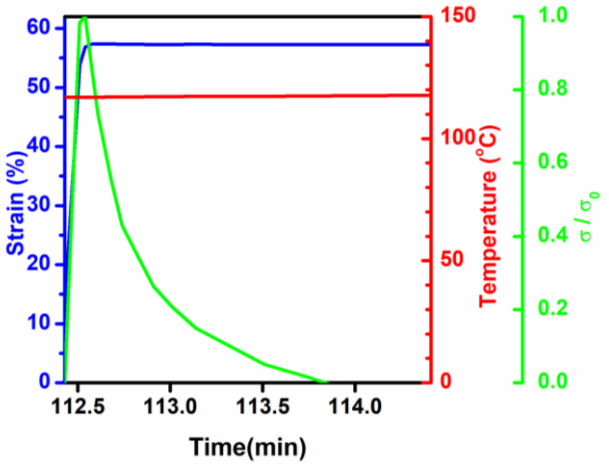

(b)

Figure 5.4. (a) Reversible shape memory cycle (segments I and III) and stress relaxation (II) measurements by DMA of the same taPEVA sample. (b) Stress relaxation curve of taPEVA at 120 °C in segment II, the instantaneous stress relative to the initial stress was shown.

The thermadapt RSME could also be displayed by visual deformation. A newly fabricated sample with a permanent shape I was first heated to 80 °C for 10 min, then programmed and folded to a V shape and cooled to 0 °C. The external force was removed after 2 min at 0 °C, when the temporary shape V was fixed. In Figure 5.5a, when the sample with an angle of 59.8° was heated to 50 °C by hot air, the angle of V shape opened to 68.8°. When cooled by cold air to 0 °C, the angle of the V shape closed back to 59.8°. These open and close actions could be repeated in the heating and cooling cycles without additional manual deformation, as recorded in Figure 5.5b, showing a good reversible shape memory effect. The angle showed a trend of slight increase with the repeat cycles, attributed to possible material relaxation that occurred after cyclic heating, as it has already been demonstrated in Figure 5.2. The sample was further heated to 120 °C for 30 min, manually reset to an S shape, and then cooled to room temperature to fix the new permanent shape S. The sample with the new permanent shape was heated at 80 °C for 10 min and then programmed to a temporary pinched shape S, as shown in Figure 5.5a. After the pinched shape S was fixed at 0 °C, the temperature was varied between 50 °C and 0 °C, the pinched shape S could also exhibit a reversible open and close shape shift, demonstrating taPEVA as a new kind of thermadapt RSMP. It should be noticed that the reversible angle shift of taPEVA shown in Figure 5.5 was smaller than that in the other reference,[16] which was due to that the PEVA used in this work has a higher content of vinyl acetate and higher melting index than that in ref 16,

indicating poorer crystallization capacity and lower molecular weight in the present taPEVA system, which resulted in a poorer ability of chain orientation. As a result, the taPEVA showed a smaller change in angle than that in ref 16. Increasing the actuating temperature and the programming strain would increase the reversible ratio and thus increase the bending and recovery angle.

(a)

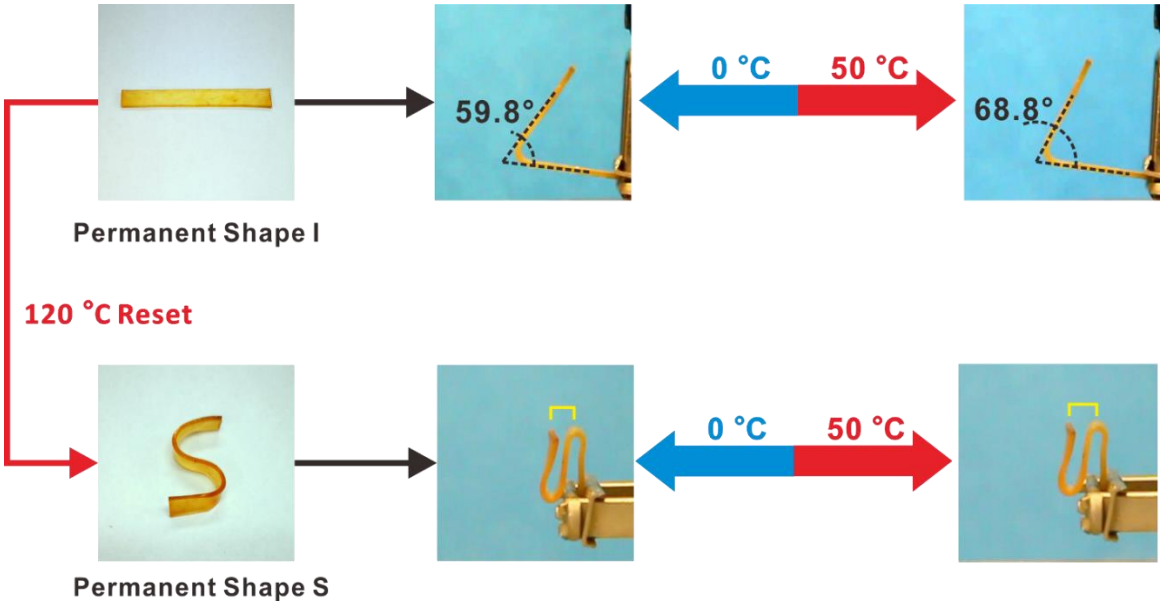

(b)

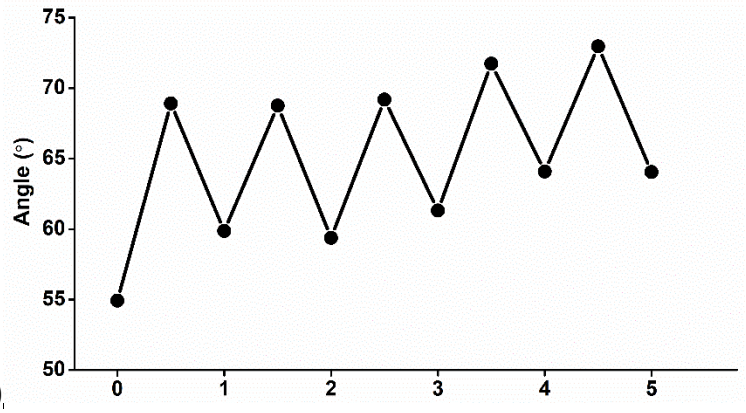

Figure 5.5. Reversible shape memory effect of taPEVA. (a) Photographs of the angle change, (b) Plot of the angle change of the temporary shape V in heating and cooling cycles.

Based on the above measurements, a mechanism for the thermadapt RSMP was proposed. As shown in Figure 5.6, PEVA materials contained abundant ester groups on the side chains, which could act as cross-linkers in the presence of TBD. The taPEVA materials performed a representative reversible shape memory behavior below its maximum melting temperature T_m. The taPEVA sample was programmed to a temporary shape 1A from its permanent shape 1 at the programming temperature (T_p). After cooling to a low temperature (T_{low}), the temporary shape 1A was fixed by crystallization. The formation of oriented crystallization was demonstrated by the XRD spectra, as shown in Figure S5.4. When the sample was heated to a high temperature (T_{high}), the small crystal domains partly melted and the sample contracted to a temporary shape 1B. The taPEVA sample achieved the RSME between the temporary shapes 1A and 1B

upon cooling and heating between T_{low} and T_{high} due to the CIE/MIC mechanism. When the sample was heated back to the programming temperature T_p, it recovered to the permanent shape 1. When the sample was further heated to the deformation temperature T_d (dynamic state temperature) above the maximum melting temperature T_m, all the crystal domains melted and the ester groups in the polymer network reached their dynamic state and transformed to dynamic covalent bonds in the presence of the transesterification catalyst TBD. The ester groups broke and re-formed dynamically and induced plasticity into the taPEVA network. Once the sample was deformed to a new shape at T_d and cooled to a temperature below T_m, the new permanent shape 2 was fixed. The reset sample also performed typical reversible shape memory cycles between the temporary shapes 2A at T_{low} and 2B at T_{high} under the same mechanism of crystallization-induced elongation (CIE) and melting-induced contraction (MIC). However, when the sample was heated back to T_p, it recovered to its permanent shape 2, but not the permanent shape 1. In addition, another new temporary shape could also be reprogrammed at T_p and refixed by cooling. Furthermore, when it was further heated again to T_d, another new permanent shape could be reset. The tensile strength and modulus of taPEVA did not decrease after a second hot pressing, as shown in Figure S5.5. The recyclability and reprocessability of the thermadapt reversible shape memory polymer were further demonstrated by recycling, as shown in Figure S5.6.

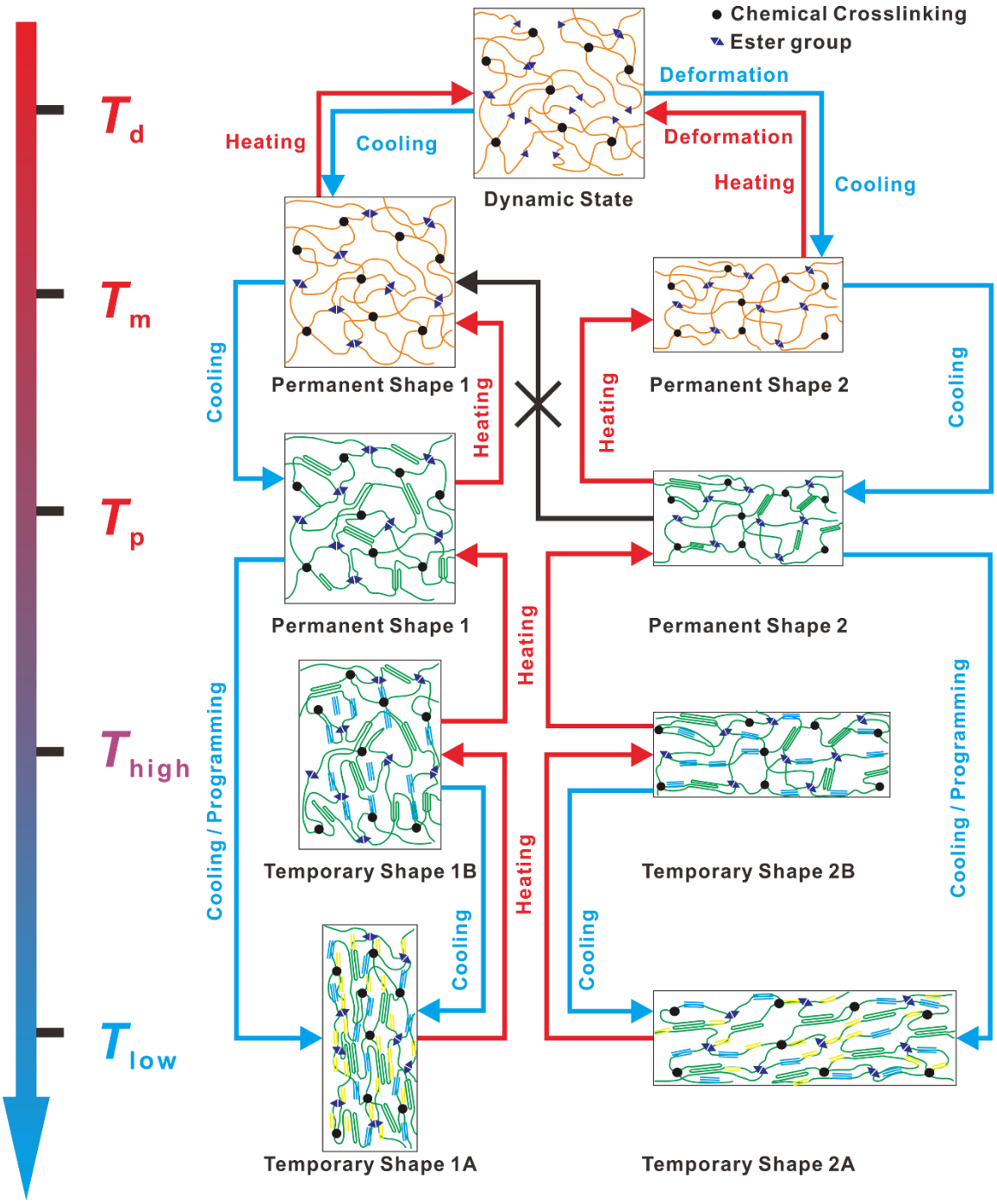

Figure 5.6. Mechanism illustration of taPEVA as the thermadapt RSMP.

§ 5.5 Conclusions

The cross-linked PEVA materials with the transesterification catalyst TBD have been demonstrated to possess both the reversible shape memory effect and thermadapt property. The broad range of melting transitions from different sized crystal domains formed by various crystalline segment lengths in the PEVA chains facilitate the crystallization-induced elongation and melting-induced contraction performance of the PEVA materials. The transesterification reactions in the presence of TBD result in a dynamic covalent polymer network, which endows PEVA an excellent thermadapt performance. This work reports the first semicrystalline thermadapt RSMP based on commercially available polymers. The idea to improve reprocessability of cross-linked RSMP through simple modification of commodity polymers provides a great opportunity for the development of commercial shape memory materials.

§ 5.6 References

(1) Hager, M. D., Bode, S., Weber, C., Schubert, U. S., Shape Memory Polymers: Past, Present and Future Developments. *Prog. Polym. Sci.* **2015**, *49-50*, 3-33.

(2) Zhao, Q., Qi, H. J., Xie, T., Recent Progress in Shape Memory Polymer: New Behavior, Enabling Materials, and Mechanistic Understanding. *Prog. Polym. Sci.* **2015**, *49-50*, 79-120.

(3) Berg, G. J., McBride, M. K., Wang, C., Bowman, C. N., New Directions in the Chemistry of Shape Memory Polymers. *Polymer* **2014**, *55* (23), 5849-5872.

(4) Meng, H., Li, G., A Review of Stimuli-Responsive Shape Memory Polymer Composites. *Polymer* **2013**, *54* (9), 2199-2221.

(5) Hu, J., Zhu, Y., Huang, H., Lu, J., Recent Advances in Shape‐Memory Polymers: Structure, Mechanism, Functionality, Modeling and Applications. *Prog. Polym. Sci.* **2012**, *37* (12), 1720-1763.

(6) Xie, T., Recent Advances in Polymer Shape Memory. *Polymer* **2011**, *52* (22), 4985-5000.

(7) Zhou, J., Sheiko, S. S., Reversible Shape-Shifting in Polymeric Materials. *J. Polym. Sci., Part B: Polym. Phys.* **2016**, *54* (14), 1365-1380.

(8) Chen, S., Hu, J., Zhuo, H., Zhu, Y., Two-Way Shape Memory Effect in Polymer Laminates. *Mater. Lett.* **2008**, *62* (25), 4088-4090.

(9) Li, M. H., Keller, P., Artificial Muscles Based on Liquid Crystal Elastomers. *Philos. Trans. R. Soc., A* **2006**, *364* (1847), 2763-2777.

(10) Chung, T., Romo-Uribe, A., Mather, P. T., Two-Way Reversible Shape Memory in a Semicrystalline Network. *Macromolecules* **2008**, *41* (1), 184-192.

(11) Pandini, S., Riccò, T., Borboni, A., Bodini, I., Vetturi, D., Cambiaghi, D., Toselli, M., Paderni, K., Messori, M., Pilati, F., Chiellini, F., Bartoli, C., Tailored One-Way and Two-Way Shape Memory Capabilities of Poly(*ε*-Caprolactone)-Based Systems for Biomedical Applications. *J. Mater. Eng. Perform.* **2014**, *23* (7), 2545-2552.

(12) Behl, M., Kratz, K., Zotzmann, J., Nöchel, U., Lendlein, A., Reversible Bidirectional Shape-Memory Polymers. *Adv. Mater.* **2013**, *25* (32), 4466-4469.

(13) Wang, K., Jia, Y., Zhu, X. X., Two-Way Reversible Shape Memory Polymers Made of Cross-Linked Cocrystallizable Random Copolymers with Tunable Actuation Temperatures. *Macromolecules* **2017**, *50* (21), 8570–8579.

(14) Zhou, J., Turner, S. A., Brosnan, S. M., Li, Q., Carrillo, J. Y., Nykypanchuk, D., Gang, O., Ashby, V. S., Dobrynin, A. V., Sheiko, S. S., Shapeshifting: Reversible Shape Memory in Semicrystalline Elastomers. *Macromolecules* **2014**, *47* (5), 1768-1776.

(15) Xie, H., Cheng, C., Deng, X., Fan, C., Du, L., Yang, K., Wang, Y., Creating Poly(tetramethylene Oxide) Glycol-Based Networks with Tunable Two-Way Shape Memory Effects Via Temperature-Switched Netpoints. *Macromolecules* **2017**, *50* (13), 5155-5164.

(16) Behl, M., Kratz, K., Noechel, U., Sauter, T., Lendlein, A., Temperature-Memory Polymer Actuators. *Proc. Natl. Acad. Sci. U.S.A.* **2013**, *110* (31), 12555-12559.

(17) Ge, F., Lu, X., Xiang, J., Tong, X., Zhao, Y., An Optical Actuator Based On Gold-Nanoparticle-Containing Temperature-Memory Semicrystalline Polymers. *Angew. Chem., Int. Ed.* **2017**, *56* (22), 6126-6130.

(18) Farhan, M., Rudolph, T., Nöchel, U., Yan, W., Kratz, K., Lendlein, A., Noncontinuously Responding Polymeric Actuators. *ACS Appl. Mater. Interfaces* **2017**, *9* (39), 33559-33564.

(19) Kolesov, I., Dolynchuk, O., Jehnichen, D., Reuter, U., Stamm, M., Radusch, H., Changes of Crystal Structure and Morphology during Two-Way Shape-Memory Cycles in Cross-Linked Linear and Short-Chain Branched Polyethylenes. *Macromolecules* **2015**, *48* (13), 4438-4450.

(20) Lu, L., Li, G., One-Way Multishape-Memory Effect and Tunable Two-Way Shape Memory Effect of Ionomer Poly(Ethylene-Co-Methacrylic acid). *ACS Appl. Mater. Interfaces* **2016**, *8* (23), 14812-14823.

(21) Biswas, A., Aswal, V. K., Sastry, P. U., Rana, D., Maiti, P., Reversible Bidirectional Shape Memory Effect in Polyurethanes through Molecular Flipping. *Macromolecules* **2016**, *49* (13), 4889-4897.

(22) Liu, W., Ojo, A. T., Wang, W., Fan, H., Li, B., Zhu, S., Preparation of Ultrahigh Molecular Weight Ethylene/1-Octene Block Copolymers Using Ethylene Pressure Pulse Feeding Policies. *Polym. Chem.* **2015**, *6* (20), 3800-3806.

(23) Gao, Y., Liu, W., Zhu, S., Polyolefin Thermoplastics for Multiple Shape and Reversible Shape Memory. *ACS Appl. Mater. Interfaces* **2017**, *9* (5), 4882-4889.

(24) Zou, W., Dong, J., Luo, Y., Zhao, Q., Xie, T., Dynamic Covalent Polymer Networks: From Old Chemistry to Modern Day Innovations. *Adv. Mater.* **2017**, *29* (14), 1606100.

(25) Denissen, W., Winne, J. M., Du Prez, F. E., Vitrimers: Permanent Organic Networks with Glass-Like Fluidity. *Chem. Sci.* **2016**, *7* (1), 30-38.

(26) Montarnal, D., Capelot, M., Tournilhac, F., Leibler, L., Silica-Like Malleable Materials from Permanent Organic Networks. *Science* **2011**, *334* (6058), 965.

(27) Fortman, D. J., Brutman, J. P., Cramer, C. J., Hillmyer, M. A., Dichtel, W. R., Mechanically Activated, Catalyst-Free Polyhydroxyurethane Vitrimers. *J. Am. Chem. Soc.* **2015**, *137* (44), 14019-14022.

(28) Scott, T. F., Schneider, A. D., Cook, W. D., Bowman, C. N., Photoinduced Plasticity in Cross-Linked Polymers. *Science* **2005**, *308* (5728), 1615 - 1617.

(29) Lawton, M. I., Tillman, K. R., Mohammed, H. S., Kuang, W., Shipp, D. A., Mather, P. T., Anhydride-Based Reconfigurable Shape Memory Elastomers. *ACS Macro Lett.* **2016**, *5* (2), 203-207.

(30) Zhao, Q., Zou, W., Luo, Y., Xie, T., Shape Memory Polymer Network with Thermally Distinct Elasticity and Plasticity. *Sci. Adv.* **2016**, *2* (1), e1501297.

(31) Zhang, G., Zhao, Q., Yang, L., Zou, W., Xi, X., Xie, T., Exploring Dynamic Equilibrium of Diels‐Alder Reaction for Solid State Plasticity in Remoldable Shape Memory Polymer Network. *ACS Macro Lett.* **2016**, *5* (7), 805-808.

(32) Fang, Z., Zheng, N., Zhao, Q., Xie, T., Healable, Reconfigurable, Reprocessable Thermoset Shape Memory Polymer with Highly Tunable Topological Rearrangement Kinetics. *ACS Appl. Mater. Interfaces* **2017**, *9* (27), 22077-22082.

(33) Zheng, N., Hou, J., Xu, Y., Fang, Z., Zou, W., Zhao, Q., Xie, T., Catalyst-Free Thermoset Polyurethane with Permanent Shape Reconfigurability and Highly Tunable Triple-Shape Memory Performance. *ACS Macro Lett.* **2017**, 326-330.

(34) Zheng, N., Fang, Z., Zou, W., Zhao, Q., Xie, T., Thermoset Shape-Memory Polyurethane with Intrinsic Plasticity Enabled by Transcarbamoylation. *Angew. Chem., Int. Ed.* **2016**, *55* (38), 11421-11425.

(35) Pei, Z., Yang, Y., Chen, Q., Terentjev, E. M., Wei, Y., Ji, Y., Mouldable Liquid-Crystalline Elastomer Actuators with Exchangeable Covalent Bonds. *Nat. Mater.* **2013**, *13* (1), 36-41.

(36) Yang, Y., Pei, Z., Li, Z., Wei, Y., Ji, Y., Making and Remaking Dynamic 3D Structures by Shining Light on Flat Liquid Crystalline Vitrimer Films without a Mold. *J. Am. Chem. Soc.* **2016**, *138* (7), 2118-2121.

(37) Meng, Y., Yang, J., Lewis, C. L., Jiang, J., Anthamatten, M., Photoinscription of Chain Anisotropy Into Polymer Networks. *Macromolecules* **2016**, *49* (23), 9100-9107.

(38) Jin, B., Song, H., Jiang, R., Song, J., Zhao, Q., Xie, T., Programming a Crystalline Shape Memory Polymer Network with Thermo- and Photo-Reversible Bonds Toward a Single-Component Soft Robot. *Sci. Adv.* **2018**, *4* (1), eaao3865.

(39) Ge, F., Zhao, Y., A New Function for Thermal Phase Transition-Based Polymer Actuators: Autonomous Motion On a Surface of Constant Temperature. *Chem. Sci.* **2017**, *8* (9), 6307-6312.

(40) Li, J., Rodgers, W. R., Xie, T., Semi-Crystalline Two-Way Shape Memory Elastomer. *Polymer* **2011**, *52* (23), 5320-5325.

(41) Gaylord, N. G., Mehta, M., Mehta, R., Maleation of Ethylene-Polar Monomer Copolymers by Reactive Processing with Maleic Anhydride-Peroxide. *J. Vinyl Addit. Technol.* **1995**, *1* (4), 261-263.

(42) Soares, B. G., Colombaretti, R. S. C., Melt Functionalization of EVA Copolymers with Maleic Anhydride. *J. Appl. Polym. Sci.* **1999**, *72* (14), 1799-1806.

§ 5.7 Supporting Information

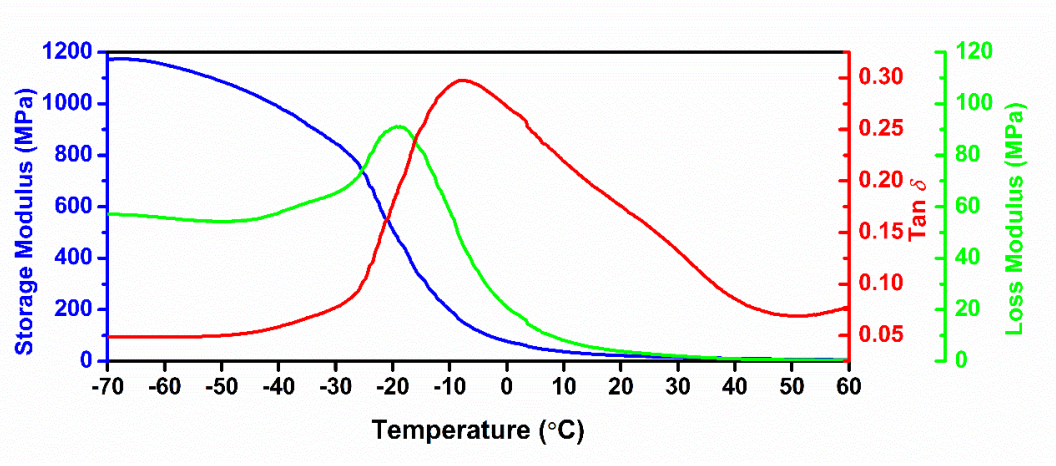

(a)

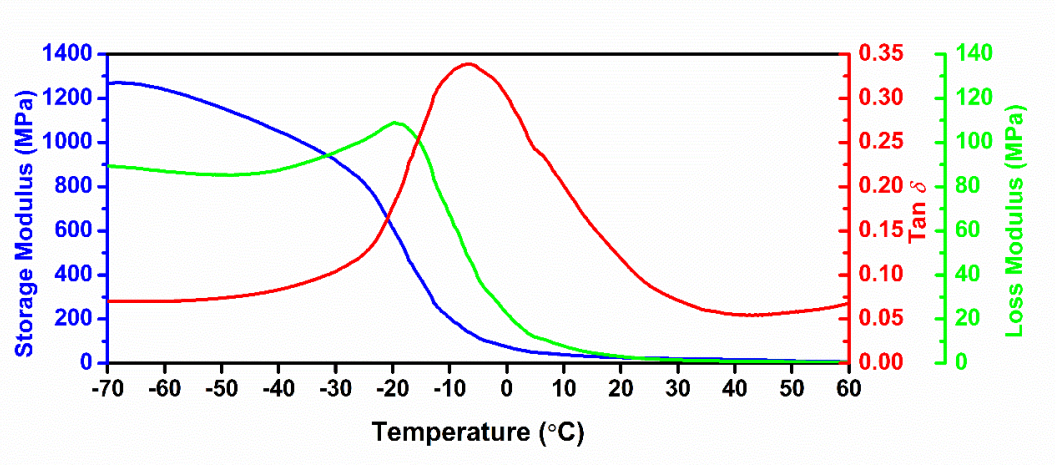

(b)

Figure S5.1. Temperature dependent modulus curves of (a) tsPEVA and (b) PEVA from -70 °C to 60 °C at a rate of 3 °C/min.

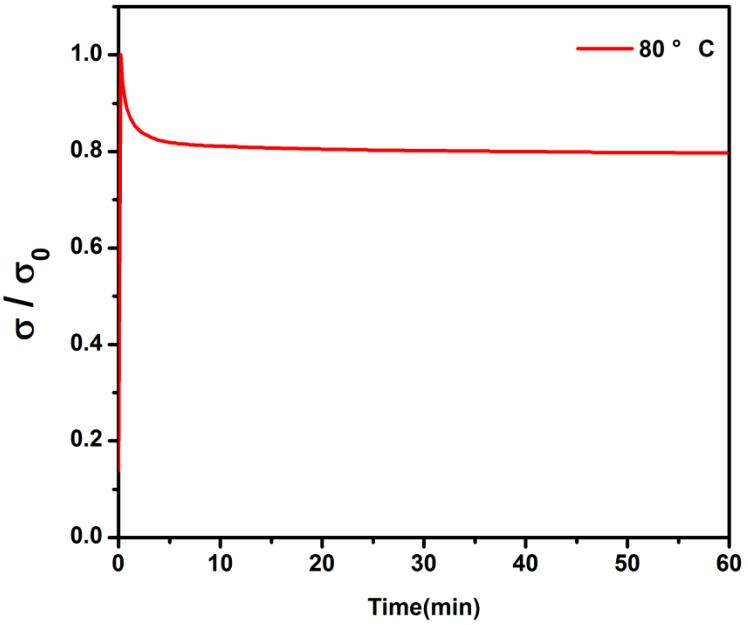

Figure S5.2. Stress relaxation curve of tsPEVA at 80 °C.

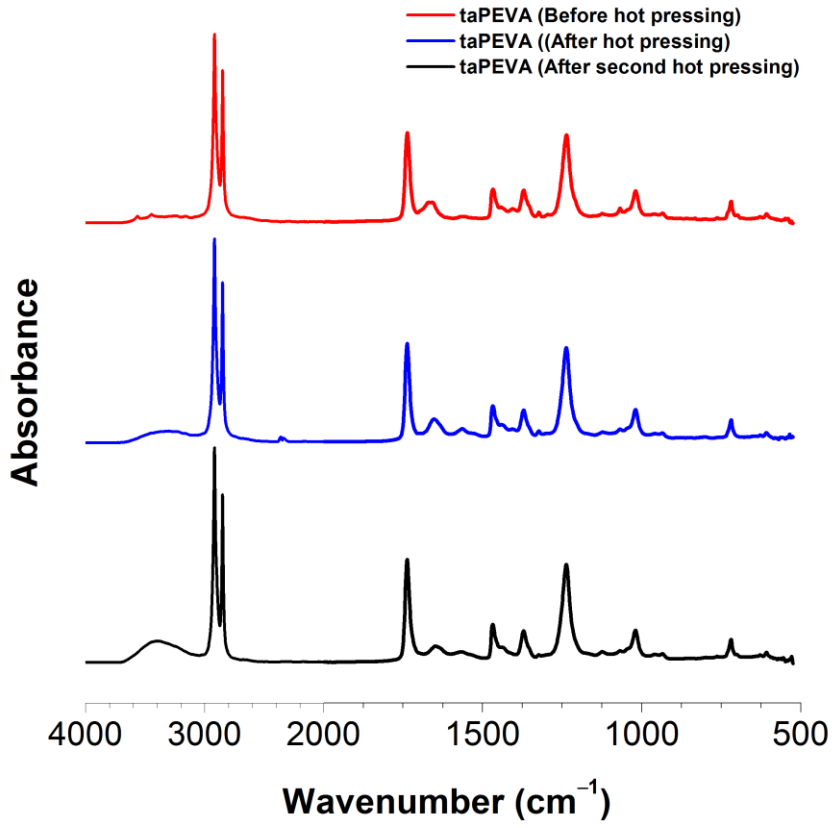

Figure S5.3. FTIR spectra of taPEVA material before hot-pressing, taPEVA, and taPEVA after reheating at 160 °C for 20 min.

The absorbance between 3200 and 3600 cm^{-1} assigning to the hydroxyl groups (OH) intensified after reheating of taPEVA, indicating the breakage of ester bonds and formation of more hydroxyl groups after reheating in the presence of the TBD catalyst. The fracture of ester bonds is the basis of dynamic crosslinking network rearrangement. Therefore, from this viewpoint, the FTIR spectra did indirectly verify the dynamic crosslinking.

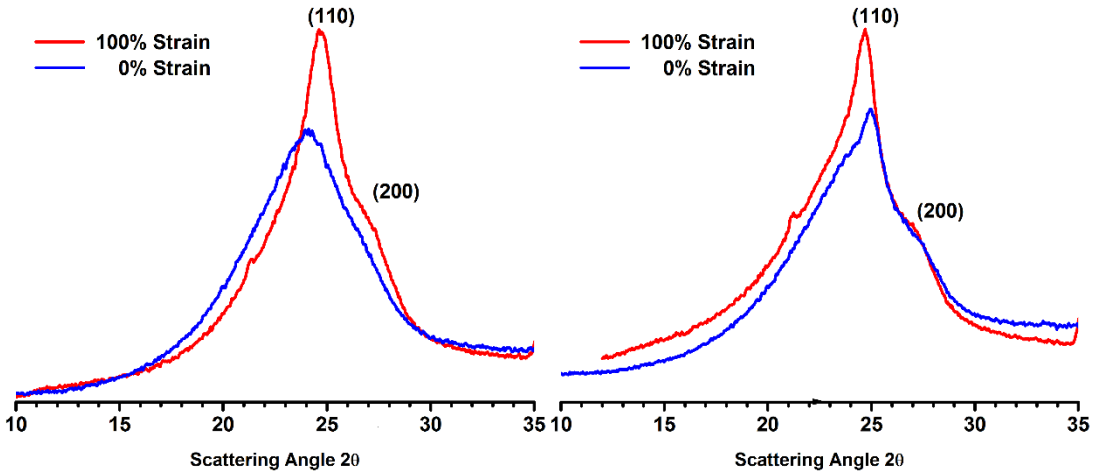

(a) (b)

Figure S5.4. XRD spectra of (a) tsPEVA and (b) taPEVA. Two samples were first heated to 75 °C for 5 min, then one sample was put into ice-water mixtures directly as the 0% strain sample, the other was stretched to 100% strain at 75 °C and then put into ice-water mixtures to form the 100% strain sample.

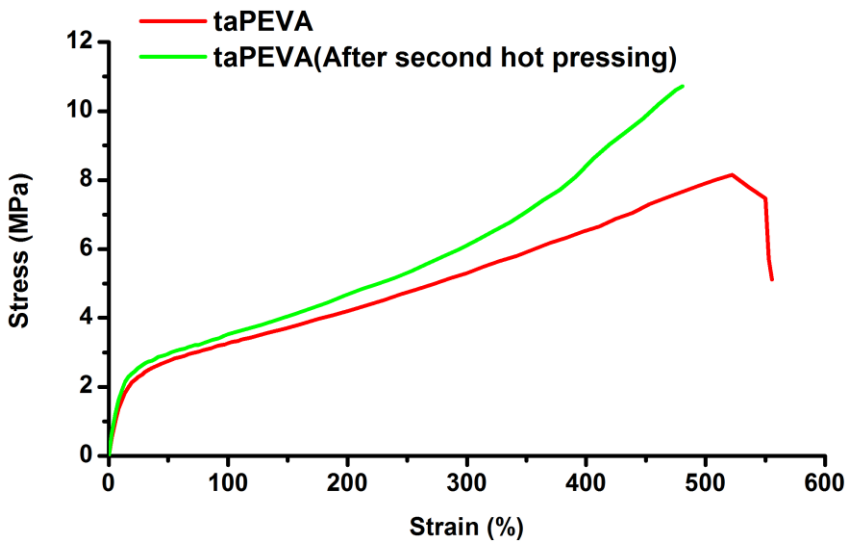

Figure S5.5. Stress-strain curves of taPEVA and taPEVA after second hot pressing. Samples were cut into dog-bone shape (30×5×1, mm) and were tested at an elongation rate of 50 mm/min with an Instron 3366 tester (Instron, Corporation; Canton, MA) at room temperature.

(a)

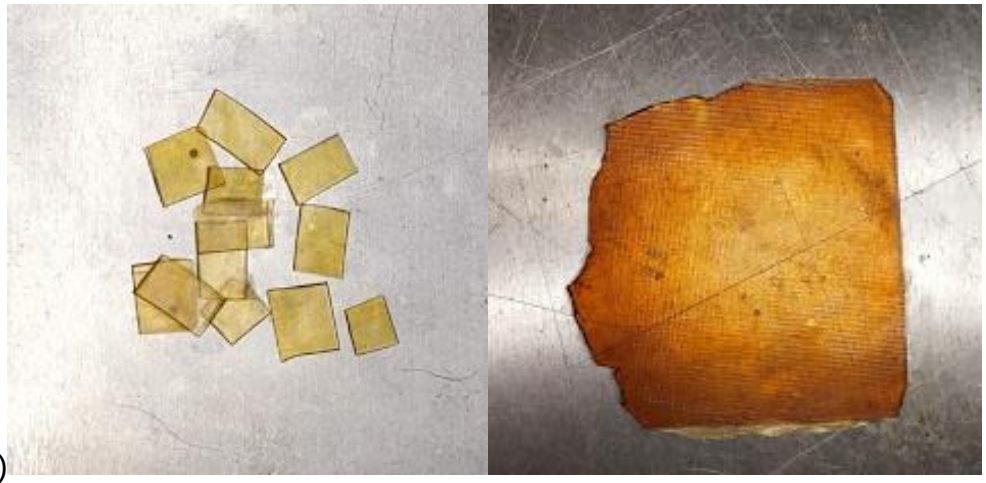

(b) 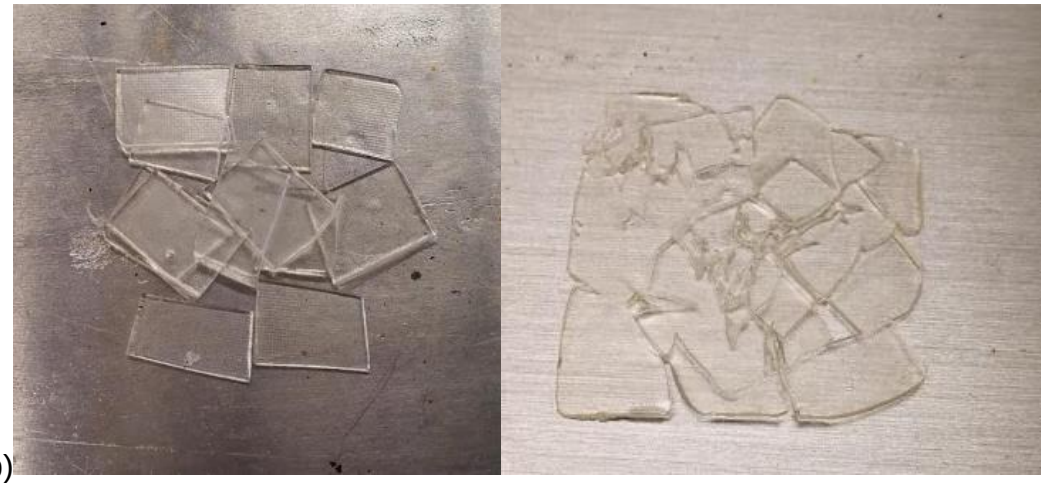

Figure S5.6. Reprocessing of (a) taPEVA and (b) tsPEVA under hot press at 160 °C for 20 min.

As shown in Figure S5.5, the tensile strength and modulus of taPEVA did not lose after recycling. The photos in Figure S5.6 also demonstrated good reprocessability of taPEVA. In comparison, tsPEVA without TBD catalyst could not be reprocessed.

6 POLYOLEFIN ELASTOMER BLEND FOAMS WITH REVERSIBLE SHAPE MEMORY EFFECT

In this chapter, the reversible shape memory effect of a polyolefin-based foam material is demonstrated and presented. This chapter is based on the manuscript entitled “Polyolefin Elastomer Blend Foams with Reversible Shape Memory Effect”.

Author contributions

Yuan Gao conducted the experiments and wrote the first draft of the manuscript under the guidance of Dr. Michael Thompson and Dr. Shiping Zhu. Dr.

Michael Thompson provided the first revision of the manuscript. The final revision was provided by Dr. Zhu.

§ 6.1 Abstract

This work reports on the first polyolefin-based reversible shape memory polymer foam. Two polyolefin elastomers (POE) are blended with differing contents and then foamed to obtain a material with broad melting transitions. The prepared foams exhibit a one-way shape memory effect and a reversible shape memory effect (RSME). The crystallization-induced elongation (CIE) and melting-induced contraction (MIC) are confirmed as the mechanisms of RSME for this material. This work demonstrated that inexpensive polyolefin-based foams could achieve novel RSME through simple blending of commercial POE resins.

§ 6.2 Introduction

During the past few decades, shape memory polymers have had a tremendous impact in industrial and academic areas due to their multifaceted behaviour, being able to “memorize” one or several temporary shapes and then recover their permanent shape under certain external stimuli, such as thermal, light, electricity, magnetic, pH, etc.[1-7] Typically in a shape memory polymer, there is a stable network with chemical or physical crosslinks to fix the permanent shape, and a reversible switch transition such as its glass transition or crystal

melting transition to fix a temporary shape(s). Responding to an external trigger, the polymer in its temporary shape can recover to its permanent shape. Any polymer material containing a stable network and a reversible switch transition should exhibit a shape memory effect. There are many different shape memory polymers currently available for industrial applications in aerospace,[8] biomedicine,[9] and textiles.[10]

Besides the conventional one-way shape memory polymers that can exhibit one or several temporary programmed shapes and recover in one direction to a permanent shape, a new two-way or reversible shape memory effect (RSME) has been recently reported for shape memory polymers that can shift between two different temporary shapes depending on an external stimulus and without the need for extra programming steps.[11] The mechanism of this shape shifting effect was discovered to be crystallization-induced elongation (CIE) upon cooling and melting-induced contraction (MIC) of the oriented crystal domains upon heating. This mechanism has been successfully demonstrated with semicrystalline polymers such as poly(cyclooctene) (PCO),[12] poly(octylene adipate),[13] polycaprolactone (PCL),[14] and poly(ethylene-co-vinyl acetate) (PEVA).[15]

In the early days, most shape memory polymers were studied in their bulk form for fundamental research, to examine shape memory effects and their related macromolecular mechanisms and mechanical properties. Besides shape memory polymers in their bulk form, recently researchers have studied other forms for potential applications, such as shape memory surfaces,[16] shape

memory hydrogels,[17] shape memory microparticles,[18] and shape memory foams.[19], Among these applications, shape memory foam or porous shape memory polymers are attracting the majority of attention from scientists since they appear to have many commercial applications and the deformational changes related to its shape memory tend to be more obvious.[20] Thus, it is of great interest to endow polymer foam materials with shape memory effects through controlled structural design. The resulting material could combine the highly valued shape memory effect with the advantages of high specific modulus, high specific strength and low density indicative of polymer foam materials.

In the last few years, many shape memory polymer foam materials have been fabricated applying various fabricating methods to obtain certain porous structures, by chemical or physical blowing agents,[21] particulate leaching,[22] polymerized high internal phase emulsions (polyHIPE),[23] electrospinning,[24] etc. Until now, the most significantly used shape memory polymer foams have been polyurethane (PU)-based and epoxy-based foams, notably applied in self-folded and self-deploying devices in aerospace assemblies [25] due to their low density, chemical stability, and excellent shape-changing ratio. The healthcare field is another area of high use, such as scaffolds in tissue engineering,[26] or biomedical implants with shape changing features to minimize the size of surgical incisions.[27]

Though there are many reports on various shape memory polymer foams, research on those with reversible behavior are still rare. In 2013, Mather and coworkers[22] prepared a highly porous foam scaffold with crosslinked

polycaprolactone (PCL) and poly(ethylene glycol), foamed by a modified porogen leaching technique. This foam exhibited reversible actuation under compression. However, the mechanical strength of the foam was not discussed in their work. Lendlein and coworkers[28] fabricated a water-blown polyurethane foam with PCL of differing molecular weights. The authors studied the RSME in compression, tension, and bending modes, and demonstrated that the RSME in tension mode was caused by CIE and MIC similar to earlier RSME mechanisms. However, in compression and bending modes, the mechanism of RSME was more complicated in their material than just CIE and MIC. Li and coworkers[29] prepared a PCL based syntactic foam by incorporating 40% (v/v) glass microspheres and crosslinking the PCL matrix with benzyl peroxide. Their crosslinked PCL syntactic foam displayed RSME with around 10% elongation upon cooling and 10% contraction upon heating at selected external loads and temperatures. Till now, the reported reversible shape memory polymer foams have all been PCL-based. It is of great significance to explore new material types for potentially reversible shape memory polymer foams.

Polyolefins can be designed as semicrystalline shape memory polymers and have been widely applied as commodity products in daily use such as heat-shrinkable tubing, packaging, etc.[30] The shape memory effect is seen with several polyolefins such as LDPE,[31] HDPE,[32] short-chain branched polyethylene,[33] trans-polyisoprene,[34] and polyolefin blends.[35] With specialized catalysts and unique methods for polyolefin polymerization being developed over

the past few decades, more and more polyolefin elastomer materials with controllable chain structures are being successfully fabricated,[36, 37] with some in commercial use already.[38] These new elastomers are opening doors to fabricating novel polyolefin-based shape memory polymer on large scale and at low cost.[39, 40] In Chapter 3, ethylene/1-octene diblock copolymer was demonstrated as a thermoplastic polyolefin elastomer with 'multiple shape memory' effect and RSME through delicate polyolefin chain structure design. Furthermore, POE blends with appropriately designed compositions were demonstrated in Chapter 4 with RSME, showing excellent potential for being produced on a large scale. With progress in polyolefin-based reversible shape memory polymers (RSMP), different forms and new applications can be expected.

Various polyolefin materials have been foamed such as polyethylene,[41] polypropylene,[42] ethylene–styrene interpolymers,[43] due to their advantages of low cost, chemical resistance, light weight, thermal insulation, skin friendliness, negligible water absorption, shock absorption, and buoyancy.[44] However, in contrast to previously mentioned PU and epoxy-based shape memory polymer foams, polyolefin-based shape memory polymer foams are not reported. In this newly report work, POE blend foams are shown to behave with the RSME and demonstrate large volume change in the display of the effect, expanding the applications of commercial polyolefin materials.

§ 6.3 Experimental Section

6.3.1 Materials and preparation

Polyolefin elastomers Engage™ 8003 and Engage™ 8180, were purchased from Dow Chemicals, while dicumyl peroxide (DCP) and sodium bicarbonate ($NaHCO_3$) were purchased from Sigma-Aldrich. All chemicals were used as received. The POE blends were fabricated in Thermo Haake Rheometer. POE raw materials were added into the mixer at 85 °C and blended for 6 min, then sodium bicarbonate and DCP were added into the mixer for 2 min. Table 6.1 summarizes the recipes of three prepared elastomer blends. For the subsequent foaming step, each POE blend was molded in a hot press (Carver; USA) at 10.3 MPa and 170 °C for 15 min to produce rectangular shapes with dimensions of 40× 40 × 30 mm^3.

Table 6.1 Recipes of the POE blend foam series

Samples	P1	P2	P3
Engage™ 8003	120 g	90 g	60 g
Engage™ 8180	60 g	90 g	120 g
$NaHCO_3$	5 g	5 g	5 g
DCP	2.7 g	2.7 g	2.7 g

6.3.2 Polymer characterization

The thermal properties were measured by differential scanning calorimetry (DSC). The crystal melting temperature T_m and crystallization temperature T_c was measured in a Model 2910 Modulated DSC (TA instruments). Samples between 6.0 mg and 9.0 mg were first heated to 160 °C with the heating rate of 50 °C/min and then kept at 160 °C for 5 min to remove their thermal history. Afterwards, the temperature was cooled to -20 °C with a rate of 10 °C/min to measure T_c, kept at -20 °C for 5 min and finally, heated back to 160 °C at a rate of 10 °C/min. The T_m was obtained from the second heating curve.

Reversible shape memory effects in tension mode were measured by dynamic mechanical analysis (DMA) with a Model DMA850 from TA instruments. To test the RSME in free-standing conditions, a typical process was as follows: a sample (e.g. P1) was heated to 85 °C for 4 min, and the strain was recorded as ε_{f0}. It was then stretched at a constant stress of 0.2 MPa, cooled from 80 to -5 °C at a rate of 5 °C/min, and then annealed at -5 °C for 3 min still under stress. After removing the stress, the sample was kept at -5 °C for another 2 min, then heated to 55 °C and annealed for 3 min to obtain the reversible strain ε_{rb}. After another cooling process to -5 °C, a stable strain ε_s was obtained. The cooling-heating segments between -5 °C and 55 °C were repeated for 4 cycles. The reversible ratio R_{rb} was calculated from:

$$R_{\mathrm{rb}} = \frac{\varepsilon_{\mathrm{s}} - \varepsilon_{\mathrm{rb}}}{\varepsilon_{\mathrm{s}} - \varepsilon_{\mathrm{f0}}}$$

An angle change demonstration was operated as followed. Foam sample was cut into flat shape with the dimensions of 40 × 8 × 8 mm^3. The sample was first put into an oven with 85 °C for 5 min to reach the programming temperature, then the sample was folded and quenched to -5 °C by cold air. After removing the external force, the temporary shape with a small angle of 0° was fixed. Then the sample was treated to several heating and cooling cycles by hot air and cold air stream and the temperature range was controlled as -5 °C and 50 °C.

The foam micromorphology was measured by TESCAN VEGA II LSU SEM. Each sample was fractured in liquid nitrogen, and then the samples were sputter-coated with 5 nm of gold prior to observation.

The X-ray diffraction (XRD) analysis was performed on a Bruker D8 DISCOVER with DAVINCI.DESIGN diffractometer using Co as the anode material. The sample was scanned from 10° to 35° with a scanning increment of 0.02° at 35 kV generator voltage and 45 mA current. The sample stage of the machine could provide heat so that the samples could be tested at various temperatures *in situ*.

§ 6.4 Results and discussion

The series of crosslinked POE blend foam samples were designed and fabricated as the recipe shown in Table 1. Commercial POE Engage™ 8003 and Engage™ 8180 were blended together to contribute a broad melting transition, and $NaHCO_3$ was selected as the blowing agent to coordinate with the

approximate crosslinking temperature at 170 °C. The density of each sample was controlled at around 0.40 g/cm^3.

6.4.1 Thermal properties

The crystal melting transition range of each polyolefin blend foam was measured first for identifying the range of the programming temperature T_p that could be selected for shape memory effect test. DSC curves corresponding to the second heating cycle for crosslinked POE blend foam samples P1, P2, and P3 and the two original polyolefin elastomers, Engage™ 8003, Engage™ 8180 are shown in Figure 1. Engage™ 8003 showed a melting transition with a peak at 85.1 °C, while Engage™ 8180 showed a broader melting transition with a peak at 52.1 °C. Both POEs contained a size distribution of the crystalline domains with the crystalline domains in Engage™ 8003 being larger. According to the similar composition and chemistry environment, blends of these two POEs should be compatible, giving a broadened melting transition peak because the polymer chains with different hard segment lengths were more likely homogeneously mixed and a series of new crystal domains with different sizes were formed. The three foam samples showed melting transitions spanning from 85 °C to -5 °C, which could be utilized as the switch transition in a shape memory polymer. As Engage™ 8180 content progressively increased in the foam samples from P1 to P3, a melting peak at 52.1 °C was not obvious for P1 but it was significantly noticed in P3. Thus, according to the DSC curves, the range of the programming temperature T_p could be confirmed.

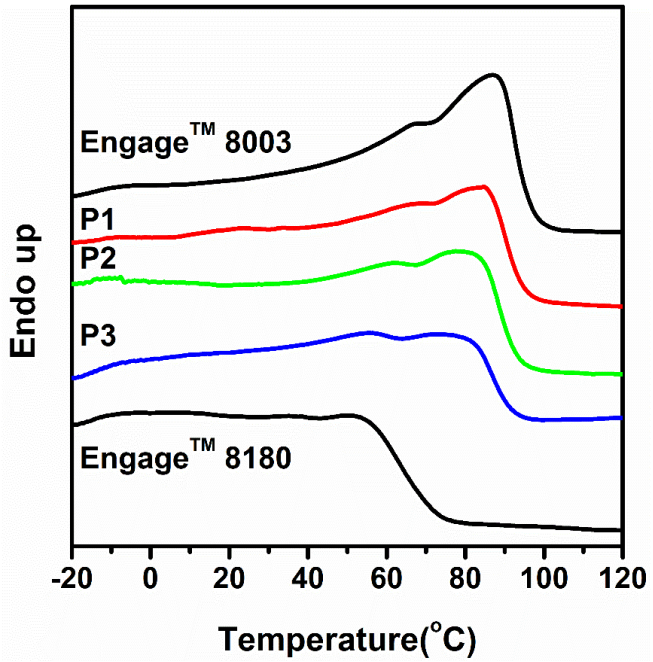

Figure 6.1. DSC heating curves of Engage™ 8003, Engage™ 8180 and the three POE blend foams prepared in the study: P1, P2, and P3.

6.4.2 Micromorphology

The foaming agent $NaHCO_3$ of the POE blend foams was chosen to match the foaming (decomposition) temperature with the reaction using DCP to arrive at a desired density of 0.4 g/cm^3 and appropriate crosslink density. The gel contents of the 3 samples were all measured around 90%. The controlled morphology had significant importance on the shape memory effect, as discussed later.

SEM micrographs of the three POE blend foams are shown in Figure 2. All samples exhibited closed-cell structures with cell diameters ranging from 200 μm to 500 μm, which is small but not very homogeneous. On the other hand, the

micrographs showed cells of irregular shape, which may affect the physical properties. Despite the different POE contents, the micromorphology of three POE blend foam samples appeared similar to one another under the same foaming and crosslinking conditions.

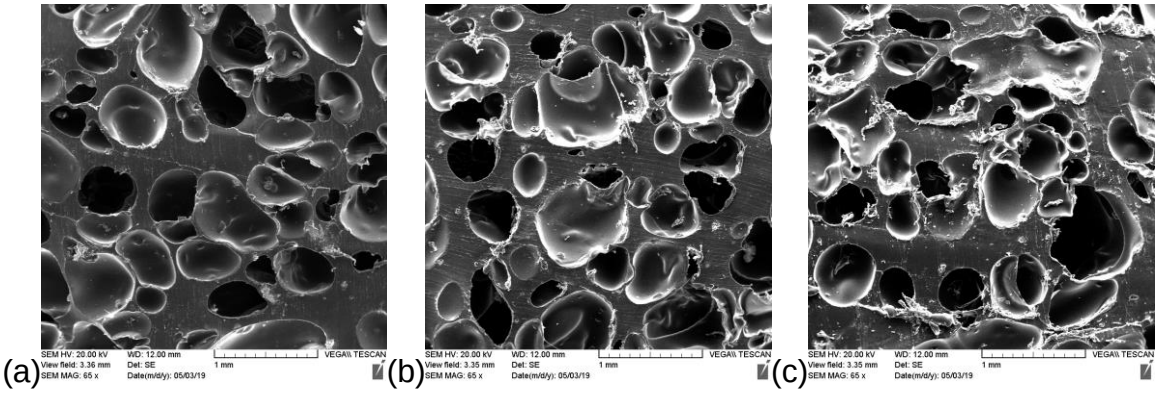

Figure 6.2. SEM micrographs of POE blend foams: (a) P1, (b) P2, and (c) P3.

6.4.3 Reversible shape memory effect

Shape memory responses seen in tension mode by DMA for the POE blend foams are displayed in Figure 3. The data shows that the stretched samples under external loading of 0.14 MPa exhibited a higher elongation rate during cooling from 60 °C to 0 °C, which represented the crystallization temperature range of the POE blend foams; the higher elongation rate was considered to be an indication of the CIE effect of the material under external loading. As the temperature subsequently increased from -5 °C to 55 °C, the sample partially contracted with a reported reversible strain ε_{rb} of 64.75% in P1, 56.93% in P2 and

44.33% in P3 since the crystal domains of low melting temperature had melted and any previous temporary shape could not be fixed as a result. In the following cooling step, the temperature decreased from 55 °C to -5 °C with the rate of 5 °C/min while the sample was remained mounted in the DMA without applied stress. As shown in Figure 3, all of the samples P1, P2, and P3 showed elongation during cooling. Then the stable strain ε_s of the sample could be recorded as 74.83% in P1, 67.05% in P2 and 51.62% in P3, and the reversible ratio R_{rb} of the POE blend foams P1, P2 and P3 were 13.6%, 15.3%, and 15.0%, which was a relatively high value compared to other reversible shape memory foams or polyolefin-based RSMPs in the literature when treated with similar prestrain.[28, 45, 46] The cooling and heating cycle could be repeated for at least 4 times per specimen in this test. Thus the RSME of the POE blend foam was successfully demonstrated. Currently, this work is the first know demonstration of a reversible shape memory polymer foam based-on polyolefin materials.

(a)

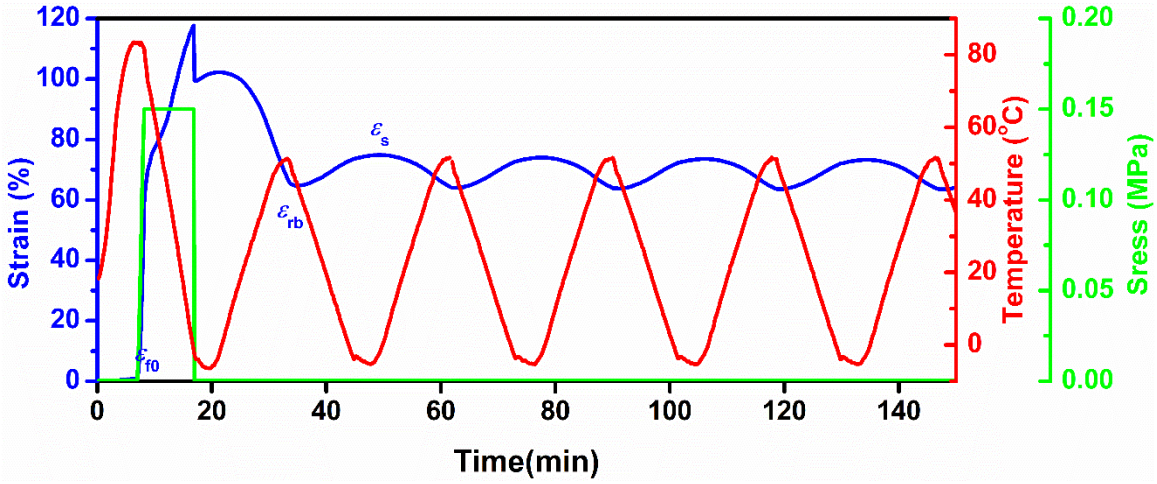
Strain (%)
Temperature (°C)
Sress (MPa)
Time(min)
ε_s
ε_{rb}
ε_{f0}

(b)

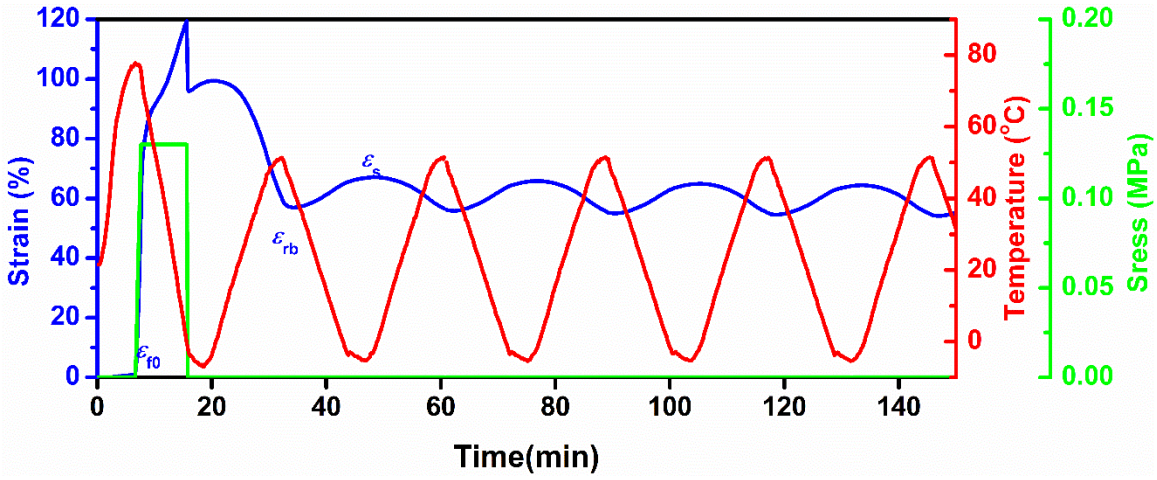
Strain (%)
Temperature (°C)
Sress (MPa)
Time(min)
ε_s
ε_{rb}
ε_{f0}

(c)

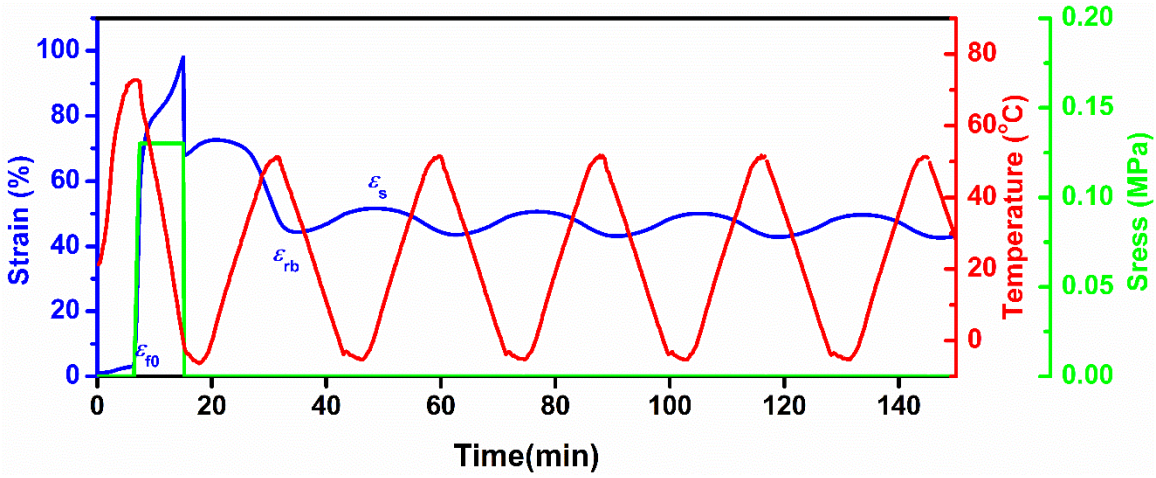

Figure 6.3. RSME of POE blend foams (a) P1, (b) P2, and (c) P3 in tension mode and in loading-free condition.

The RSME of the POE blend foams could also be demonstrated directly in bending mode through the angle change test.[47, 48] Sample P1 was selected for the demonstration, with results shown in Figure 4. As the temperature increased to 55 °C, the angle of the sample changed by 22°, and when the sample was lower temperature to -5 °C again, the angle of the sample decreased to 2°. The 20° angle change of the foam sample could be observed and could repeat for at least 4 cycles, as shown in Figure 4. This is a more qualitative method compared to the DMA results but it is considered equally as evidence of RSME.

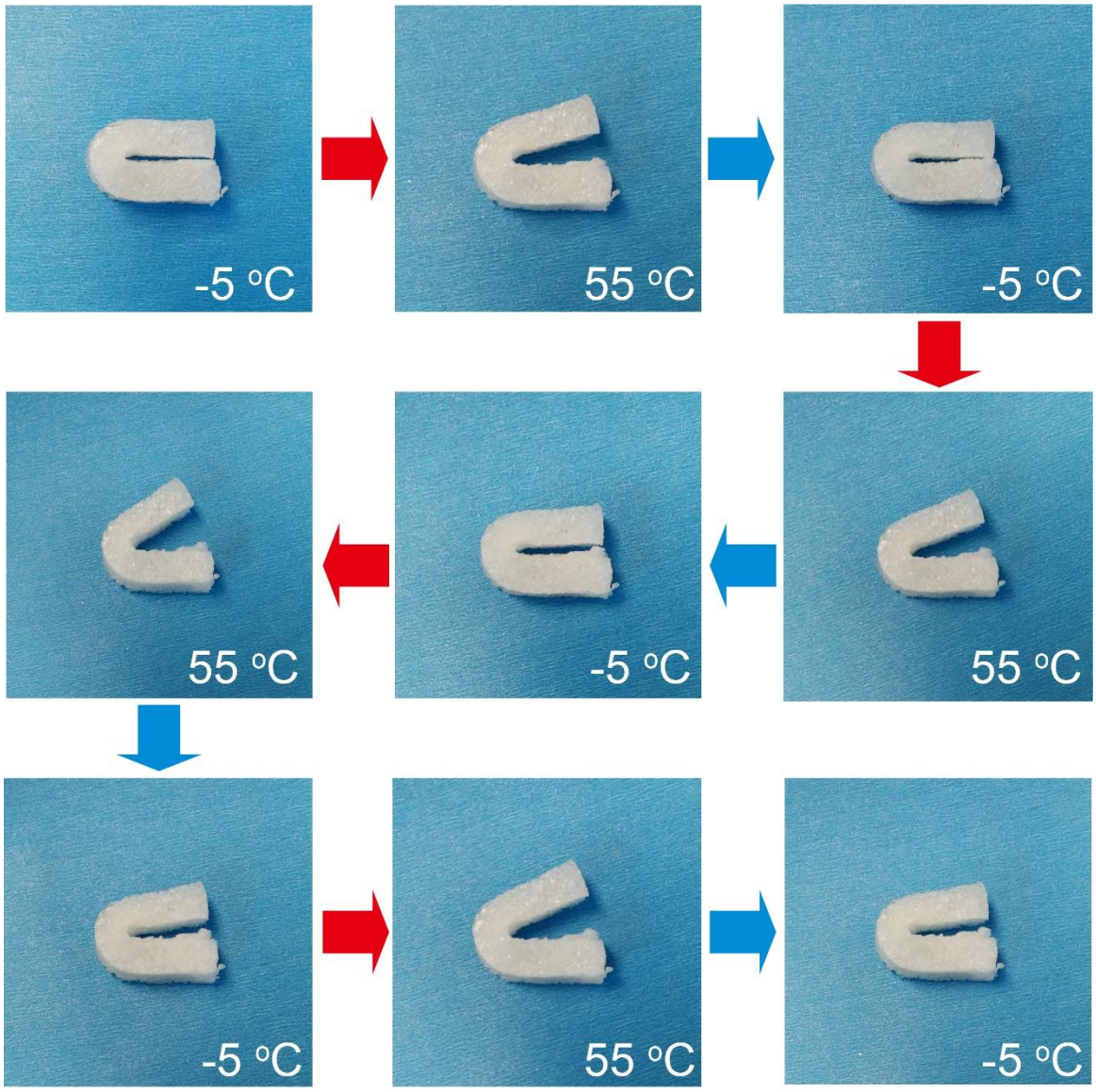

Figure 6.4. An angle change of POE blend foam P1.

6.4.4 XRD analysis

The XRD analysis of the POE blend foam was shown in Figure 5 to explore crystallinity changes at the different stages of the shape memory response cycle. In Figure 5 (a-c), the three POE blends were characterized at room temperature

after first being deformed to 50% strain at 85 °C to program their temporary shape then cooling to -5 °C to fix the temporary shapes. In these three plots, the blend samples were compared to their unstrained counterparts (experiencing the same thermal treatment but no strain). Each sample equilibrated in the XRD sample stage for 5 min before testing. Seen in the diffractogram of Figure 5(a) for P1, there were broad peaks at 23° attributed to the amorphous phase, and all blend samples showed higher signal peaks at 25° which was attributed to reflections in the (110) crystallographic plane. The peak at 27° represented reflections in the (200) crystallographic plane. The samples with frozen strain showed the highest ratio value between the (110) peak and amorphous phase peak in P1 while the lowest ratio value was found in P3, showing the ratio was significantly influenced by Engage™ 8003 content as a dominant contributor of crystallizability. The higher reflection peaks in the curves of strained POE blend foams compared to their unstrained counterparts also indicated that the strained POE blend foams generate more crystalline domains, though oriented and frozen in place from the programming.

Thermophysical changes in the crystallinity of each of the three strained foam samples, relevant to their programming for RSME, are depicted in Figure 5(d-f). The samples were studied at the programming temperature T_p 85 °C and an intermediate temperature (55 °C) in RSME testing cycle to compare crystalline morphology with samples at room temperature. As the temperature increased from 25 °C to 55 °C, all three strained samples exhibited a decrease on the

reflection intensity of the (110) plane, indicating crystallinity decreased due to the melting of crystal domains. However, there were still crystal domains remaining according to the XRD spectra at 55 °C which were able to still constrain many of the stretched and oriented polymer chains. At 85 °C, the reflection intensity of (110) plane of the three samples had almost disappeared due to the melting of nearly all crystal domains in the samples.

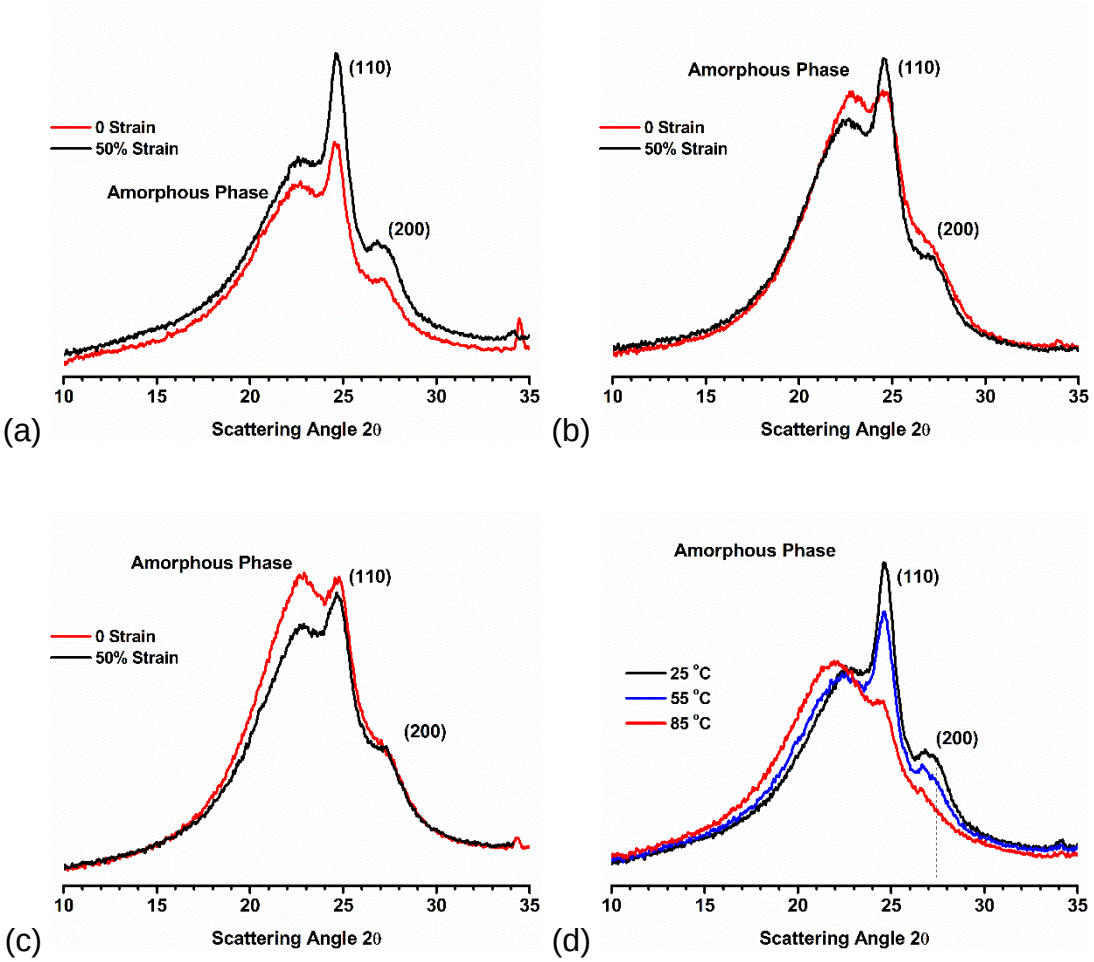

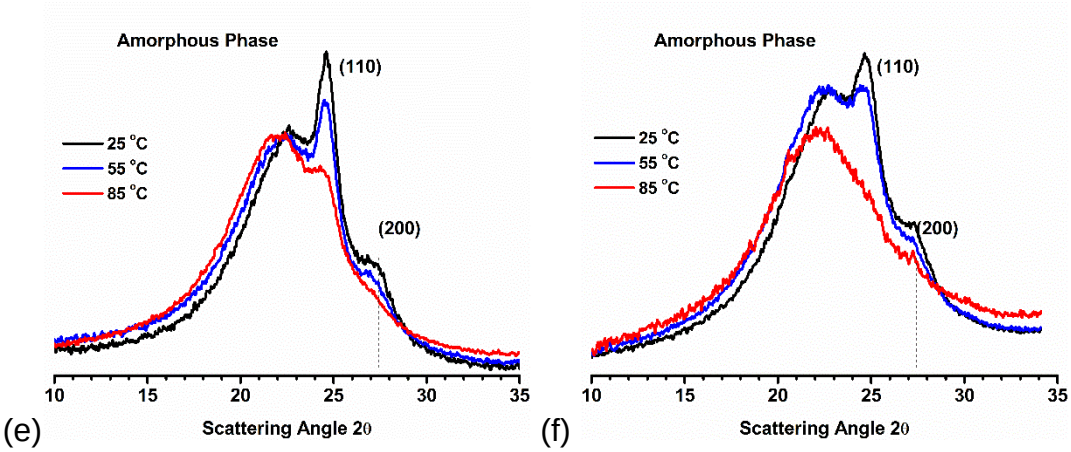

Figure 6.5. XRD diffractograms of foam samples (a) P1, (b) P2, and (c) P3 in 0 and 50% strain being evaluated at room temperature (25 °C); and 50% strained foam samples (d) P1, (e) P2, and (f) P3 being heated during the characterization to 25 °C, 55 °C and 85 °C.

6.4.5 Mechanism

Based on the results shown in this chapter, a mechanism of POE blend foam could be proposed and conceptually shown in Figure 6. The porous materials based on the POE blends had broad melting transitions and crystal size distributions. The crosslinks in the materials provided sufficient network strength for the shape recovery as well as constrained the chain conformation for further crystallization steps.[13] The crystal domains with different sizes could fix certain chain conformations while the material was kept below their crystallization temperatures. Thus, once the foam sample was shaped at their programming temperature and cooled down to a lower temperature T_{low}, the newly deformed

temporary shape ‘A’ would be fixed after external forces were removed. On the other hand, when the temperature increased the temporary sample shape ‘A’ would begin to recover aspects of its permanent shape gradually, since the crystal domains melted in order of smallest to largest crystallites. When a relatively high temperature T_{high} was reached, though still within the melting range of the material, a temporary shape ‘B’ could then be fixed by the remained crystal domains. Because the strained chain conformation still existed in the foams, when the temperature decreased again, the small crystal domains would crystalize along the stretched chain and induced an elongation according to the CIE effect, thus the sample shape would change to temporary shape ‘A’ again to demonstrate the RSME. Due to the porous structure, the samples exhibit a larger volume change than denser counterparts. Once a foam sample was heated back to the programming temperature, the sample would recover to its permanent shape and loss its memory of the temporary shapes due to the disappearance of the oriented chain conformation.

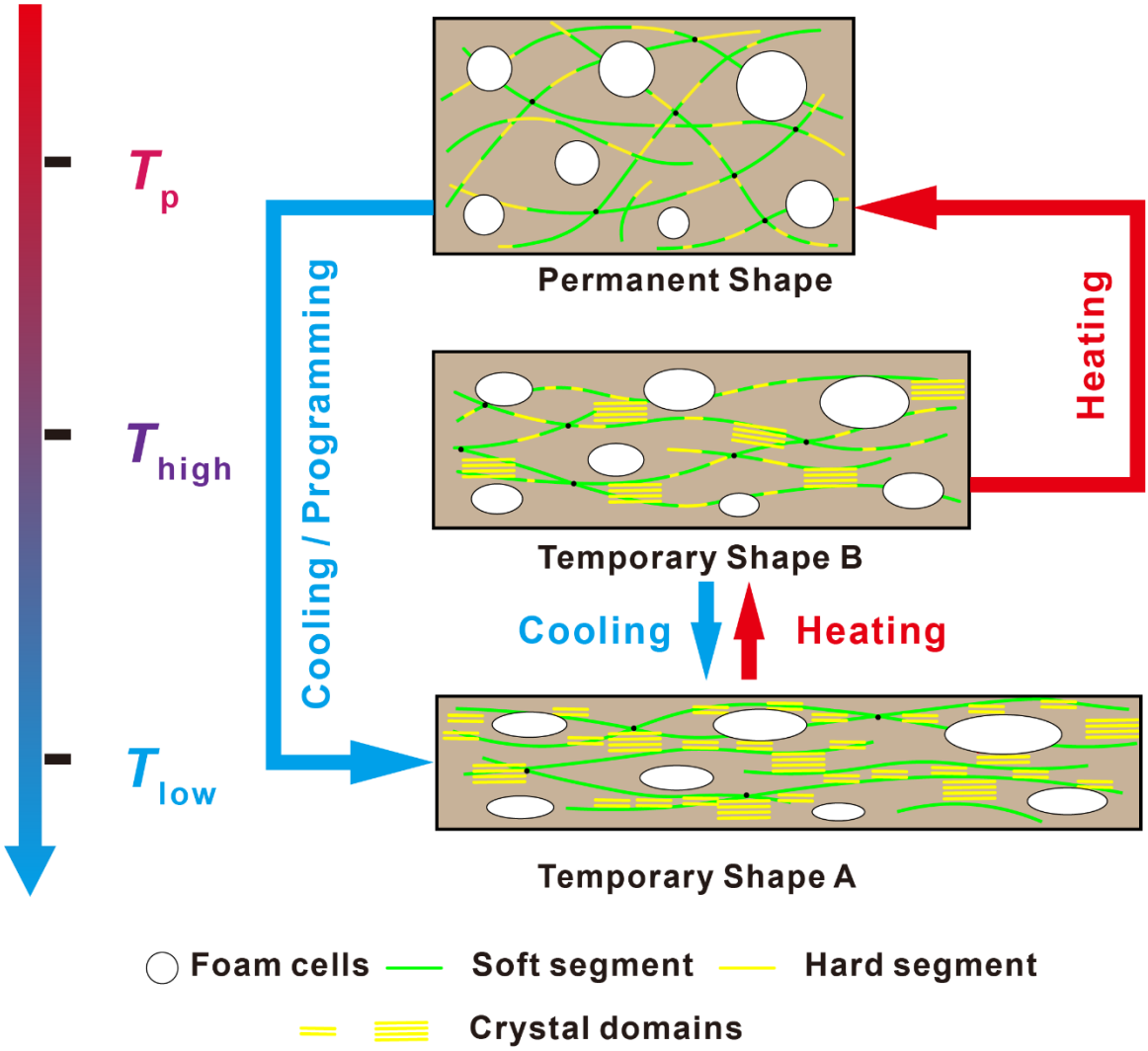

Figure 6.6. Mechanism of reversible shape memory POE blend foams.

§ 6.5 Conclusions

In summary, POE blend foams with tunable composition were demonstrated to exhibit the RSME was possible with polyolefin-based materials. A mechanism for the reversible shape memory POE foam was proposed, which was CIE and MIC effect of the oriented crystal domains. The current POE blend foam was the

first reported reversible shape memory foam based on polyolefin materials. This work would expand the material resource for obtaining RSMP foams, especially from commercial POE products.

§ 6.6 References

(1) Hager, M. D.; Bode, S.; Weber, C.; Schubert, U. S., Shape memory polymers: Past, present and future developments. *Prog. Polym. Sci.* **2015**, 49-50, 3-33.

(2) Zhao, Q.; Qi, H. J.; Xie, T., Recent progress in shape memory polymer: New behavior, enabling materials, and mechanistic understanding. *Prog. Polym. Sci.* **2015**, 49-50, 79-120.

(3) Meng, H.; Li, G., A review of stimuli-responsive shape memory polymer composites. *Polymer* **2013**, 54, (9), 2199-2221.

(4) Meng, H.; Li, G., Reversible switching transitions of stimuli-responsive shape changing polymers. *J. Mater. Chem. A* **2013**, 1, (27), 7838-7865.

(5) Hu, J.; Zhu, Y.; Huang, H.; Lu, J., Recent advances in shape‐memory polymers: Structure, mechanism, functionality, modeling and applications. *Prog. Polym. Sci.* **2012**, 37, (12), 1720-1763.

(6) Xie, T., Recent advances in polymer shape memory. *Polymer* **2011**, 52, (22), 4985-5000.

(7) Behl, M.; Zotzmann, J.; Lendlein, A., Shape-Memory Polymers and Shape-Changing Polymers. In *Shape-Memory Polymers*, Lendlein, A., Ed Springer Berlin Heidelberg: Berlin, Heidelberg, **2010**, 1-40.

(8) Liu, Y.; Du, H.; Liu, L.; Leng, J., Shape memory polymers and their composites in aerospace applications: a review. *Smart Mater. Struct.* **2014**, 23, (2), 23001.

(9) El Feninat, F.; Laroche, G.; Fiset, M.; Mantovani, D., Shape Memory Materials for Biomedical Applications. *Adv. Eng. Mater.* **2002**, 4, (3), 91-104.

(10) Hu, J.; Chen, S., A review of actively moving polymers in textile applications. *J. Mater. Chem.* **2010**, 20, (17), 3346-3355.

(11) Zhou, J.; Sheiko, S. S., Reversible shape-shifting in polymeric materials. *J. Polym. Sci., Part B: Polym. Phys.* **2016**, 54, (14), 1365-1380.

(12) Chung, T.; Romo-Uribe, A.; Mather, P. T., Two-Way Reversible Shape Memory in a Semicrystalline Network. *Macromolecules* **2008**, 41, (1), 184-192.

(13) Zhou, J.; Turner, S. A.; Brosnan, S. M.; Li, Q.; Carrillo, J. Y.; Nykypanchuk, D.; Gang, O.; Ashby, V. S.; Dobrynin, A. V.; Sheiko, S. S., Shapeshifting: Reversible Shape Memory in Semicrystalline Elastomers. *Macromolecules* **2014**, 47, (5), 1768-1776.

(14) Huang, M.; Dong, X.; Wang, L.; Zhao, J.; Liu, G.; Wang, D., Two-way shape memory property and its structural origin of cross-linked poly(ε -caprolactone). *RSC Adv.* **2014**, 4, (98), 55483-55494.

(15) Li, J.; Rodgers, W. R.; Xie, T., Semi-crystalline two-way shape memory elastomer. *Polymer* **2011**, 52, (23), 5320-5325.

(16) Ebara, M.; Uto, K.; Idota, N.; Hoffman, J. M.; Aoyagi, T., Shape-Memory Surface with Dynamically Tunable Nano-Geometry Activated by Body Heat. *Adv. Mater.* **2012**, 24, (2), 273-278.

(17) Harris, R. D.; Auletta, J. T.; Motlagh, S. A. M.; Lawless, M. J.; Perri, N. M.; Saxena, S.; Weiland, L. M.; Waldeck, D. H.; Clark, W. W.; Meyer, T. Y., Chemical and Electrochemical Manipulation of Mechanical Properties in Stimuli-Responsive Copper-Cross-Linked Hydrogels. *ACS Macro Lett.* **2013**, 2, (12), 1095-1099.

(18) Wischke, C.; Schossig, M.; Lendlein, A., Shape-Memory Effect of Micro-/Nanoparticles from Thermoplastic Multiblock Copolymers. *Small* **2014**, 10, (1), 83-87.

(19) Nejad, H. B.; Baker, R. M.; Mather, P. T., Preparation and characterization of triple shape memory composite foams. *Soft Matter* **2014**, 10, (40), 8066-8074.

(20) Hasan, S. M.; Nash, L. D.; Maitland, D. J., Porous shape memory polymers: Design and applications. *J. Polym. Sci., Part B: Polym. Phys.* **2016**, 54, (14), 1300-1318.

(21) Hearon, K.; Singhal, P.; Horn, J.; Small, W.; Olsovsky, C.; Maitland, K. C.; Wilson, T. S.; Maitland, D. J., Porous Shape-Memory Polymers. *Polym. Rev.* **2013**, 53, (1), 41-75.

(22) Baker, R. M.; Henderson, J. H.; Mather, P. T., Shape memory poly(ε -caprolactone)-co-poly(ethylene glycol) foams with body temperature triggering and two-way actuation. *J. Mater. Chem. B* **2013**, 1, (38), 4916.

(23) Livshin, S.; Silverstein, M. S., Crystallinity in Cross-Linked Porous Polymers from High Internal Phase Emulsions. *Macromolecules* **2007**, 40, (17), 6349-6354.

(24) Bao, M.; Lou, X.; Zhou, Q.; Dong, W.; Yuan, H.; Zhang, Y., Electrospun Biomimetic Fibrous Scaffold from Shape Memory Polymer of PDLLA-co-TMC for Bone Tissue Engineering. *ACS Appl. Mater. Interfaces* **2014**, 6, (4), 2611-2621.

(25) Sokolowski, W. M.; Tan, S. C., Advanced Self-Deployable Structures for Space Applications. *J. Spacecr. Rockets* **2007**, 44, (4), 750-754.

(26) Correia, C. O.; Leite, Á. J.; Mano, J. F., Chitosan/bioactive glass nanoparticles scaffolds with shape memory properties. *Carbohydr. Polym.* **2015**, 123, 39-45.

(27) Zhang, D.; George, O. J.; Petersen, K. M.; Jimenez-Vergara, A. C.; Hahn, M. S.; Grunlan, M. A., A bioactive "self-fitting" shape memory polymer scaffold with potential to treat cranio-maxillo facial bone defects. *Acta Biomater.* **2014**, 10, (11), 4597-4605.

(28) Zharinova, E.; Heuchel, M.; Weigel, T.; Gerber, D.; Kratz, K.; Lendlein, A., Water-Blown Polyurethane Foams Showing a Reversible Shape-Memory Effect. *Polymers* **2016**, 8, (12), 412.

(29) Lu, L.; Cao, J.; Li, G., A polycaprolactone-based syntactic foam with bidirectional reversible actuation. *J. Appl. Polym. Sci.* **2017**, 134, (34), 45225.

(30) Mishra, J. K.; Raychowdhury, S.; Das, C. K., Heat-shrinkable polymer blends based on grafted low-density polyethylene and polyurethane elastomer. Part I. *Polym. Int.* **2000**, 49, (12), 1615-1623.

(31) Morshedian, J.; Khonakdar, H. A.; Mehrabzadeh, M.; Eslami, H., Preparation and properties of heat-shrinkable cross-linked low-density polyethylene. *Adv. Polym. Technol.* **2003**, 22, (2), 112-119.

(32) Khonakdar, H. A.; Morshedian, J.; Mehrabzadeh, M.; Wagenknecht, U.; Jafari, S. H., Thermal and shrinkage behaviour of stretched peroxide-crosslinked high-density polyethylene. *Eur. Polym. J.* **2003**, 39, (8), 1729-1734.

(33) Kolesov, I. S.; Kratz, K.; Lendlein, A.; Radusch, H., Kinetics and dynamics of thermally-induced shape-memory behavior of crosslinked short-chain branched polyethylenes. *Polymer* **2009**, 50, (23), 5490-5498.

(34) Sun, X.; Ni, X., Block copolymer of trans-polyisoprene and urethane segment: Crystallization behavior and morphology. *J. Appl. Polym. Sci.* **2004**, 94, (6), 2286-2294.

(35) Zhao, J.; Chen, M.; Wang, X.; Zhao, X.; Wang, Z.; Dang, Z.; Ma, L.; Hu, G.; Chen, F., Triple Shape Memory Effects of Cross-Linked Polyethylene/Polypropylene Blends with Cocontinuous Architecture. *ACS Appl. Mater. Interfaces* **2013**, 5, (12), 5550-5556.

(36) Liu, W.; Zhang, X.; Bu, Z.; Wang, W.; Fan, H.; Li, B.; Zhu, S., Elastomeric properties of ethylene/1-octene random and block copolymers synthesized from living coordination polymerization. *Polymer* **2015**, 72, 118-124.

(37) Liu, W.; Ojo, A. T.; Wang, W.; Fan, H.; Li, B.; Zhu, S., Preparation of ultrahigh molecular weight ethylene/1-octene block copolymers using ethylene pressure pulse feeding policies. *Polym. Chem.* **2015**, 6, (20), 3800-3806.

(38) Arriola, D. J., Catalytic Production of Olefin Block Copolymers via Chain Shuttling Polymerization. *Science* **2006**, 312, (5774), 714-719.

(39) Zhang, Q.; Feng, J., Difunctional olefin block copolymer/paraffin form-stable phase change materials with simultaneous shape memory property. *Sol. Energy Mater. Sol. Cells* **2013**, 117, 259-266.

(40) Zhang, Q.; Cui, K.; Feng, J.; Fan, J.; Li, L.; Wu, L.; Huang, Q., Investigation on the recovery performance of olefin block copolymer/hexadecane form stable phase change materials with shape memory properties. *Sol. Energy Mater. Sol. Cells* **2015**, 132, 632-639.

(41) Liu, G.; Park, C. B.; Lefas, J. A., Production of low-density LLDPE foams in rotational molding. *Polym. Eng. Sci.* **1998**, 38, (12), 1997-2009.

(42) Pop-Iliev, R.; Liu, F.; Liu, G.; Park, C. B., Rotational foam molding of polypropylene with control of melt strength. *Adv. Polym. Technol.* **2003**, 22, (4), 280-296.

(43) Park, C. P.; Clingerman, G. P., Compatibilizing PE-PS blends with ethylene-styrene copolymers. *Plast. Eng.* **1997**, 53, (3), 97-99.

(44) Rodríguez-Pérez, M. A., Crosslinked Polyolefin Foams: Production, Structure, Properties, and Applications. In *Crosslinking in Materials Science*, Springer Berlin Heidelberg: Berlin, Heidelberg, 2005, 97-126.

(45) Kolesov, I.; Dolynchuk, O.; Jehnichen, D.; Reuter, U.; Stamm, M.; Radusch, H., Changes of Crystal Structure and Morphology during Two-Way

Shape-Memory Cycles in Cross-Linked Linear and Short-Chain Branched Polyethylenes. *Macromolecules* **2015**, 48, (13), 4438-4450.

(46) Ma, L.; Zhao, J.; Wang, X.; Chen, M.; Liang, Y.; Wang, Z.; Yu, Z.; Hedden, R. C., Effects of carbon black nanoparticles on two-way reversible shape memory in crosslinked polyethylene. *Polymer* **2015**, 56, 490-497.

(47) Wang, L.; Razzaq, M. Y.; Rudolph, T.; Heuchel, M.; Nöchel, U.; Mansfeld, U.; Jiang, Y.; Gould, O. E. C.; Behl, M.; Kratz, K.; Lendlein, A., Reprogrammable, magnetically controlled polymeric nanocomposite actuators. *Mater. Horiz.* **2018**, 5, (5), 861-867.

(48) Fan, L. F.; Huang, Y. N.; Rong, M. Z.; Zhang, M. Q.; Chen, X., Imparting External Stress-Free Two-Way Shape Memory Effect to Commodity Polyolefins by Manipulation of Their Hierarchical Structures. *ACS Macro Lett.* **2019**, 1141-1146.

7 CONTRIBUTIONS AND RECOMMENDATIONS

In this chapter, the major contributions of this thesis work are summarized. The recommendations on future potential directions in the field of reversible shape memory polymer is then provided by the author.

§ 7.1 Contributions

The major contributions in this thesis on polyolefin-based reversible shape memory polymers are highlighted as follows:

- A new reversible shape memory polymer based on thermoplastic pure hydrocarbon material is firstly proposed and its multiple and reversible shape memory effect were demonstrated. It is shown that thermoplastic

polyolefin elastomer with designed chain structure can form a broad distribution of crystalline domain sizes, and physical crosslinks sufficient to constrain the orientation of these crystal domains, both of which contribute to the reversible shape memory effect and the excellent reprocessability.

- A simple strategy for fabricating thermoplastic reversible shape memory polymer through blending is considered and the multiple and reversible shape memory effect of commercial thermoplastic polyolefin elastomer blends are demonstrated. This strategy blended materials with various melting transitions to construct a broad and continuous melting transition for achieving the reversible shape memory effect. It can also be applied in reversible shape memory polymer production at low cost and at large scale.
- A new reversible shape memory polymer structure with reconfigurable polymer network by introducing transesterification catalyst into crosslinked poly(ethylene-co-vinyl acetate) system is represented. The idea improved the reprocessability of crosslinked RSMP through simple modification of commodity polymers, which as a result provided a great opportunity for the development of commercial shape memory materials.
- A new reversible shape memory polymer foam based on polyolefin material is designed and fabricated. The reversible shape memory effect of polyolefin elastomer blend foams in tension and bending mode is

demonstrated. This approach extended the material source of current reversable shape memory polymer.

§ 7.2 Recommendations for the future work

As summarized in Chapter 2, reversible shape memory polymers have attracted much attention due to their unique shape shifting behaviors and have potential applications in the areas of soft actuators, microrobotics, etc. In the past few years, this field has been the focus of new materials design, new structure design, and new trigger selections. Despite the significant progress, it has to be acknowledged that research on RSMP is still in its early stages, and that there are still many challenges and possibility in this field. The following perspectives are listed for some recommendations for future research of RSMP.

- Designing and synthesizing RSMP materials with various working temperature range for different applications scenarios, e.g. outer space.
- Designing and synthesizing new RSMP forms, such as foams, fibres, etc.
- Designing and synthesizing RSMP materials that can response to other trigger such as light, electricity, magnetic field, etc.

- Designing and synthesizing functional RSMP materials or devices that can exhibit response other than shape changing, such as fluorescence emitting, conductivity change, etc.
- Exploring the new mechanisms of reversible shape memory effect through both theoretical and experimental route.